APPLICATIONS OF IRREVERSIBLE THERMODYNAMICS TO TRANSPORT PROCESSES IN ELECTROLYTE SOLUTIONS.

a thesis presented for the degree of

Ph. D.

by

ANDREW AGNEW

FACULTY OF SCIENCE

CHEMISTRY DEPARTMENT

JANUARY 1975

ProQuest LLC.
789 East Eisenhower Parkway
P.O. Box 1346
Ann Arbor, MI 48106 – 1346

Acknowledgements.

I am happy to be able to express my gratitude to all who helped me throughout the preparation of this thesis. I am greatly indebted to Dr. Russell Paterson for his guidance and supervision and especially for many useful discussions about theoretical aspects of the work. I must also thank Dr Helen S. Dunsmore whose assistance with the preparation of computer programs was invaluable. I am also indebted to Stephen Anderson for his assistance in the measurement of cell emf transference numbers, and to Lutfullah for making availiable the preliminary results of his potentiometric study of aqueous zinc chloride. Last, but by no means least, my thanks to John Anderson, Ian Burke, Ronald Cameron, and Jim Walker, both for their help with all aspects of the work and for their continuing friendship which helped make the period of study such a pleasent one.

I also thank the Science Research Council for the receipt of a maintainance grant.

Contents.

Summary.

Non-equilibrium thermodynamics is applied to isothermal vector transport processes in concentrated aqueous binary electrolyte solutions. It is shown that this branch of thermodynamics gives rise to linear mobility coefficients, L_{ij}, and frictional coefficients, R_{ij}, which measure the effect on ion-constituent, i, of a thermodynamic force on ion-constituent, j. The cross coefficients, L_{ij} and R_{ij} where $i \neq j$, are of especial interest as they provide a measure of the interactions between species i and j. The transport coefficients are considered to be more fundamental than the more commonly reported transport properties which can be shown to be combinations of the L_{ij} or the R_{ij}.

The interpretation of the concentration dependance of transport coefficients is qualitative and must therefore be based on a comparison between similar salts. Zinc chloride and zinc perchlorate were selected for experimental study as zinc chloride exhibits extensive self complexing in aqueous solution whereas zinc perchlorate does not. The effects of self-complexing are therefore assessed using the experimental results for these two salts, in conjunction with transport coefficients availiable in the literature for several other salts.

Four experimental measurements are required to evaluate the four independent transport coefficients of a binary electrolyte solution. These are of electrical conductivity, salt diffusion coefficient, Hittorf transference number, and cell emf transference number, as a function of concentration. Each of these experiments is analysed and equations are derived which express the mobility and frictional coefficients in terms of these experimental quantities. It is shown that the equality of the two transference numbers is a consequence of the Onsager reciprocal relations, which state that $L_{ij} = L_{ji}$ and $R_{ij} = R_{ji}$

for $i \neq j$. These relations require experimental proof which is given.

The experimental section describes the preparation of aqueous solutions of zinc chloride and zinc perchlorate and the measurement of their transport properties. Electrical conductivity was measured using standard methods. Diffusion coefficients were measured using an optical technique which allowed the progress of restricted diffusion in a closed rectangular glass cell to be followed as a function of time. Hittorf transference numbers were measured for both salts using a glass cell based on the design of MacInnes and Dole. Cell emf transference numbers were measured for zinc chloride only using cells of similar design to those described by Pikal and Miller. Values for zinc perchlorate were obtained from the literature.

The experimental results are collected and used to calculate the transport coefficients for zinc chloride and zinc perchlorate. The relative merits of the mobility and frictional coefficients for interpretative purposes are discussed. Both schemes have merits, but the frictional representation has the advantage that it provides coefficients which measure the interactions between ions and solvent as well as those which measure interactions between ion and ion. Also the cation - anion frictional coefficient reflects the difference between strong ion association, as exhibited by aqueous silver nitrate, and self-complexing, as exhibited by the zinc and cadmium halides, whereas the corresponding mobility coefficient does not. Finally it is demonstrated that the mobility coefficients of a self-complexing salt can be expressed as a combination of the mobility coefficients of each of the individual species. The concentration dependance of each of these latter coefficients can be estimated qualitatively from theoretical considerations and combined to explain experimental trends.

In the final chapter the effect of the weak ion association in dilute aqueous solutions of 2:2 electrolytes on their diffusion coefficients is considered. It is shown that for the four salts for which

experimental data are availiable the observed diffusion coefficient is equal to the diffusion coefficient calculated from electrolyte theory using the concentration of free ions in solution. This relation is found to be valid within experimental error to a total salt concentration of 0.1mol dm^{-1}. Calculations were also carried for three weak organic acids for which experimental diffusion coefficients are availiable, but in these systems the above relation was found not to be valid.

Nomenclature

(Symbols are inserted in order of appearance)

dS	total entropy change
dQ	heat exchanged with exterior
T	Absolute temperature
$d_e S$	flow of entropy due to interaction with exterior
$d_i S$	production of entropy inside system
σ	rate of production of entropy per unit volume
V	volume
S_v	entropy density per unit volume
t	time
J_s	flow of entropy
J_q	flow of heat
J_i	flow of matter
A	affinity of chemical reaction
$\tilde{\mu}_i$	electrochemical potential
μ_i	chemical potential
Φ	rate of dissipation of free energy
X_i	thermodynamic driving force
n_i	number of moles of species i
C_i	concentration of i per unit volume
v_i	velocity of species i
L_{ik} R_{ik}	phenomenological coefficients
r_1, r_2	stoichiometric coefficients for ionisation
Z	valency
I	current density
κ	specific conductance

$\frac{\partial x}{\partial n}$	gradient of electrical potential
F	Faraday's constant
Λ	equivalent conductance
N	equivalent concentration.
t_i^h	Hittorf transference number
t_i^c	cell emf transference number
R	gas constant
$\overline{M}$	thermodynamic diffusion coefficient
$(D)_o$	diffusion coefficient on apparatus fixed reference frame
$y_{\pm}$	mean molar activity coefficient
D_v	diffusion coefficient on volume fixed reference frame
m	molal concentration
$\gamma^{\pm}$	mean molal activity coefficient
C_o	solvent concentration
E	electro-motive force
ξ	distance parameter in diffusion cell
λ	wavelength of light
l	thickness of diffusion cell
m	fringe displacement in a Rayleigh interference pattern
n	(in chapter 4 only) refractive index
m_i, m_f, m_c	concentration of solution in compartments of a Hittorf cell in moles per Kg of solution
W	weight of solution in electrode compartment of a Hittorf cell
	duration of a Hittorf run
T_i	integral transference number

f_{ij}	coefficient of kinetic friction.
l_{ij}	mobility coefficient of complex species in solution.
$y_{\pm}$	mean molar activity coefficient.
$\mathring{a}$	distance of closest approach of Debye-Huckel theory.
η_0	viscosity of solvent in poise.
$\mathcal{D}$	dielectric constant.
κ	reciprocal distance of Debye-Hückel theory.
α	degree of dissociation of a weak electrolyte.
K_D	dissociation constant.

Chapter 1

Introduction

A large section of electrochemistry is concerned with the transport of mass and charge which takes place in an electrolyte solution under the influence of an applied thermodynamic force. The processes traditionally considered are the electrical conductivity, which describes a flow of ions when the force is an applied electrical field, and diffusion, which describes the flow of solute when the applied force is a gradient of concentration, or more properly of chemical potential. Much effort has been devoted over the last 40 years to the theoretical description of these processes, but with only limited success. Despite the vast improvement in mathematical and computational techniques in recent years the upper concentration limit for classical electrolyte transport theories is only 0.05 mol dm^{-3} (molar) in the most favourable cases.

An alternative, and in many ways complementary description of transport processes has received increasing attention in recent years. This is the framework of irreversible thermodynamics which was first developed by Onsager [1] in 1931 and was later expanded and generalised by several other authors [2,3,4]. Irreversible thermodynamics gives rise to a set of phenomenological equations which describe the flow of each component in a system in terms of the independent forces on it, and on all the other components in the system. Thus irreversible thermodynamics gives rise to parameters which measure the direct effect of a force on a component, and also to parameters which measure the interaction or coupling between the flows of pairs of components. When the system is an electrolyte solution the components

are the ions and the solvent and the independent forces are the gradients of electrochemical potential of the ions. (The electrochemical potential of an ion, a concept first introduced by Guggenheim,[5] is the sum of the chemical and electrostatic potentials of the ion). The irreversible thermodynamic parameters therefore measure the kinetic interactions between ion and ion and between ion and solvent. A major advantage of this scheme is that it can be applied to electrolyte solutions of any concentration.

A detailed analysis of the application of irreversible thermodynamics to transport processes in electrolyte solutions was published by Miller[6], who was able to show that the traditional transport properties, equivalent conductivity, transference numbers, and diffusion coefficients, could all be expressed in terms of the irreversible thermodynamic parameters. Miller concluded that these parameters were more fundamental than the traditional transport properties and were, therefore, more worthy of experimental and theoretical consideration.

The interpretation of the irreversible thermodynamic parameters is at present mainly qualitative, and must, therefore, be based on the comparison of a series of similar salts. Miller[6a] chose the three alkali chlorides for which data were at that time available, lithium, sodium and potassium chloride. Paterson and Jalota[7-10] provided the experimental data required for the analysis of rubidium and cesium chloride and extended Miller's interpretation of the parameters for the alkali chloride series.

Paterson and Jalota explained some anomalies in the

irreversible thermodynamic parameters of caesium and rubidium chlorides in terms of the ion association present in solutions of these salts. For this reason it was decided to investigate a system which showed extensive interactions between the cations and anions present in solution. The system chosen for study was aqueous zinc chloride, which is well known to exhibit extensive self-complexing in concentrated solutions [11,12]. For the purposes of comparison zinc perchlorate was also studied since this salt was not expected to exhibit extensive ion association or self-complexing. The concentration range studied was 0.1 - 3.0 molar in each case.

In chapter 2 the application of irreversible thermodynamic theories to transport processes in a binary electrolyte solution is discussed, and special reference is made to the influence of self-complexing on the development of the theory. It is shown that four experimental transport properties require to be measured to evaluate the irreversible thermodynamic parameters, the equivalent conductivity, the diffusion coefficient, the Hittorf transference number, and the cell emf transference number. The latter two properties are commonly taken to be identical, but it will be shown that this is an assumption which must be verified experimentally. Of these four properties only cell emf transference number data are available in the literature for zinc chloride [11] and zinc perchlorate[13]. The experimental work of this thesis consisted of measuring the 'missing' transport properties.

The measurement of equivalent conductivity is described in chapter 3. This chapter also contains an account of the preparation of exactly stoichiometric solutions of zinc chloride, a task which was

much more difficult than might have been expected. Chapter 4 describes the measurement of diffusion coefficients by an optical technique, and chapter 5, the measurement of Hittorf transference numbers. Also reported in chapter 5 are the results of a potentiometric study on zinc chloride solutions which extended the cell emf transference number data to cover all the required concentration range. In chapter 6 the results of the transport experiments are collected and the irreversible thermodynamic parameters calculated and discussed.

In chapter 7 the application of classical electrolyte theory to diffusion in ion associated systems is discussed and the behaviour of 2:2 salts, which are slightly associated in solution, is compared with that of the weak organic acids, which are extensively associated. Several computer programmes which were written to perform involved or repetitive calculations are reproduced in the Appendix.

Chapter 2

The Theory of Irreversible Thermodynamics and its Application to Transport Processes in Electrolyte Solutions

Classical thermodynamics, although a harmonious and self-consistent structure, is somewhat limited in scope by being essentially confined to the description of reversible processes and true equilibrium states. It is known, however, that in a great number of systems true thermodynamic equilibrium is only rarely attained. The theory of non-equilibrium thermodynamics was developed to describe such irreversible processes, most notably by Onsager,[1] Meixner,[2] Casimir,[3] and Prigogine[4]. This chapter, describing the application of this theory to transport processes in electrolyte solutions, is compiled mainly from four excellent treatises on the subject,[5,6,7,8] and the recent papers of Miller[9a,b,c].

2.1 The Production of Free Energy in an Irreversible Process:- The Dissipation Function

2.1.1 The Production of Entropy by an Irreversible Process

The theory of non-equilibrium thermodynamics has its basis in the Second Law of thermodynamics; that the entropy production of an irreversible process must be positive. Systems undergoing irreversible processes may be divided into local sub-systems which are macroscopically small, but contain sufficient molecules to render microscopic fluctuations negligible. If the perturbation of the system from equilibrium is not large each

subsystem can be considered to be at local equilibrium, and the laws of classical thermodynamics will hold; in particular the Second Law :-

$$dS \geq {}^{dQ}/_{T} \qquad (2.1)$$

where dS is the entropy change, dQ is the heat exchanged with the exterior, and T is the absolute temperature.

The entropy change, dS, can be split into two terms :-

$$dS = d_e S + d_i S \qquad (2.2)$$

where $d_e S$ is the flow of entropy due to interaction with the exterior, and $d_i S$ is the production of entropy inside the system. $d_i S$ is zero for a reversible process and positive for an irreversible process. It is a central postulate of non-equilibrium thermodynamics, justifiable by statistical mechanics,[10] that $d_i S \geq 0$ for every macroscopic subsystem considered. Therefore if we have a system, I, enclosed by another system, II, such that both systems are isolated, the statement of the Second Law becomes :-

$$dS = dS^{I} + dS^{II} \geq 0 \qquad (2.3)$$

and the postulate means that a situation where

$$d_i S^{I} < 0, \; d_i S^{II} > 0 \quad \text{where} \quad d_i(S^{I} + S^{II}) \geq 0$$

is not allowed.

The rate of entropy production of a system can be considered to be the sum of contributions from each subsystem so that in the limit

$$\frac{d_i S}{dt} = \int_V \sigma \, dV \qquad (2.4)$$

where σ is the local rate of production of entropy per unit volume, V. The rate of flow of entropy into the system is related to the local flow of entropy, J_s, by

$$\frac{d_e S}{dt} = \int_V - \text{div } J_s \, dV \qquad (2.5)$$

The total entropy of the system can also be defined in terms of the local entropy density throughout the system, S_v, by

$$S = \int_V S_v dV \qquad (2.6)$$

Differentiating equation (2.6) w.r.t time gives the rate of change of total entropy

$$\frac{dS}{dt} = \int_v \frac{\partial S_v}{\partial t} .dV \qquad (2.7)$$

By differentiating equation (2.2) w.r.t time and substituting equations (2.4), (2.5) and (2.7) we get

$$\int_V \frac{\partial S_v}{\partial t} \, dV = - \int_V \text{div } J_s .dV + \int_V \sigma \, dV \qquad (2.8)$$

This describes the total rate of change of entropy with time. For any local change it becomes

$$\frac{\partial S_v}{\partial t} = -\text{div } J_s + \sigma \qquad (2.9)$$

The conditions for equilibrium are that

$$\frac{\partial S_v}{\partial t} = 0 \quad \text{and div } J_s = 0 \qquad (2.10)$$

and therefore from equation (2.9) σ will also be zero. For a system in the steady state, however, only the rate of change of the total entropy need vanish, and therefore the conditions are

given by equation (2.11)

$$\frac{\partial S_v}{\partial t} = 0$$

$$\text{and} \qquad \text{div} J_s = \sigma \qquad (2.11)$$

i.e. the rate of entropy production must equal the rate at which entropy leaves the system.

2.1.2 The Dissipation Function For a continuous system the rate of entropy production, σ, can be shown to be given by[11] equation (2.12)

$$\sigma = \frac{J_q}{T} \text{ grad } (-T) + \sum_{i=1}^{n} \frac{J_i}{T} \text{ grad } (-\tilde{\mu}_i) + J_{ch} \left|\frac{A}{T}\right| \qquad (2.12)$$

where J_q, J_i and J_{ch} are the flows of heat and matter, and the rate of chemical reaction respectively, and grad $(-T)$, grad $(-\tilde{\mu}_i)$, and $\left|\frac{A}{T}\right|$ are the corresponding driving forces; the negative gradients of temperature and electrochemical potential and the affinity of the chemical reaction respectively. A more convenient form of (2.12) is obtained by replacing σ with the dissipation function, $T\sigma = \Phi$

$$\Phi = J_s \text{ grad } (-T) + \sum_{i=1}^{n} J_i \text{ grad } (-\tilde{\mu}_i) + J_{ch} \cdot A \qquad (2.13)$$

Φ has the dimensions of energy per unit time and it is a measure of the local rate of dissipation of free energy. Both equations (2.12) and (2.13) show σ or Φ as the product of flows and conjugate driving forces. We are concerned here with isothermal transport processes in electrolyte solutions in the

absence of chemical reactions, therefore equation (2.13) simplifies to equation (2.14)

$$\Phi = \sum_{i=o}^{n} J_i X_i \qquad (2.14)$$

For a system of solvent, o, and n solute species J_i is the mass fixed flow of species i in units of moles $cm^{-2} sec^{-1}$ and X_i is the corresponding thermodynamic force (equivalent to grad $(-\tilde{\mu}_i)$) with units of Joule $mole^{-1} cm^{-1}$.

2.1.3 Frames of Reference for Flows The derivations so far have assumed a barycentric frame of reference for the flows, but it has been shown that provided the system is in mechanical equilibrium any arbitrary frame of reference can be used[12]. In the study of transport properties of electrolyte solutions the most generally useful reference frame is the solvent fixed one.

Equation (2.14) describes a system of (n + 1) components in which (as a result of the Gibbs-Duhem equation) there are only n independent flows and forces. This states that

$$\sum_{i=o}^{n} n_i d\tilde{\mu}_i = 0 \qquad (2.15)$$

where n_i is the total number of moles of species i present.

Dividing by the volume V and differentiating with respect to the spatial co-ordinates transforms equation (2.15) to

$$\sum_{i=o}^{n} C_i \text{ grad } (\tilde{\mu}_i) = 0$$

or

$$\sum_{i=o}^{n} C_i X_i = 0 \qquad (2.16)$$

where C_i is the concentration of i per unit volume. Eliminating X_o (solvent) from equation (2.16) and substituting in the dissipation function gives

$$\Phi = \sum_{i=1}^{n} \left(J_i - \frac{C_i}{C_o} J_o\right) X_i \qquad (2.17)$$

The flow of species i, J_i is given by the product of its concentration, C_i, and its velocity with respect to some arbitrary frame of reference, v_i, so that

$$J_i - \frac{C_i}{C_o} J_o = C_i(v_i - v_o) = J_i^o \qquad (2.18)$$

J_i^o is the flow of species i referred to a solvent fixed frame of reference. From now on all flows will be referred to this frame of reference unless otherwise stated, and the superscript o will be dropped for typographical convenience.

2.2 The Relation between Flows and Forces. The Phenomenological Equations and the Onsager Reciprocal Relations

The dissipation function is of little practical use unless some relation can be found between conjugate pairs of flows and forces. Many linear relations have been found between flows and conjugate forces, e.g. Fick's law of diffusion, Ohm's law of electrical conduction, and Fourier's law of heat conduction, and also between flows of one type and forces of another type, e.g. the Seebeck and Peltier thermo-electric effects. Consideration of those results and others led Onsager to postulate a general set of linear phenomenological equations :-

$$J_i^* = \sum_{i=o}^{n} L_{ik}^* X_k \qquad (i = 0, 1, 2, 3 \ldots\ldots n) \quad (2.19)$$

where J_i^* is the flow of species i on any arbitrary reference frame, and X_i is the thermodynamic force acting on species k. The L_{ik}^* are phenomenological co-efficients independent of the forces. These equations hold for slow processes in a system not too far from equilibrium, and in particular can be assumed to hold for transport processes in electrolyte solutions[13].

For a one flow-one force system equation (2.19) becomes

$$J_i^* = L_{ii}^* X_i \qquad (2.20)$$

where L_{ii}^* is a specific measure of the mobility of species i. From equation (2.20) Ohm's law and Fick's law can be easily abstracted by substituting the appropriate values for the force, X_i. In a system of two components, for example a binary electrolyte solution on a solvent fixed frame of reference, equation (2.19) becomes

$$\begin{aligned} J_1 &= L_{11}X_1 + L_{12}X_2 \\ J_2 &= L_{21}X_1 + L_{22}X_2 \end{aligned} \qquad (2.21)$$

Here the direct coefficients L_{11} and L_{22} remain, and in addition two cross coefficients, L_{12} and L_{21} are introduced. These cross or coupling coefficients are a measure of the interaction between species 1 and 2. For example, when X_1 is zero L_{12} controls the magnitude of the flow of species 1, J_1, caused by the non-zero force, X_2, on species 2.

The coefficients of equation (2.19) are independent, but

the absolute magnitude of the cross coefficients L_{ik}, is restricted by the magnitude of the direct coefficients, L_{ii}, as a consequence of the requirement that entropy production should be positive. In the binary case equations (2.14) and (2.21) give

$$\Phi = L_{11}X_1^2 + (L_{12} + L_{21})X_1X_2 + L_{22}X_2^2 > 0 \qquad (2.22)$$

Equation (2.22) must be true for all positive or negative values of X_1 and X_2 provided both are not zero simultaneously. Setting first X_2 and then X_1 equal to zero gives

$$L_{11} > 0 \quad \text{and} \quad L_{22} > 0 \qquad (2.23)$$

Given the inequalities (2.23) the left hand term in inequality (2.22) can only have imaginary roots. This can only be true if

$$(L_{12} + L_{21})^2 - 4L_{11}L_{22} < 0$$

$$\text{or} \qquad 4L_{11}L_{22} > (L_{12} + L_{21})^2 \qquad (2.24)$$

The above conditions are easily generalised to the n-component case, where the constraints on the magnitudes of the various coefficients are

$$L_{ii} > 0 \quad (i = 0, 1, 2 \ldots n) \qquad (2.25)$$

$$4L_{ii}L_{kk} > (L_{ik} + L_{ki})^2 \quad (i,k = 0, 1, 2 \ldots n) \qquad (2.26)$$

i.e. the direct coefficients are always positive but the cross coefficients may be positive, negative or zero.

As formulated so far the application of the phenomenological laws to a system of n flows and forces requires the determination of n^2 coefficients from n^2 independent experiments. However Onsager has shown, using the principle of microscopic reversibility, that

the matrix of phenomenological coefficients is symmetric, i.e.

$$L_{ik} = L_{ki} \qquad i,k = 1, 2, 3 \ldots n \qquad (2.27)$$

The equations (2.27) are commonly referred to as the Onsager Reciprocal Relations (ORR). The ORR reduce the number of independent coefficients required to characterise a system of n flows and forces to $\frac{1}{2}n(n + 1)$. The ORR were proved, by Onsager, only for systems very close to equilibrium, but experimental evidence indicates that they are valid well beyond the range of theoretical justification[13,14,15].

The physical interpretation of the mobility coefficients, L_{ik}, for electrolyte solutions will be considered in detail later. Briefly, however, the direct coefficients, L_{ii}, are taken as a measure of the intrinsic mobility of species i in the absence of interactions with species L, whilst the cross coefficients, L_{ik}, give a measure of the kinetic coupling between the two species, i and k. All the coefficients are dependent on the frame of reference chosen for the flows, and therefore on the solvent fixed reference frame. Both direct and cross coefficients contain contributions from the solvent.

2.2.1 The Inverse Form of the Phenomenological Equations

The inverse form of equation (2.19) is

$$X_i = \sum_{k=o}^{n} R_{ik} J_k^{*} \qquad i = 0, 1, 2, \ldots n \qquad (2.28)$$

in which the flows are referred to an arbitary reference frame. The coefficients, R_{ik}, are frictional rather than mobility coefficients.

In an electrolyte solution the direct coefficients, R_{ii} represent frictional interactions between like species, and the cross coefficients, R_{ik}, interactions between the two different species i and k.

The coefficients in equation (2.28) are not uniquely defined as neither the flows nor the forces are independent. However, the condition that there shall be no dissipation of free energy when the velocities of all species are equal implies equation (2.24)[16,17]

$$\sum_{k=o}^{n} C_k R_{ik} = 0 \qquad (i = 0, 1, 2 \ \ldots \ n) \qquad (2.29)$$

The R_{ij} now become uniquely specified and reference frame independent. Thus multiplying equation (2.29) by $(v_i - v_*)$, where v_i is the velocity of species i and v_* is the velocity of the arbitrary reference frame, and subtracting from equation (2.28) gives

$$X_i = \sum_{k=o}^{n} R_{ik} C_k (v_k - v_i) \qquad (i = 0, 1, \ldots n) \qquad (2.30)$$

Since the v_* have cancelled out the R_{ik} are reference frame independent. As with the mobility coefficients, the frictional coefficients can be shown to obey the ORR

$$R_{ik} = R_{ki} \qquad (i,k = 0, 1, \ldots n) \qquad (2.31)$$

It can also be shown that the direct coefficients are always positive whilst the cross coefficients can be positive, negative or zero, i.e.

$$R_{ii} > 0 \qquad (i = 0, 1, \ldots n) \qquad (2.32)$$

$$4R_{ii}R_{kk} > (R_{ik} + R_{ki})^2 \qquad (i,k = 0, 1, \ldots n)$$

For a binary electrolyte system with flows defined on a solvent fixed (SF) reference frame J_o becomes zero and an independent set of equations can be written

$$\begin{aligned} X_1 &= R_{11}J_1 + R_{12}J_2 \\ X_2 &= R_{21}J_1 + R_{22}J_2 \end{aligned} \qquad (2.33)$$

Equation (2.33) is the exact inverse of equation (2.21) and can be obtained from it by matrix inversion. Thus the frictional coefficients can be expressed in terms of the mobility coefficients. The results are

$$R_{11} = \frac{L_{22}}{|L|} \qquad R_{12} = \frac{L_{22}}{|L|} \qquad (2.34)$$

$$R_{22} = \frac{-L_{21}}{|L|} \qquad R_{22} = \frac{L_{11}}{|L|}$$

where $$|L| = L_{11}L_{22} - L_{12}L_{21} \qquad (2.35)$$

Combining equations (2.29) and (2.34) then allows R_{10}, R_{20} and R_{00} to be calculated.

2.3 Measurement of the Phenomenological Coefficients - Analysis of Transport Experiments in Aqueous Electrolytes

We consider the isothermal system of a binary electrolyte in a neutral solvent which exists in solution as

$$C_{r_1}A_{r_2} \rightleftharpoons r_1C^{z_1} + r_2A^{z_2} \qquad (2.36)$$

Here r_1 and r_2 are the stoichiometric coefficients for ionisation of the salt into cation, C, and anion, A, with signal valencies z_1 and z_2 respectively. It will be shown later that the following

derivations are also valid for a system where ion association is present if C and A represent the cation and anion constituents respectively instead of the simple ions. The cation or anion constituent is the total amount of cation or anion which would be present if all associated species of the type $C_{n_1} A_{n_2}^{(Z_1 n_1 + Z_2 n_2)}$ were completely dissociated. From equation (2.36) the electrochemical potentials of the ions, $\tilde{\mu}_1$ and $\tilde{\mu}_2$, and the chemical potential of the electrolyte as a whole, μ_{12}, are seen to be related by

$$\mu_{12} = r_1\tilde{\mu}_1 + r_2\tilde{\mu}_2 \qquad (2.37)$$

whilst electroneutrality requires that

$$r_1 Z_1 + r_2 Z_2 = 0 \qquad (2.37)$$

The SF reference frame is chosen and the phenomenological equations (2.21) used where the thermodynamic forces, X_i, are identified as the negative gradients of electrochemical potential.

$$X_i = \frac{-\partial\tilde{\mu}_i}{\partial x} = \frac{-\partial\mu_i}{\partial x} + Z_i F \frac{-\partial\psi}{\partial x} \qquad i = 1,2 \qquad (2.38)$$

where x is the distance parameter. The 1-dimensional case only is considered as this corresponds to the normal experimental conditions. The $\frac{\partial\mu_i}{\partial x}$ are gradients of chemical potential of the ions in joule $\text{mole}^{-1}\text{cm}^{-1}$ and $\frac{\partial\psi}{\partial x}$ is the gradient of electrical potential in the system in volts cm^{-1}, and F is Faraday's constant in coulomb equiv^{-1}.

The four independent experimental quantities needed to evaluate the four L_{ik} coefficients are the equivalent conductance, Λ, the diffusion coefficient, D, the Hittorf transference number, t_i^h, and the emf transport number, t_i^C. The ORR imply that one of these experiments is redundant, and it will be shown that the ORR imply that the Hittorf and emf transference numbers are identical.

2.3.1 Electrical Conductance The electrical conductance of an electrolyte solution obeys Ohm's law :

$$I = \kappa \frac{-\partial \psi}{\partial x} \tag{2.39}$$

where I is the current density in Amp cm^{-2} and κ is the specific conductance in $Ohm^{-1}cm^{-1}$. In terms of flows of ion constituents I becomes

$$I = (Z_1 J_1 + Z_2 J_2)F \tag{2.40}$$

In a conductance experiment the concentration is uniform throughout the cell and therefore the chemical potential gradients vanish and X_i becomes, equation (2.41)

$$X_i = Z_i F \frac{-\partial \psi}{\partial x} \quad i = 1, 2 \tag{2.41}$$

Substituting equations (2.21) and (2.41) in (2.40), rearranging, and comparing the result with equation (2.39) gives equation (2.42).

$$\kappa = (Z_1^2 L_{11} + Z_1 Z_2 (L_{12} + L_{21}) + Z_2^2 L_{22})F^2 \tag{2.42}$$

The more commonly reported experimental quantity is the equivalent conductance, defined by equation (2.43)

$$\Lambda = \frac{1000\,\kappa}{N} \tag{2.43}$$

where N is the concentration in equiv l^{-1}, and 1000 is really 1000 $cm^3 l^{-1}$. Combining equations (2.42) and (2.43) gives

$$\Lambda = \frac{1000 \alpha F^2}{N} \tag{2.44}$$

where

$$\alpha = Z_1^2 L_{11} + Z_1 Z_2 (L_{12} + L_{21}) + Z_2^2 L_{22} \tag{2.45}$$

Λ is normally measured on an apparatus fixed reference frame, but can be shown to be reference frame independent[18].

2.3.2 The Hittorf Transference Number The Hittorf transference number, t_i^h, is defined as the fraction of the total electrical current carried by the i th ion constituent in a solution of constant composition. It is defined on a SF reference frame. In terms of flows this definition becomes

$$t_i^h = \frac{Z_i J_i F}{I} \tag{2.46}$$

Combining equations (2.21), (2.40), (2.41), (2.45) and (2.46) gives for the cation transference number, t_1^h,

$$t_1^h = \frac{Z_1^2 L_{11} + Z_1 Z_2 L_{12}}{\alpha} \tag{2.47}$$

It is easily verified that in a binary electrolyte solution

$$t_1 + t_2 = 1 \tag{2.48}$$

2.3.3 E.m.f. Transference Numbers An electrochemical cell with transference consists of two compartments each containing an identical electrode and an electrolyte. The concentration of the electrolyte in each compartment is different, and the two compartments are joined by a liquid junction. Such a cell is represented by

$$Ag/AgCl \quad ZnCl_2(C_1) \quad || \quad ZnCl_2(C_2) \quad AgCl/Ag$$

where C_1 and C_2 are concentrations with $C_2 > C_1$. Diffusion occurs across the liquid junction, and as a result of the unequal ionic mobilities charge separation occurs. In a very short time (10^{-9}s or less) powerful coulombic effects slow the faster ions and speed up the slower ions so that no net current flows and a liquid junction potential is set up. Thus

$$I = Z_1 J_1 + Z_2 J_2 = 0 \tag{2.49}$$

The gradients of chemical and electrical potential are non-zero. Substituting equations (2.21) and (2.38) in equation (2.49) and solving for $F\left(-\frac{\partial \psi}{\partial x}\right)$ gives

$$F\left(-\frac{\partial \psi}{\partial x}\right) = \frac{(Z_1L_{11} + Z_2L_{21})}{\alpha}\frac{\partial \mu_1}{\partial x} + \frac{(Z_1L_{12} + Z_2L_{22})}{\alpha}\frac{\partial \mu_2}{\partial x} \tag{2.50}$$

We can define the cell or emf cation transference number t_1^c as

$$t_1^c = \frac{Z_1^2L_{11} + Z_1Z_2L_{21}}{\alpha} \tag{2.51}$$

and similarly for the anion transference number, t_2^c. Substituting in equation (2.50) gives the classical equation for the diffusion potential

$$F\left(-\frac{\partial \psi}{\partial x}\right) = \frac{t_1^c}{Z_1}\frac{\partial \mu_1}{\partial x} + \frac{t_2^c}{Z_2}\frac{\partial \mu_2}{\partial x} \tag{2.52}$$

Equation (2.25) must be transformed by including the electrode reactions for the system considered. Assuming, as in the cell depicted above, that the electrode is reversible to the anion, and integrating from the anode, α, through the cell to the cathode, β, the classical result is obtained

$$E = -\frac{1}{F}\int_{\alpha}^{P}\frac{t_1^c}{r_1Z_1}d\mu_{12} = -\frac{RT}{F}\cdot\frac{1}{r_1Z_1}\int_{\alpha}^{\beta} t_1^c \, d\ln a_{12} \tag{2.53}$$

where E is the emf of the cell at zero current and R is the gas constant in J deg^{-1} mol^{-1}. For electrodes reversible to the anion subscripts 1 and 2 are interchanged.

Experimental values of t_1^c are obtained from the derivative of equation (2.53) by measuring the emf of cells where the concentration

of the solution around one electrode is varied and that of the solution around the other is held constant. This gives

$$t_1^c = \frac{r_1 Z_1 F}{RT} \cdot \frac{\partial E_2}{\partial \ln a_{12}} \qquad (2.54)$$

Equation (2.54) applies when a_{12} is known from other studies. It can be seen by comparing equations (2.51) and (2.47) that the Hittorf and emf transference numbers are identical if and only if the ORR hold.

2.3.4 Diffusion Isothermal diffusion occurs in the presence of a concentration gradient. The flows of anion and cation are coupled so that the net current is zero and equation (2.49) applies. When combined with equation (2.37) this gives equation (2.55)

$$\frac{J_1}{r_1} = \frac{J_2}{r_2} = J \qquad (2.55)$$

Here J is the flow of the solute as a whole since $\frac{J_1}{r_1}$ and $\frac{J_2}{r_2}$ represent the flows of cations and anions in the proportions found in the electrolyte compound $C_{r_1} A_{r_2}$. The diffusion coefficient is now defined by Fick's Law

$$J = \frac{(D)_o}{1000} \left(- \frac{\partial c}{\partial x} \right) = \bar{M} \left(- \frac{\partial \mu_{12}}{\partial x} \right) \qquad (2.55)$$

where $(D)_o$ is the diffusion coefficient on the SF frame of reference, in $cm^2 sec^{-1}$ $\bar{M}$ is the thermodynamic diffusion coefficient in $mol^2 J^{-1} cm^{-1} s^{-1}$ and 1000 is really 1000.027 $cm^3 l^{-1}$. Equation (2.55) can be written

$$\frac{(D)_o}{1000} \left(- \frac{\partial c}{\partial x} \right) = \bar{M} \left(\frac{\partial \mu_{12}}{\partial c} \right) \left(- \frac{\partial c}{\partial x} \right) \qquad (2.56)$$

where $\left(\frac{\partial \mu_{12}}{\partial c} \right)$ is given by

$$\frac{\partial \mu_{12}}{\partial c} = \frac{rRT}{c} \cdot \left(1 + \frac{\partial \ln y}{\partial \ln c} \right) \qquad (2.57)$$

where $r = r_1 + r_2$ and y is the mean molar activity coefficient. Equations (2.55), (2.56) and 2.57) give

$$1000\ rRT\ \frac{\bar{M}}{c} = {}^{(D)}{}_{o}/(1 + \frac{\partial \ln y}{\partial \ln c}) \qquad (2.58)$$

As a matter of experimental convenience diffusion coefficients are normally measured on a volume fixed reference frame and reported as such, D_v. $(D)_o$ and D_v are only equal at infinite dilution although in dilute solutions the difference is small and commonly neglected. This is not valid in concentrated solutions however, where the relation between the two can be expressed as[19]

$$\frac{(D)_o}{1 + \frac{\partial \ln y}{\partial \ln c}} = \frac{D_v}{1 + \frac{\partial \ln \gamma}{\partial \ln m}} \qquad (2.59)$$

where m is the molality in moles per kilogram of solvent and γ is the mean molal activity coefficient.

An expression for $\bar{M}$ or D_v in terms of the L_{ik} is required. Equations (2.21), (2.38) and (2.55) give

$$J = \frac{J_1}{r_1} = \frac{1}{r_1}\left[L_{11}\left(\frac{-\partial \mu_1}{\partial x}\right) + L_{12}\left(\frac{-\partial \mu_2}{\partial x}\right) + (2_1 L_{11} + 2_2 L_{12})\, F\, \left(\frac{-\partial \psi}{\partial x}\right)\right] \qquad (2.60)$$

By substituting for $F\left(-\frac{\partial \psi}{\partial x}\right)$ from equation (2.50) and rearranging equation (2.61) is obtained, which, when compared with equation (2.55) gives equation (2.62)

$$J = \frac{Z_1 Z_2}{r_1 r_2} - \left[\frac{L_{11}L_{22} - L_{12}L_{21}}{\alpha}\right]\left(- \frac{\partial \mu_{12}}{\partial n}\right) \qquad (2.61)$$

$$\bar{M} = - \frac{Z_1 Z_2}{r_1 r_2}\left[\frac{L_{11}L_{22} - L_{12}L_{21}}{\alpha}\right] \qquad (2.62)$$

On substituting from equations (2.58) and (2.59) equation (2.63) is obtained

$$D_v = \frac{1000rRT}{c}\left(1 + \frac{\partial \ln\gamma}{\partial \ln m}\right)\left[-\frac{Z_1Z_2}{r_1r_2}\,\frac{L_{11}L_{22} - L_{12}L_{21}}{\alpha}\right] \qquad (2.63)$$

2.4 Calculation of the Transport Coefficients from Measured Quantities

The mobility coefficients, L_{ik}, are obtained from the measured transport properties by the simultaneous solution of equations (2.44), (2.47), (2.51) and (2.63). The result is

$$\frac{L_{ik}}{N} = \frac{t_i^h t_k^c \Lambda}{10^3 F^2 Z_i Z_k} + \frac{r_1 r_k D_v}{10^3 RTrr_1 Z_1\left(1 + \frac{\partial \ln\gamma}{\partial \ln m}\right)} \qquad (i,k = 1,2) \qquad (2.64)$$

If the ORR are assumed the distinction between t^h and t^c can be omitted. When the physical constants have the units quoted in section (2.3) the units of $\frac{L_{ik}}{N}$ are mol $l.J^{-1}cm^{-1}s^{-1}equiv^{-1}$. The L_{ik} are divided by the equivalent concentration to reduce their concentration dependence and give them a more readily appreciated physical significance, just as the equivalent conductance, as opposed to the specific conductance is chosen for comparisons between electrolytes. As J_i must tend to zero as concentration tends to zero, no matter the values of the forces, all the L_{ik} must tend to zero at zero concentration. However, on division by N, the direct coefficient for any ion will tend to a common non-zero limit no matter the valency type of the electrolyte considered. The cross coefficients will still tend to zero at zero concentration and be more heavily concentration dependent because Z_2 is negative and thus causes the first and second terms on the right hand side of equation (2.64) to partially cancel.

The frictional coefficients are obtained from the L_{ik}/N

calculated from equation (2.64) by direct substitution in equations (2.34) and use of equations (2.29). The results are

$$NR_{11} = \frac{L_{22}}{N} \Big/ \left|\left(\frac{L}{N}\right)\right| \qquad NR_{12} = \frac{-L_{12}}{N} \Big/ \left|\left(\frac{L}{N}\right)\right|$$

$$NR_{21} = \frac{-L_{21}}{N} \Big/ \left|\left(\frac{L}{N}\right)\right| \qquad NR_{22} = \frac{L_{11}}{N} \Big/ \left|\left(\frac{L}{N}\right)\right|$$

where $$\left|\left(\frac{L}{N}\right)\right| = \frac{L_{11}}{N}\,\frac{L_{22}}{N} - \frac{L_{12}L_{21}}{N^2} \qquad (2.65)$$

Substituting in equations (2.29) from (2.64) gives

$$\begin{aligned} C_oR_{10} &= -(r_1NR_{11} + r_2NR_{12})\,Z \\ C_oR_{20} &= -(r_1NR_{12} + r_2NR_{22})\,Z \\ \frac{R_{oo}}{N} &= -(r_1C_oR_{10} + r_2C_oR_{20})\,\frac{C_o^2}{Z} \end{aligned} \qquad (2.66)$$

where Z is the number of equivalents per mole of solute and C_o is the solvent concentration, given by

$$C_o = \frac{1000}{mM_o}\,C \qquad (2.67)$$

where M_o is the molecular weight of the solvent. As for the L_{ik}, the R_{ik} are multiplied by the appropriate concentration to give them a physically more realistic interpretation. The units of these frictional coefficients are J cm s equiv $mol^{-2}l^{-1}$.

2.5 The Influence of Ion Association

The principal object of study in this thesis is ion-association and complex formation in aqueous binary electrolyte solutions and it seems prudent, therefore, to confirm that the thermodynamic analysis outlined above applies to such systems. Consider

the case of the binary electrolyte $C_{r_1}A_{r_2}$ which dissociates formally as represented in equation (2.36), but where complexes between cation and anion of the form $CA_i^{Z_1 + iZ_2}$ are formed in a stepwise manner.

$$\begin{aligned} C^{Z_1} + A^{Z_2} &\rightleftharpoons CA^{Z_1 + Z_2} \\ CA^{Z_1 + Z_2} + A^{Z_2} &\rightleftharpoons CA_2^{Z_1 + Z_2} \\ CA_{n-1}^{Z_1 + (n-1)Z_2} + A^{Z_2} &\rightleftharpoons CA_n^{Z_1 + nZ_2} \end{aligned} \qquad (2.68)$$

Let the electrochemical potentials of cation, anion, and complex species i be $\tilde{\mu}_c$, $\tilde{\mu}_A$ and $\tilde{\mu}_i$ respectively. From equations (2.68) they are seen to be related by

$$\tilde{\mu}_c + i\tilde{\mu}_A = \tilde{\mu}_i \qquad (i = 1, 2 \ldots n) \qquad (2.69)$$

The dissipation function for this system can be written as

$$T\sigma = J_1X_1 + J_2X_2 = j_cx_c + j_Ax_A + \sum_{i=1}^{n} j_ix_i > 0 \qquad (2.70)$$

and the corresponding phenomenological equations as

$$\begin{aligned} J_1 &= L_{11}X_1 + L_{12}X_2 \\ J_2 &= L_{22}X_1 + L_{22}X_2 \end{aligned} \qquad (2.21)$$

and

$$j_i = l_{ic}x_c + l_{iA}x_i + \sum_{k=1}^{n} l_{ik}x_k \qquad (i = c, A, 1, \ldots n) \qquad (2.71)$$

As before J_1 and J_2 are the S.F. flows of cation and anion constituent respectively, X_1 and X_2 are their conjugate forces, and the L_{ik} are mobility coefficients. Similarly j_c, j_A and j_i are the flows of free cation, free anion, and the i th complex respectively, on the SF reference frame. The conjugate forces, x_c, x_A and x_i, are given by the negative gradients of the electrochemical potential of

these discrete species. From equation (2.69) these are seen to be related by equation (2.72)

$$x_1 = x_c + ix_A \quad (i = 1, \ldots n) \tag{2.72}$$

It is required to show that equations (2.71) can be reduced to the form of equations (2.21). Firstly it is noted that the total free energy of the solution can be expressed as the sum of the free energies of each of its components. This gives equation (2.73)

$$C_{12}\mu_{12} = C_c\tilde{\mu_c} + C_A\tilde{\mu}_A + \sum_{i=1}^{n} C_i\tilde{\mu}_i \quad i = 1, 2 \ldots n \tag{2.73}$$

Substituting for μ_i in equation (2.73) from equation (2.69) gives equation (2.74)

$$C_{12}\mu_{12} = \mu_c(C_c + \sum_{i=1}^{n} C_i) + \mu_A (C_A + \sum_{i=1}^{n} iC_i) \tag{2.74}$$

From the stoichiometry of equations (2.68) it is obvious that

$$\begin{aligned} r_1 &= \frac{1}{C_{12}} \cdot (C_c + \sum_{i=1}^{n} C_i) \\ r_2 &= \frac{1}{C_{12}} \cdot (C_A + \sum_{i=1}^{n} iC_i) \end{aligned} \tag{2.75}$$

When equations (2.75) are substituted in equation (2.74) the result is seen to be identical to equation (2.37). This proves that equation (2.37) is valid for any electrolyte in which ion association is present when the chemical potentials on the right hand side of the equation are taken to be those of the free cations and anions. It also shows that in equations (2.21) and (2.71) X_1 can be identified as equivalent to x_c and X_2 as equivalent to x_A.

The stoichiometry of equations (2.68) also gives equations (2.76)

$$J_1 = j_c + \sum_{i=1}^{n} j_i$$
$$J_2 = j_A + \sum_{i=1}^{n} i j_i \qquad (2.76)$$

Substituting equations (2.76) and (2.72) in equations (2.71), and collecting terms in x_c and x_A gives equations (2.77) which are seen to be identical to equations (2.21)

$$J_1 = BX_1 + DX_2$$
$$J_2 = EX_1 + FX_2 \qquad (2.77)$$

where

$$B \equiv L_{11} = l_{cc} + \sum_{i=1}^{n} (l_{ii} + l_{ic} + l_{ci}) + \sum_{\substack{i=1 \\ i\neq k}}^{n} \sum_{k=1}^{n} l_{ik}$$

$$D \equiv L_{12} = l_{cA} + \sum_{i=1}^{n} l_{iA} + i(l_{ii} + l_{ci}) + \sum_{\substack{i=1 \\ i\neq k}}^{n} \sum_{k=1}^{n} k l_{ik}$$

$$E \equiv L_{21} = l_{Ac} + \sum_{i=1}^{n} l_{Ai} + i(l_{ii} + l_{ic}) + \sum_{\substack{i=1 \\ i\neq k}}^{n} \sum_{k=1}^{n} i l_{ik}$$

$$F \equiv L_{22} = l_{AA} + \sum_{i=1}^{n} \left[i(l_{Ai} + l_{iA}) + i^2 l_{ii} \right] + \sum_{\substack{i=1 \\ i\neq k}}^{n} \sum_{k=1}^{n} i.k.l_{ik}$$

Thus the derivations given in sections (2.3) and (2.4) can be seen to be valid for systems where complexing or ion association are present.

Chapter 3

Preparation and Characterisation of Aqueous Solutions of Zinc Salts

3.1 Preparation of the Stock Solutions

Solutions of zinc chloride, zinc nitrate and zinc perchlorate were prepared and investigated. The preparation of each solution will be described in turn. In all cases high grade distilled water, suitable for electrical conductivity measurements, was used for preparing stock solutions. All solutions were filtered through a millipore filter before use. This filter contains a small amount of detergent to facilitate flow through it, and this was removed in each case by pre-washing with at least 1 litre of distilled water.

3.1.1 Zinc Nitrate This salt is available in high purity from several chemical manufacturers; we obtained our supplies from Merck and Co. Ltd. The salt was supplied as a mixed hydrate, making it impossible to prepare accurate solutions by weight.

A sample of this material was recrystallised from water by cooling a saturated solution from room temperature to $0^{\circ}C$ and collecting the resulting crystals. The concentration and conductance of a solution of those crystals in water was measured and compared with values obtained for solutions prepared from the original material. The agreement was within the estimated experimental error of $\pm$ 0.05%, and therefore all subsequent solutions were prepared from the original sample.

3.1.2 Zinc Perchlorate Zinc Perchlorate is also commercially available in high purity, but it is expensive and obtainable only from American suppliers. It was found to be simpler, quicker, and cheaper to prepare this salt in the laboratory by adding excess spectroscopically pure zinc oxide (Koch Light) to Analar perchloric acid (B.D.H.) and filtering off the unreacted zinc oxide. The solution prepared in this way gave a slight milky precipitate on dilution, probably due to excess dissolved zinc oxide. A sample of zinc perchlorate was recrystallised from this solution by the method described above. The crystals obtained were also found to give a slight precipitate when used to make very dilute solutions. The original solution was then made slightly acid (approximately pH 2) by the addition of a few drops of perchloric acid and another sample recrystallised. Care was taken to remove as much of the mother liquor as possible from the crystals to ensure that no excess acid was carried forward. These crystals gave clear solutions at all dilutions and this method of recrystallisation was therefore adopted for the preparation of the experimental material.

3.1.3 Zinc Chloride The preparation of exactly stoichiometric solutions of zinc chloride presents great practical difficulties, mainly occasioned by the fact that, because of its enormous solubility in water and other common solvents, zinc chloride is virtually impossible to recrystallise, even from highly acid solutions. Zinc chloride of claimed high purity is readily available commercially, but in all cases it was found to contain excess zinc which is precipitated as the insoluble oxychloride when the clear concentrated solutions formed by commercial zinc chloride are diluted.

3.1.3.1 Methods of Preparation described in the Literature:

A fair amount of work has been done on zinc chloride and several methods of preparation are described in the literature[20-24]. Hamilton and Butler[20] passed dry hydrogen chloride gas through dry ether covering zinc metal. Zinc chloride was formed and dissolved in the ether. When solution of the metal was complete the ether was evaporated under vacuum and the product gently warmed to remove the last traces of ether. The zinc chloride formed was claimed to give clear dilute solutions. The method does not, however, seem suited to the preparation of large quantities of zinc chloride, and was consequently not investigated any further. A similar method was used by Lunden[21]. He passed dry chlorine gas over strongly heated zinc metal and obtained zinc chloride. Again this method does not seem suited to the preparation of large quantities of material, and, since Lunden was working with molten salts, no evidence exists as to whether or not his material would give clear solutions.

Most workers have prepared their zinc chloride by adding hydrochloric acid to zinc oxide or commercial zinc chloride. Scatchard and Tefft[22] simply added excess zinc oxide to hydrochloric acid and corrected their results for the presence of excess zinc (they were measuring the emf of cells of the type Zn/Hg $ZnCl_2$ Ag/AgCl). Harris and Parton[24] and Robinson and Stokes[23], each analysed commercial zinc chloride for zinc and chloride content, and added a calculated amount of hydrochloric acid to the solution to neutralise the excess zinc oxide. Robinson and Stokes were not, however, satisfied with this solution and prepared another batch by adding just enough hydrochloric

acid to a solution of commercial zinc chloride to avoid precipitation of oxychloride on dilution. This solution they estimated to contain zinc and chloride in the ratio of 1.0055:2.

3.1.3.2 Selection of a Method of Preparation: Several methods of preparing zinc chloride were tested in this work. The obvious starting point was to try the direct addition of zinc oxide to hydrochloric acid in the quantities required for direct neutralisation. Spectroscopically pure zinc oxide was dried by roasting in an oven at 900°C for 24 hours and stored in a vacuum dessicator over phosphorous pentoxide to give a moisture free product which could be weighed as ZnO. Analar concentrated hydrochloric acid was diluted with an equal volume of distilled water, and the concentration of this acid determined by measuring the electrical conductivity of diluted samples of the solution, using the published data of Stokes[25]. The calculated weight of dried zinc oxide was then added to a weighed amount of hydrochloric acid (calculated from the published density data[26]) and the solution left aside for a few days for reaction to take place.

The resulting solution was clear with no trace of oxide remaining, but had a pH = 2.5, indicating that excess acid was present. As the solution was approximately 2.5 molar in zinc this corresponds to an error of only 0.06% in the quantity of acid added. The amount of zinc oxide required to neutralise the remaining acid was calculated and added to the solution. This dissolved completely to give a solution whose zinc to chloride ratio was 1:2 within the estimated experimental error of $\pm$.07%. This solution, which was approximately 2.5 molar, had a pH of four. Unfortunately a faint

precipitate of zinc oxychloride was formed on extreme dilution, indicating a slight excess of zinc in the solution. Similar results were obtained when the preparation was repeated.

Thus the "stoichiometric" method of preparing zinc chloride was found to be unsatisfactory because a very small error in the preparation caused excessive pH variations. The next method to be tried was the technique of Robinson and Stokes of adding small quantities of acid to these solutions until no precipitate is formed on dilution. This was done for three separate solutions, hydrochloric acid being added dropwise from a fine Pasteur pipette. In each case the pH of the final solution was around four, and the stoichiometric ratio was 1:2 within experimental error.

The most sensitive test of whether or not these three solutions were identical was considered to be the identity or otherwise of their electrical conductivities at the same concentration. This property should be extremely sensitive to the presence of even a slight excess of acid in solution owing to the exceptionally high mobility of hydrogen ions in aqueous solution. Therefore the specific conductances of several dilutions of each of the solutions A, B and C were measured in the concentration range 0.3 to 0.7 molar. The results were compared graphically as shown in Fig. 3.1, where the points from the three different solutions are shown labelled, along with the best line through the points, obtained by a computer executed least squares curve-fit. It can be seen that the points all lie very close to the line, and the computer calculation indicates that the standard deviation of the points from the line is approximately

0.05%, which corresponds to the expected accuracy of measurement of the concentration of the test solutions. Thus the solutions have been shown to be identical within experimental error.

The above method was adopted for the preparation of all subsequent solutions, with the minor alteration that in some cases extra acid was added to solutions of commercially obtained zinc chloride. The results shown in Fig. 3.1 were taken as standards, and the solutions being prepared were adjusted for zinc or chloride content until the specific conductances of diluted samples fell on the curve fit line within experimental error.

Another method of preparation tried, and subsequently rejected, deserves a brief mention. The idea was to form zinc chloride in solution by the displacement of copper ions from cupric chloride solution by addition of zinc shot. The reaction was tried, and found to proceed vigorously to give a colourless solution above a dense white precipitate which was not positively identified, but probably consisted of a mixture of zinc oxide and zinc oxychloride. Cuprous chloride could also have been present, as the conditions in the reaction flask, viz a boiling, acidic solution of cupric chloride in the presence of copper, were ideal for its formation. The solution was filtered and left for a few hours over zinc shot to ensure that any cuprous ions in solution were reacted. The resulting solution was perfectly clear and had a zinc to chloride ratio of 1:2 within experimental error; but it gave a white precipitate on dilution. The electrical conductance of the solution was measured and found to be significantly below the standard curve, implying the

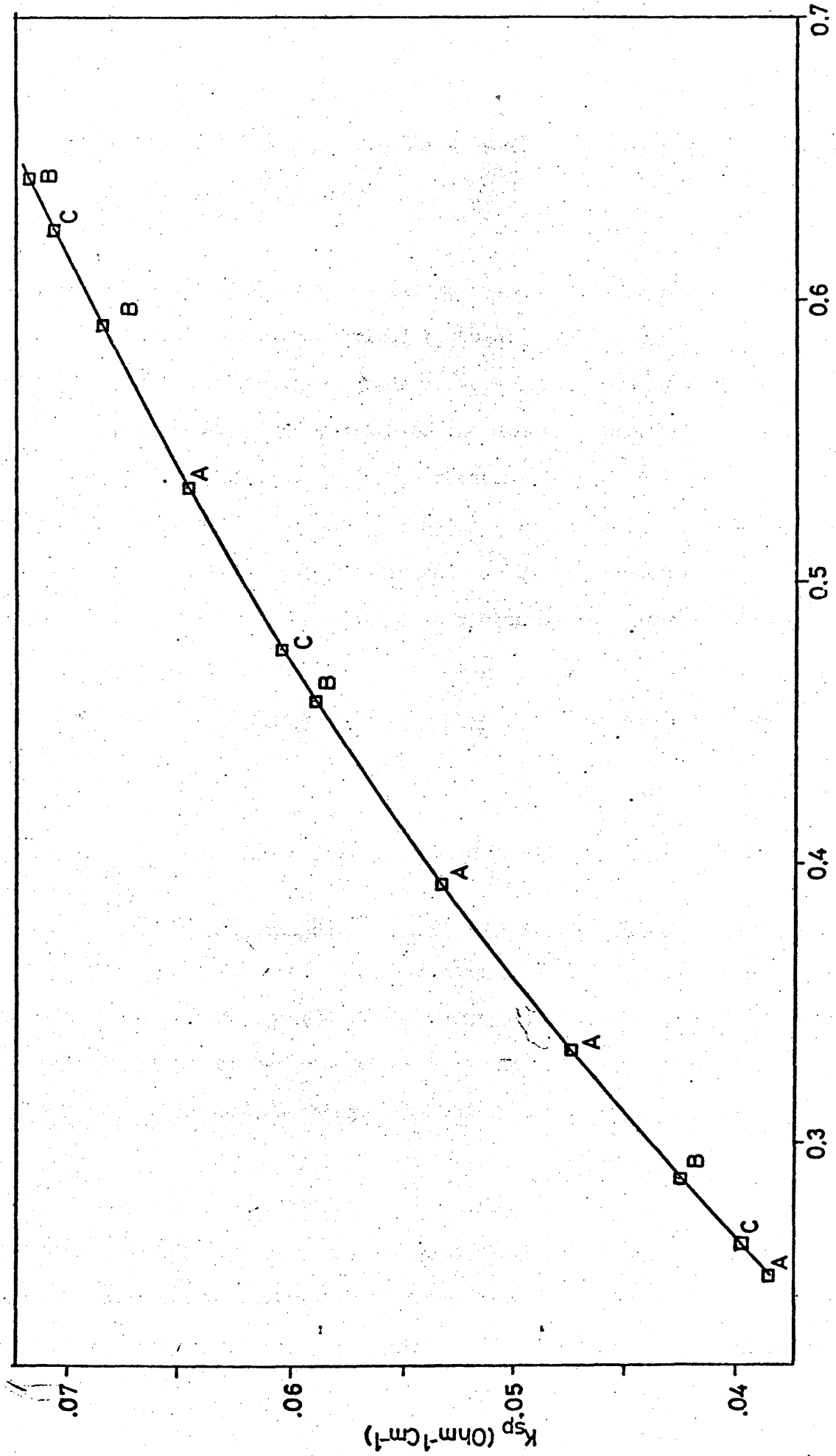

Fig 3.1

presence of excess zinc. Therefore this method gives similar results to the direct addition of zinc oxide to hydrochloric acid, and was pursued no further.

3.2 Analytical Methods All the methods used were standard volumetric techniques described by Vogel. All items of volumetric glassware used were pyrex grade A, and were all calibrated as described in Vogel[27a] by weighing the amount of distilled water they delivered or contained. The correction factors were all found to be within grade A limits, but were nevertheless always applied. Volume measurement errors were further reduced by carrying out all volumetric operations in a room maintained at a constant temperature of 25°C ± 1°C. The reproducibility of duplicate calibrations was ± 0.05%. Most of the analyses for zinc were made by standard E.D.T.A. titration, although a few were carried out potentiometrically using potassium ferrocyanide as reagent. The chloride estimations were all made using a potentiometric titration with silver nitrate as reagent.

3.2.1 Estimation of the End Point of a Potentiometric Titration: This was done using the linear plot method of Gran[28,29], by which the titration curve of emf (or pH) plotted against volume of titrant added can be transformed by a numerical manipulation into straight lines intersecting at the equivalence point. The derivation of the function to be plotted against titre to give a straight line is straightforward but rather lengthy, and therefore only the relevant result is quoted here. It was also found that in the systems used accurate, stable, potential readings were more conveniently obtained after the equivalence point, and therefore only one line was plotted.

The appropriate Gran function is given by :-

$$F = (V_o + V) \text{ antilog}_{10} \; 17 \; (k - E) \qquad (3.1)$$

where V_o is the initial sample volume, V is the titre, E is the corresponding potential reading (E is taken always as +ve), and k is an arbitary constant greater than the largest value of E obtained after the equivalence point. A plot of F against titre should give a straight line which when extrapolated to F = 0 gives the titre corresponding to the equivalence point of the titration. In all experiments V_o was kept much larger than the titre, V, and therefore the factor $(V_o + V)$ remained approximately constant throughout the titration and could be omitted.

3.2.2 Estimation of zinc by EDTA titration E.D.T.A. solutions were prepared by dissolving a weighed quantity of Analar disodium dihydrogen ethanediaminetetraacetate in distilled water in a graduated flask, and standardised by titration with a solution of known zinc content. This standard zinc solution was prepared by dissolving a weighed spectroscopically pure zinc rod in excess hydrochloric acid and diluting to the mark in a graduated flask. The solutions to be titrated were diluted to 200 mls with distilled water and buffered to pH 10 with an ammonium chloride/ammonium hydrochloride buffer. The indicator used was eriochrome black T. Duplicate analyses normally agreed to better than 0.07% and were rejected if they did not.

The maximum useful concentration of E.D.T.A. solution that can be prepared is about 0.15 molar, which means that for the more concentrated zinc solutions studied the sample volumes required to

give reasonable titres were rather small. For these solutions it was judged to be more accurate to weigh out the sample and use the accurate density data being obtained at the same time to give the volume. This procedure was also followed in the analysis of Hittorf transport number experiments where the number of moles of solute associated with a fixed weight of solvent was required. The concentration of a solution estimated in this was expressed in units of moles/Kg. (mmoles/g) and converted to a molarity by multiplication by the solution density; obtained from a least squares curve fit polynomial of density as a function of concentration in units of moles/Kg.

3.2.3 Estimation of zinc content by Potentiometric Titration[27c]

Potassium ferrocyanide and zinc ions react to give a sparingly soluble precipitate of potassium zinc ferrocyanide.

$$3\ Zn^{2+} + 2K_4Fe(CN)_6 \rightleftharpoons K_2Zn_3\left[Fe(CN)_6\right]_2 + 6K^+$$

The reaction can be followed potentiometrically if a little potassium ferricyanide is present to form a redox couple with the ferrocyanide. Zinc ferricyanide is more soluble than the ferrocyanide, and is not, therefore, precipitated under the reaction conditions. Thus the concentration of ferricyanide ion remains fairly constant throughout the titration whereas that of the ferrocyanide ion rises sharply at the end point, giving a correspondingly rapid rise in the reduction potential sensed by a platinum electrode placed in the reaction flask.

A diagram of the experimental apparatus is shown in Fig. 3.2.

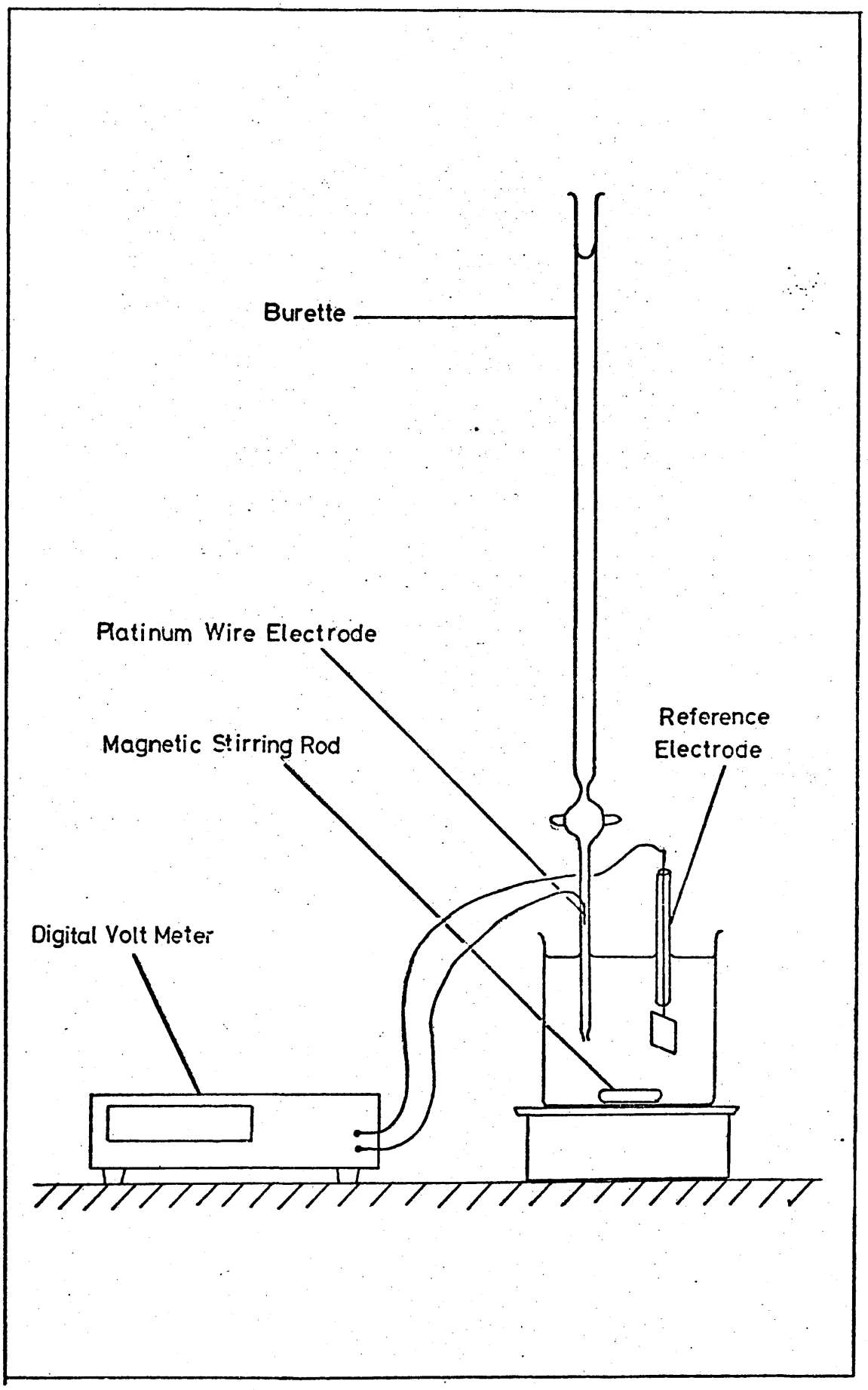

Fig 3.2

Apparatus for Potentiometric Titrations

The titrant, potassium ferrocyanide solution containing a trace of ferricyanide, was contained in a 25 ml grade A burette which had a platinum wire sealed into its tip below the stopcock. The tip of the burette dipped into the titrand, which consisted of a zinc solution sample acidified with 50 ml of 4N sulphuric acid, diluted to 200 ml with distilled water, and treated with 1 gm of ammonium sulphate. The solution was stirred by a magnetic stirrer and had a bright platinum electrode dipping into it. The two platinum electrodes were connected to a Solatron LM 1867 Digital Voltmeter which read the emf of the cell directly.

The titration was carried out by running the ferrocyanide solution fairly rapidly from the burette until a rise in the rate of change of the digital voltmeter reading showed that the end point was near. The zinc sample was chosen so that this happened after approximately 20 ml of ferrocyanide solution had been added. After thorough mixing of the solution the stirring was stopped and the system left for a few minutes until a steady reading was obtained on the voltmeter. This potential, along with the corresponding burette reading, was noted, and the procedure repeated about 10 times until the last 5 ml or so of reagent had been added. The end point of the titration was then determined by a Gran plot. A typical plot for the titration of potassium ferrocyanide and a zinc standard solution is shown in Fig. 3.3. Duplicate analyses were found to agree within $\pm$ 0.05%.

3.2.4 Choice of Method for Routine Analysis of Zinc Both methods of analysis gave accurate, reproducible, results, which were consistent

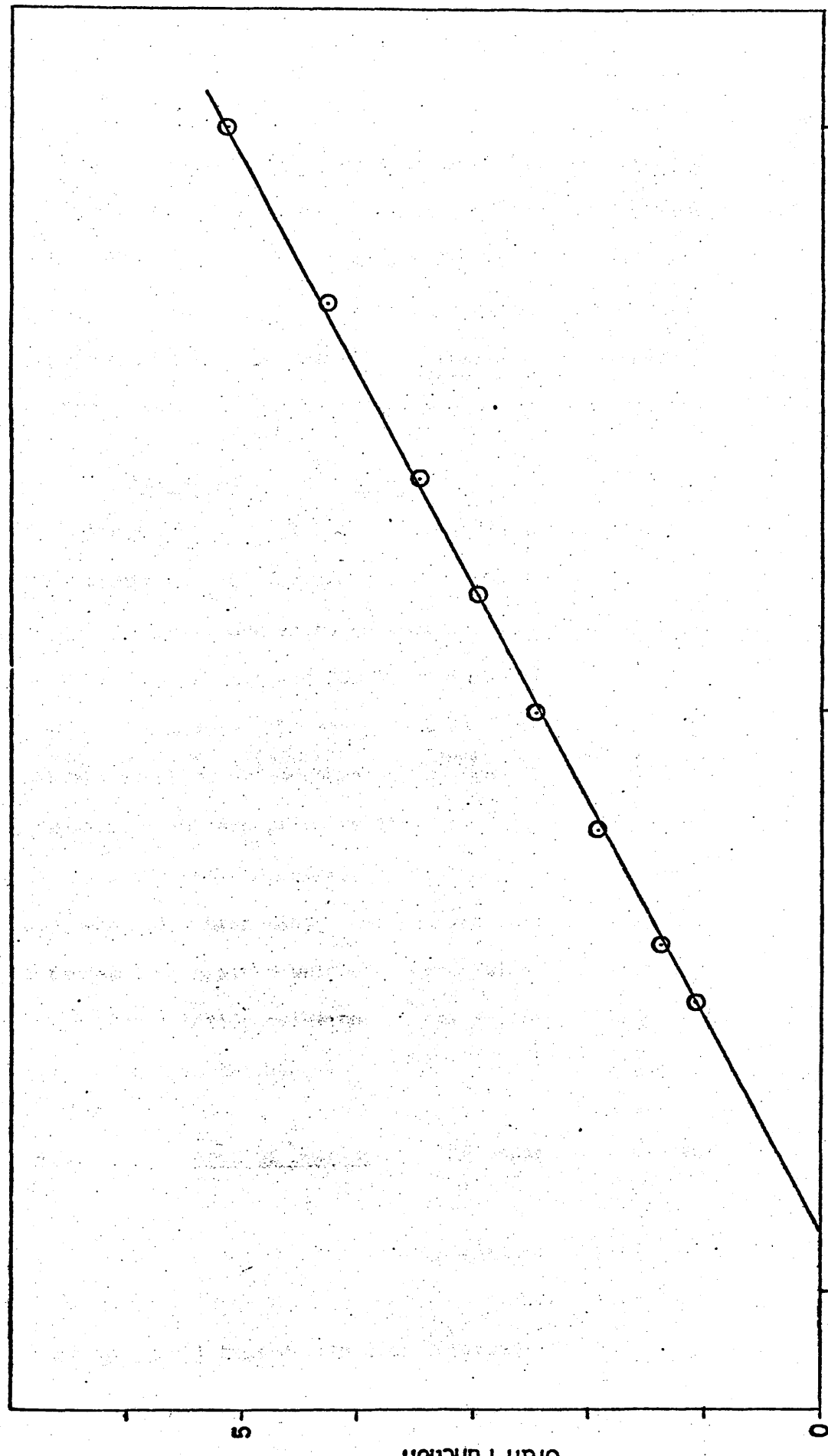

Fig 3.3

with one another well within experimental error. Most of the routine analyses were done by means of E.D.T.A. titrations as a matter of convenience. In cases where the concentration had to be determined with the highest possible accuracy, e.g. in the analysis of Hittorf experiments or the measurement of electrical conductance, titrations were performed in triplicate, and the results rechecked if they deviated from the mean by more than 0.05%.

3.2.5 Estimation of Chloride Content[27d] This was done by potentiometric titration of the sample with silver nitrate solution. The apparatus used was identical to that shown in Fig. 3.2 except that the platinum electrodes were replaced with silver. The chloride solution was diluted to 200 ml with distilled water and titrated as described above. The system formed a concentration cell with the liquid junction at the burette tip, and the emf of this cell fell rapidly at the end point as the concentration of silver ions in the titration vessel increased. The end point was determined as above by means of a Gran plot. The silver nitrate solutions were standardised against weighed amounts of dried, thrice recrystallised potassium chloride solutions. The reproducibility of the results was $\pm$ 0.07% as before.

3.3 Measurement of Density The density of the test solutions as a function of concentration was required in order to allow conversions to be made between the various concentration units used. Five pyknometers, each with a capacity of approximately 30 ml, were used, each being calibrated with distilled water.

The pyknometer was weighed clean and dry, filled with cool

distilled water, and suspended for a few hours in a water bath whose temperature was maintained at 25°C ± .005, until thermal equilibrium had been obtained. The pyknometer was then removed, rinsed with cold water to contract the contents, dried by rinsing with Analar acetone, and reweighed. The weight of the contents was corrected to vacuum[27e] and used to calculate the volume of the pyknometer from the known density of water. Unknown solutions were treated in the same way to determine the weight of solution contained by the pyknometer, and hence the density of the solution relative to water at 4°C. Duplicate measurements or calibrations agreed to ± .02%.

The results are given in table 3.1 as values of the density at round number molarities. These were calculated from least squares curve fit expressions of density v molarity which reproduced the experimental data within the expected experimental uncertainty of ± 0.05%. The major part of this uncertainty arose from the measurement of concentration. All the curve fit expressions are polynomials of the form of equation (3.2)

$$y = \sum_{i=o}^{n} a_i x^i \qquad (3.2)$$

The coefficients, a_i, for the three salts are given in table (3.2).

3.4 Measurement of Electrical Conductance The electrical conductance of an electrolyte solution represents one of the transport properties required for a complete irreversible thermodynamic analysis. In the case of zinc chloride it was also used as a measure of the reproducibility of different batches of solution. The methods of measuring conductance have been reviewed by several authors[30,31,32], and require no general description here. The techniques and apparatus

Table 3.1 Density of Zinc Salt Solution

Molarity	Density Kg l^{-1}		
	Zinc Chloride	Zinc Perchlorate	Zinc Nitrate
0	.99707	.99707	.99707
0.1	1.0099	1.0172	1.0124
0.2	1.0214	1.0369	1.0276
0.3	1.0328	1.0566	1.0428
0.4	1.0441	1.0762	1.0579
0.5	1.0552	1.0958	1.0730
0.6	1.0662	1.1154	1.0880
0.7	1.0771	1.1349	1.0300
0.8	1.0879	1.1543	1.1179
0.9	1.0985	1.1737	1.1328
1.0	1.1091	1.1931	1.1474
1.2	1.1298	1.2317	1.1771
1.4	1.1502	1.2701	1.2064
1.6	1.1702	1.3083	1.2355
1.8	1.1900	1.3464	1.2644
2.0	1.2094	1.3844	1.2930
2.5	1.2571	1.4785	1.3638
3.0	1.3038	1.5718	1.4332
3.5	1.3503	-	1.5014
4.0	1.3971	-	1.5682

Table 3.2 Coefficient of Least Squares Curve fit of Density v Molarity

	a_0	a_1	a_2	a_3
Zinc Chloride	.998163	.117757	-.0076324	.0007811
Zinc Perchlorate	.997401	.198624	-.0024274	.00007893
Zinc Nitrate	.997037	.153368	-.00275389	.00002544

used in this work were basically these described by Jalota[33,34] in an earlier thesis produced in this department.

3.4.1 Conductance Cells The conductance cells, a typical example of which is shown in Fig. 3.4, followed closely the design of Jones and Bollinger[35]. The filling and contact tubes were kept as far apart as possible to reduce the capacitance between them, and the shunt effect which this causes. The filling tubes incorporated bulbs which facilitated rinsing and filling the cells, and also allowed mixing of the contents during measurements to eliminate any concentration changes caused by adsorption on the electrodes or the Soret effect[25,36]. The electrodes were circular pieces of platinum, 16 mm in diameter, and were connected to the contact tube by a platinum wire sealed into the glass of the cell and further sealed with araldite on the side remote from the solution. The contact tubes were filled with mercury into which dipped the copper rods used to make contact with the leads of the conductivity bridge. Four cells, each with a different cell constant, were available, the cell constant being varied by changing lengths and diameters of the central portions of the cells.

3.4.2 Platinisation of the cell electrodes This was done to minimise the effect of polarisation at the electrodes. The platinising solution was .025 M hydrochloric acid containing 0.3% platinum chloride and 0.025% lead acetate[37]. Six culombs of electricity per cm^2 of electrode area were passed using a constant current of 10 mA cm^{-2} provided by a Solartron P.S.U. AS1413 current source. The polarity of the electrodes was reversed every ten seconds by an electronic

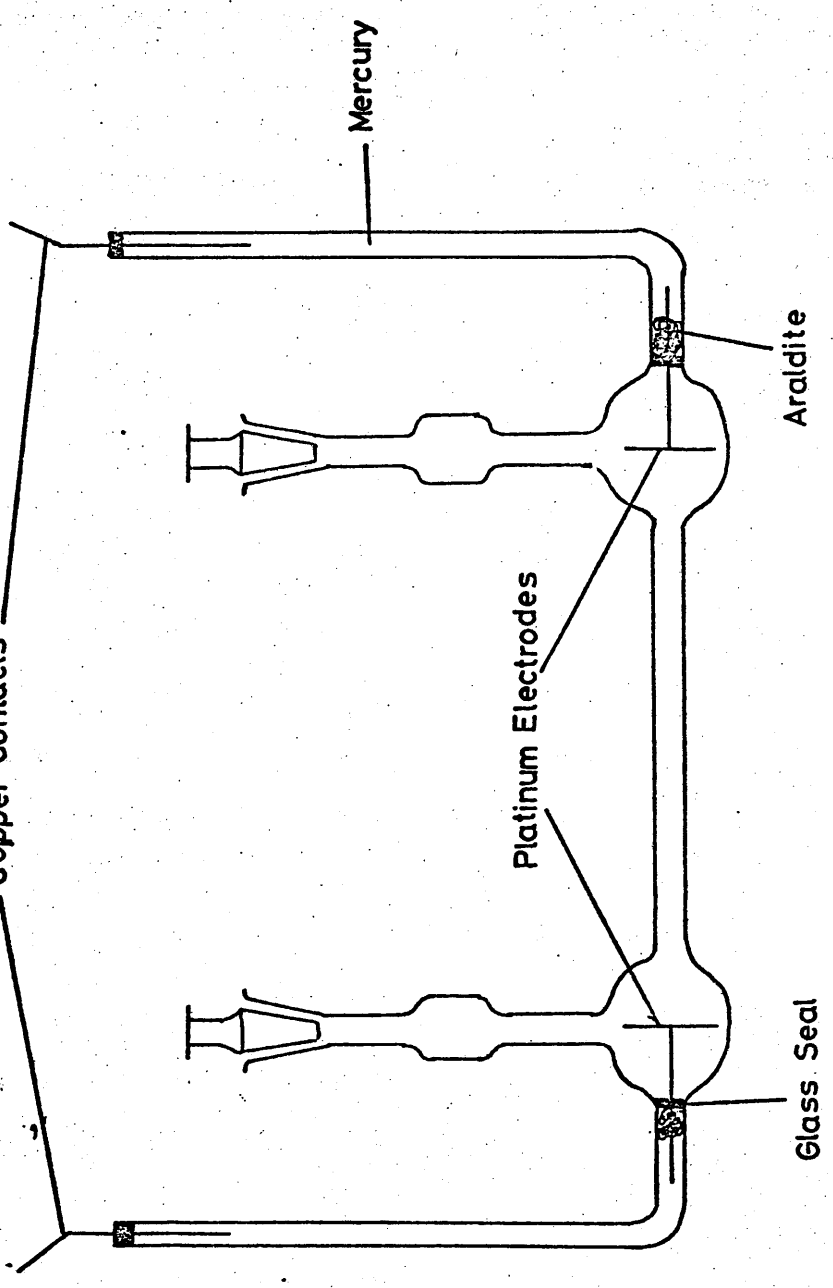

Conductivity Cell

Fig 3.4

switching device. After platinising the cells were well rinsed with distilled water and were always stored in it. The electrodes were replated from time to time, especially after a period of heavy use.

3.4.3 Temperature Control As the temperature coefficient of conductance is very high, amounting to some 2% of the total value for a $1^{o}C$ temperature change, precise temperature control is essential before accurate results can be obtained. Thermostatting was effected by immersing the conductivity cells in a bath of light mineral oil whose temperature was controlled by a mercury toluene coiled glass thermo-regulator. The bath was cooled by a coil through which passed cold water and heated by a 60 watt light bulb immersed in the oil and switched on and off by the regulator. The bath oil was vigorously stirred by an electric stirrer. Temperature was measured by an E. Mil standard thermometer, model K1 4047, calibrated to N.P.L. standards. By adjusting the rates of heating, cooling, and stirring the temperature of the bath was maintained constant at $25^{o}C$ and temperature variations were kept within $\pm$ .002^{o}C. A similar system was used for temperature control in all other transport experiments.

3.4.4 Conductivity Bridge Conductance measurements were made using a Wayne Kerr digital autobalance precision bridge, type B-331. This instrument displayed capacitance and conductance simultaneously on two meters and six digital decades, three for each property, and allowed an accuracy of 0.01% to be obtained. A "Lead eliminator" circuit was incorporated to eliminate completely any error caused by the finite resistance of the connecting leads. Measurements were made at an AC frequency of 1591.55 Hz.

3.4.5 Calibration of Conductance Cells The cells were calibrated after platinising by measuring the conductivity of 1.0, 0.1, and 0.01 demal solutions of potassium chloride. Demal solutions were introduced for this purpose by Jones and Bradshaw[38], and are defined in terms of a weight of solute (KCl) in one kilogram of solution, and are therefore independent of the atomic weight scales or volume definitions currently in fashion. The weights of potassium chloride required to prepare each of these three standards are given in table 3.3.

Table 3.3

Conc.	W. of KCl (vac)	W. of Sol. (vac)	κ(ohm^{-1} cm^{-1})
1.00 D	7.11352	100 g	.111342
0.10 D	.741913	100 g	.0128560
0.01 D	.0745263	100 g	.0014087

N.B. all weights are weights in vacuo

3.4.6 Preparation of Demal Solutions Potassium chloride for preparing the calibrating solutions was purified by recrystallising twice from distilled water, drying in an air oven at 130°C, grinding in an agate mortar, and redrying. The salt was stored over silica gel in a vacuum dessicator. Approximately seven grams of this salt was accurately weighed in a clean, dry, stoppered flask, and the weight corrected to vacuum[27e]. From this weight, and the information in table 3, the weight of solution required in vacuum was calculated

and corrected for air bouyancy. Distilled water of low conductivity (specific conductance less than 1 x 10^{-6} $Ohm^{-1}cm^{-1}$ without degassing) was added until this weight was attained exactly. 0.1 and 0.01 demal solutions were prepared by weight dilution of this solution, again with the application of vacuum corrections. Two sets of calibrating solutions were prepared, enabling the cells to be calibrated twice with solutions of the same concentration.

Three conductance cells, originally constructed by Jalota, were used in the present work. Two, each having cell constants of around 90 cm^{-1}, were used for the more concentrated solutions, and were calibrated with 1.0 and 0.1 demal KCl, while the third, with a cell constant of around 35 cm^{-1}, was used for the dilute solutions, and calibrated with 0.1 and 0.01 demal KCl.

3.4.7 Measurement of Conductance The cell to be calibrated was rinsed three times with 10 ml samples of the calibrating solution before being filled and immersed in the oil bath. It was left for approximately $\frac{1}{2}$ hour to allow temperature equilibration to take place and its conductance then measured every four minutes until the reading became constant. The solution in the cell was mixed to ensure uniform concentration and the conductance remeasured. No change in the conductance was observed showing that polarisation effects were absent.

The specific conductance of the water used to prepare the solutions was measured, using the approximate cell constant available, and added to the known specific conductances of the calibrating solutions. The cell constant was then calculated using the relation :-

$$k L_c = \kappa \qquad (3.3)$$

where k is the cell constant, L_c is the observed conductance and κ is the total specific conductance of the solution. The measured cell constants were all reproducible within ± .02%.

3.4.8 Measurement of conductance of zinc salts solutions Specific conductance was measured as a function of concentration for all three zinc salts. The conductance measurements were carried out as described for the calibration and the specific conductance calculated from equation (3.3). From this value the specific conductance of the water used in preparing and/or diluting the stock solutions was subtracted to give the experimental specific conductance due to the salt. A few of the more dilute solutions were swept clear of dissolved air and carbon dioxide with nitrogen, but since this was found to have no significant effect the practice was discontinued.

Since the specific conductance was to be measured to within ± .02%, every attempt was made to approach this accuracy in the measurement of concentration. The concentration of a concentrated stock solution was determined by titrating several times with E.D.T.A. solution. Several weight dilutions of this stock were prepared, and their concentrations checked by titration with E.D.T.A. The agreement was generally better than 0.05%, and if not the solution was rejected. The conductance of each solution was then measured.

3.4.9 Results The specific conductance, and the equivalent conductance, were obtained over the concentration range .03 M (.1 Normal) to 4 Molar for zinc chloride and zinc nitrate, and over the range

Table 3.4 Conductance of Solutions

Concentration	Zinc Chloride		Zinc Perchlorate		Zinc Nitrate	
mol l^{-1}	κ	Λ	κ	Λ	κ	Λ
0.0	0.0	129.15	0.0	120.16	0.0	124.26
0.1	17.861	89.307	17.514	87.571	17.705	88.525
0.2	32.122	80.431	32.662	81.654	32.296	80.740
0.3	43.996	73.327	46.589	77.648	45.450	75.750
0.4	54.217	67.771	59.615	74.519	57.593	71.991
0.5	62.558	62.559	71.664	71.664	68.608	68.608
0.6	69.469	57.891	82.784	68.989	78.630	65.525
0.7	75.201	53.715	93.028	66.449	87.838	52.741
0.8	79.970	49.981	102.446	64.029	96.237	60.148
0.9	83.954	46.641	111.113	61.729	103.856	57.698
1.0	87.338	43.625	119.048	59.524	110.719	55.360
1.2	92.473	38.571	132.666	55.227	122.272	50.947
1.4	96.537	34.462	143.352	51.197	131.094	46.819
1.6	99.673	31.097	151.184	47.244	137.382	42.932
1.8	102.010	28.295	156.259	43.405	141.335	39.260
2.0	103.663	25.912	158.694	39.673	143.213	35.803
2.5	105.460	21.092	154.162	30.832	140.462	28.092
3.0	104.875	17.481	136.676	22.779	129.550	21.592
3.5	102.682	14.669	-	-	113.409	16.201
4.0	99.153	12.426	-	-	94.664	11.833

The units of κ are $10^{3}ohm^{-1}cm^{-1}$ and of Λ are $cm^{2}ohm^{-1}equiv^{-1}$

Table 3.5 Coefficients of Curve Fit Repressions of κ v Molarity

	a_0	a_1	a_2	a_3	a_4	a_5
Zinc Chloride 0.0 - 0.3 M	0.186215	196.4972	-212.0752	146.1963	-	-
Zinc Chloride 0.25 - 1.1 M	2.315346	171.9464	-191.1111	32.0959	-	-
Zinc Chloride 1.0 - 4.7 M	39.73947	70.61746	- 27.37462	4.68844	-0.332509	-
Zinc Perchlorate * 0 - 0.35 M	4.833594	.774400	- .0482702	- .0060896	-.00020910	-
Zinc Perchlorate .3 - 1.0 M	1.061359	168.8805	- 59.80346	8.90389	-	-
Zinc Perchlorate .9 - 3.1 M	5.650279	151.2674	- 37.3532	-1.02225	.506203	-
Zinc Nitrate 0.0 - 0.6 M	.071483	201.1285	-313.3423	751.5797	-1033.401	542.8099
Zinc Nitrate 0.5 - 1.9 M	5.07562	150.4805	-48.95298	4.11555	-	-
Zinc Nitrate 1.9 - 4.7 M	3.34422	156.4210	-54.71261	6.140655	-0.202983	-

* this fit is of ln (κ) v Ln (molarity)

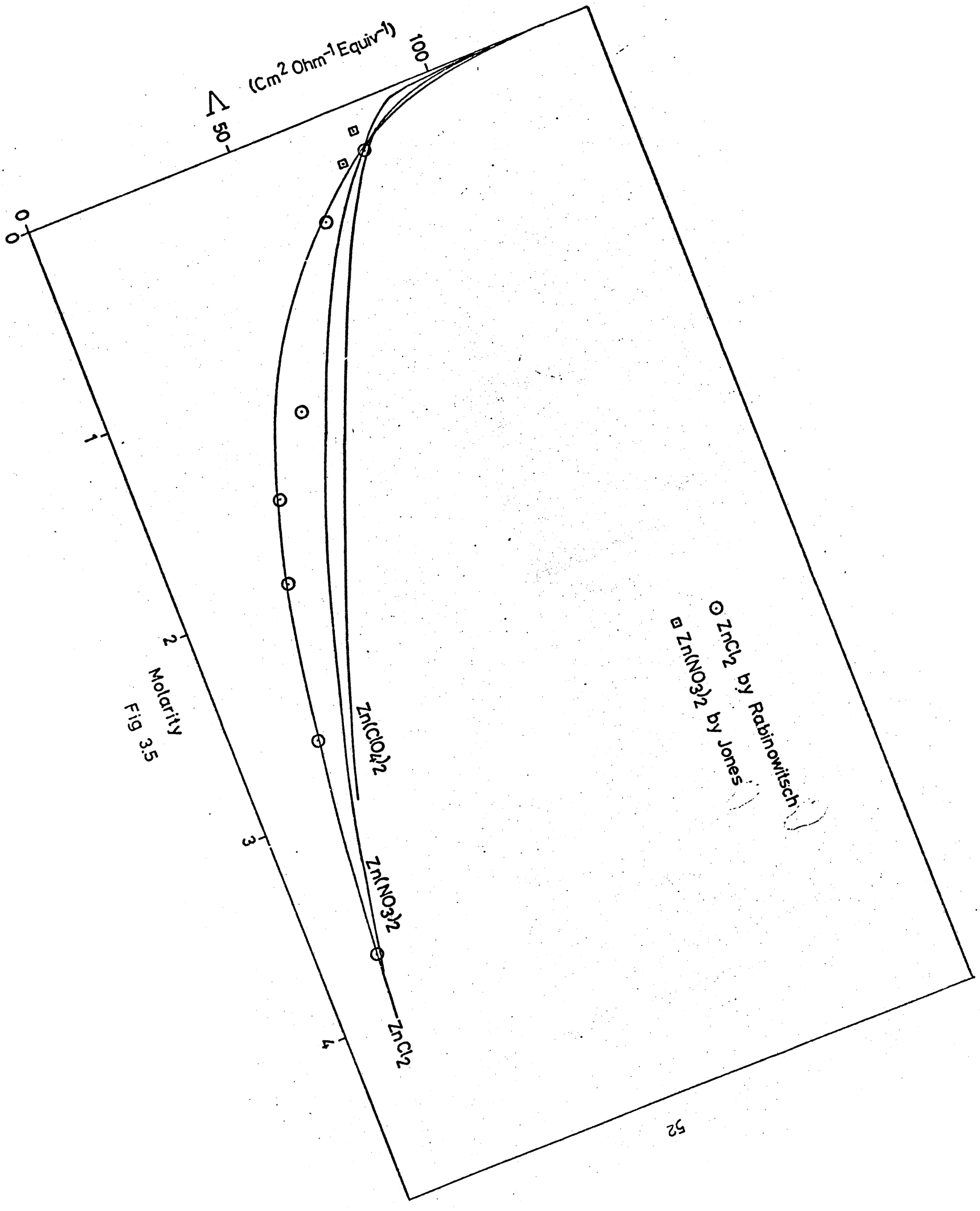
Λ (Cm² Ohm⁻¹ Equiv⁻¹)
0
50
100
0
1
2
3
4
5
Molarity
⊙ ZnCl₂ by Rabinowitsch
▫ Zn(NO₃)₂ by Jones
Zn(ClO₄)₂
Zn(NO₃)₂
ZnCl₂

Fig 3.5

.03 Molar to 3.2 Molar (saturation) for zinc perchlorate. The results are shown at round number molarities in table 3.4 and in table 3.5 the coefficients of the curve fit expressions between specific conductance and molar concentration are given. The results are also shown graphically in Fig. 3.5 as a plot of the equivalent conductance against molarity. Also shown in Fig. 3.5 are the experimental results of Rabinowitsch[39] for zinc chloride and Jones[40] for zinc nitrate. In neither case is the agreement with the present work very good. Jones' results are about 4% lower than the present ones and must be considered seriously in error, whereas Rabinowitsch's results for $ZnCl_2$ are only 1% lower than the present work. Although it is not entirely clear how Rabinowitsch prepared his solutions, it seems likely that the major cause of this discrepancy is an incorrect Zn:Cl ratio in his solutions.

Chapter 4 The Measurement of Diffusion

Several excellent reviews of the measurement of diffusivity are available[41,42,43,44], and therefore only the more important will be mentioned here. The quantity of interest is the diffusion coefficient, D, which is defined by Ficks 1st and 2nd laws :-

$$J = D \left(-\frac{\partial c}{\partial x} \right) \tag{4.1}$$

$$\frac{\partial c}{\partial t} = \frac{\partial}{\partial x} D \left(\frac{\partial c}{\partial x} \right) \tag{4.2}$$

The diffusion coefficient is in general concentration dependent. D, defined above is specific to one concentration, C, and is called the differential diffusion coefficient. All the important methods for measuring the diffusion coefficient depend on a solution of equation (4.2) with suitable boundary conditions. In free diffusion methods one of the conditions is that the concentrations at the extremities of the diffusion cell should remain constant with time, whilst in restricted diffusion methods these concentrations must change with time.

4.1.1 The Diaphragm Cell Method[41,45] Diffusion takes place in a vertical cell divided into two compartments by a porous diaphragm. The lower compartment is filled with the more concentrated solution, and the top with the more dilute. Both compartments are well stirred so that the diffusion process is confined to the diaphragm pores. This has the advantage of reducing the adverse effects of vibration and temperature fluctuation, but does mean that the method cannot be absolute; calibration with a solution of known diffusion coefficient

is required. The method is unsuitable for the study of dilute solutions because of adsorption effects on the large surface area of the diaphragm pores.

4.1.2 The Porous Frit Method[42,46] This is a restricted diffusion method. A porous frit is soaked in solution and suspended from the arm of a balance in a bath of solvent or dilute solution. As diffusion from the frit proceeds the weight of the frit falls. From the change of weight with time a value for the diffusion coefficient of the solution in the frit can be obtained. The method is quick and moderately accurate, and has the advantage of cheapness since no special equipment is required. For these reasons it is most suitable for a rapid but approximate survey of diffusion coefficients.

4.1.3 The Harned Conductimetric Method[41,42,43,47] This is a restricted diffusion method. A concentration gradient is formed in a closed rectangular cell and the concentration changes with time near the ends of the cell are measured by the change in electrical conductivity of the solution by means of electrodes placed at these points. The method is very accurate but requires great care experimentally and is confined to very dilute solutions by problems with the electrodes.

4.1.4 Optical Methods[41,42,43,44] There are a great number of these, most of which have been surveyed by Longsworth[4]. All make use of the fact that for most electrolytes the refractive index of a solution is very nearly a linear function of its concentration. Thus measurement of the refractive index profile of a diffusing system

gives a direct measurement of the concentration profile in that system. The various optical methods differ mainly in the exact optical system used to measure the refractive index profile, and in the choice of free or restricted diffusion as the boundary condition in the solution of equation (4.2). The two most important optical systems are the Rayleigh and the Gouy systems.

4.1.4.1 The Gouy Interference Method[48,49,50] Monochromatic light from a horizontal slit is passed through a vertical cell in which a concentration gradient is present. An interference pattern containing a finite number of lines is produced. The depth of the interference band is dependent on the maximum value of the refractive index between the top and bottom of the cell. The Gouy method is used to study free diffusion. It is capable of high precision, but is not applicable to dilute solutions.

4.1.4.2 The Rayleigh Interference Method[51,52,53,54] Monochromatic light from a point source is split into two beams. One beam is passed through a cell containing a concentration gradient and the other passed through a medium of constant refractive index. The two beams when recombined give a band of interference fringes which form a direct map of the refractive index gradient in the cell. This method is capable of high precision and has been used to study both free[53] and restricted[54] diffusion.

4.2 Choice of Method

The method chosen for this study was Rayleigh interferometry applied to restricted diffusion. Rayleigh interferometry has been

applied by Longsworth[53] to the study of free diffusion, and recently by Chapman and Newman[54] to the study of restricted diffusion. Chapman and Newman showed that this method was capable of giving a well defined differential diffusion coefficient for one concentration to an accuracy of 0.2% from one experiment, and was applicable over a wide range of concentrations. The equipment required was a standard Tiselius electrophoresis apparatus which was made available to us through a grant awarded by the S.R.C.

The diaphragm cell technique was considered, but was thought to be less suitable as it is not an absolute method, and is less accurate than the Rayleigh method.

4.3 The Theory of Restricted Diffusion

In the normal experimental set up restricted diffusion takes place in one dimension in a closed vertical cell of height, a, (see Fig. 4.1).

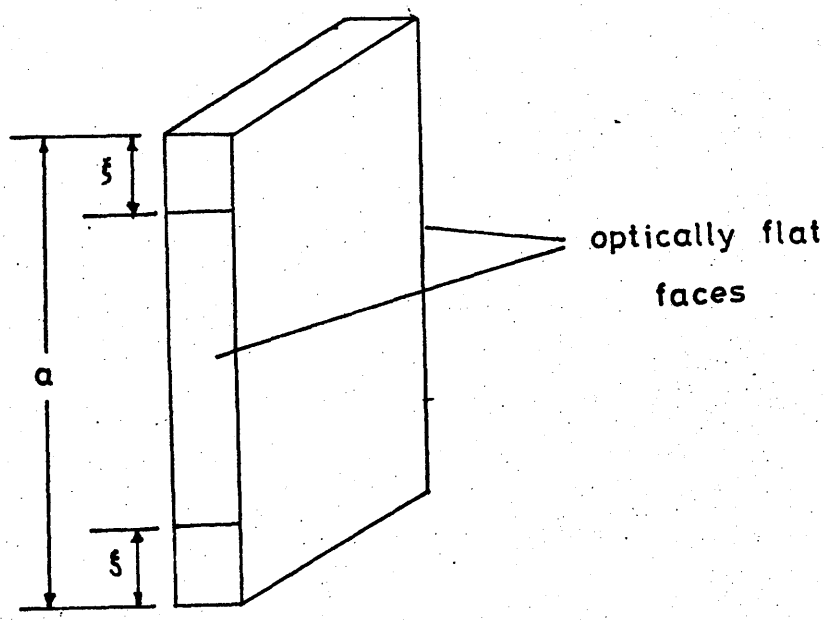

Fig. (4.1) Diffusion Cell

Free diffusion takes place from an initially sharp boundary between solutions of differing concentration until the concentration changes reach the top and bottom of the cell and the concentration profile becomes symmetrical. When this happens the conditions for restricted diffusion are obtained. These are

$$\frac{\partial c}{\partial x} = 0 \quad \text{for } x = 0 \text{ and } x = a \tag{4.3}$$

Harned assumed that D was independent of concentration, in which case the solution of equation (4.2) is a Fourier series of the form

$$C = C_o + \sum_{n=1}^{\infty} B_n \exp\left(-\frac{n^2\pi^2}{a^2}\right) \cdot \cos\left(\frac{n\pi x}{a}\right) . \tag{4.4}$$

where C is the concentration at time, t, at a position, n, in the cell, C_o is the uniform which will be obtained in the cell after infinite time, and the B_n are constants. The difference in concentration between any two symmetrical points in the cell, $x = \xi$ and $x = (a - \xi)$ is therefore given by :-

$$\Delta C = C_\xi - C_{a-\xi} = \sum_{n=1}^{\alpha} B_n \exp\left(-\frac{n^2\pi^2}{a^2} \cdot D\right) \cos\left(\frac{n}{a} \cdot \xi\right) - \cos\left(\frac{n}{a}(a - \xi)\right) \tag{4.5}$$

Harned observed that all the terms of even value of n in equation (4.5) vanish and that a choice of $\xi = a/6$ would also cause the n = 3 term to vanish. Equation (4.5) then becomes :-

$$\Delta C = \sqrt{3}\, B_1 \exp\left(-\frac{\pi^2}{a^2} \cdot Dt\right) - \sqrt{3}\, B_5 \exp\left(-\frac{25\pi^2}{a^2} \cdot Dt\right) + \text{——} \tag{4.6}$$

The higher terms in equation (4.6) quickly become negligible as the value of t rises until at suitably large times only the first term is

important. Taking logarithms of equation (4.6) for the first term only gives

$$\ln (\Delta C) = \ln (\sqrt{3}\ B_1) - (\frac{\pi^2 D}{a^2}) . t \qquad (4.7)$$

Thus a plot of ln (ΔC) against time should give a straight line of slope, $- \frac{\pi^2 D}{a^2}$. The linearity or otherwise of such a plot will be proof of the assumptions made in the derivation.

The results derived above were used by Harned only in very dilute solutions where volume changes and frame of reference effects on diffusion are negligible. Chapman and Newman have carried out an analysis of restricted diffusion in concentrated solutions[54], taking those effects into account, and their results are stated here. Their equivalent expression to equation (4.6) is

$$\Delta C = A_1 \sqrt{3} \exp (- \frac{D^\infty \pi^2}{a^2} . t) + A_2 \exp (- \frac{3D^\infty \pi^2}{a^2} . t) + \cdots \qquad (4.8)$$

where A_1 and A_2 are constants for any one experiment and are dependent on the initial conditions in the cell. D^∞ is defined in the analysis as the volume fixed differential diffusion coefficient of the uniform solution present in the cell after infinite time (or thorough mixing). The second term in equation (4.8) is of order e^3 rather than e^{25} as suggested by Harned's analysis, but it will, however, still become negligible at sufficiently large times. Chapman and Newman have thus shown that restricted diffusion can be applied to binary electrolyte solutions of any concentration to yield directly a differential diffusion coefficient.

4.4.1 Rayleigh Interferometry

The basis of Rayleigh interferometry is the ability of two coherent beams of light to interfere constructively or destructively depending on the phase difference in their waveforms. A simple arrangement for producing interference fringes is to pass coherent light through two parallel slits in a mask and let the resulting light pattern fall on a screen, as shown in Fig. 4.2. Consider the point M on the screen at distance y from the optical axis. M receives light from both slit A and slit B, but the light beam from slit A has to traverse a distance d sin θ greater than that from slit B (where $\theta = \tan^{-1} y/R$; R being the distance from mask to screen). The two beams of light are in phase at the mask, and they will be in phase at M, and hence produce an intensity maximum, if and only if d sin θ is an integral number of wavelengths λ .

Now consider the case when two optical samples A and B of thickness l and refractive indices n_A and n_B are placed in front of slits A and B respectively. The optical path length in any medium is the actual length multiplied by the refractive index, and hence the condition for constructive interference at M becomes

$$d \sin \theta + l(n_A - n_B) = m \lambda \qquad m = 1, 2, \ldots \qquad (4.9)$$

Now consider the effect of changing the refractive index of sample A from n_A to $n_A + \Delta n_A$ whilst keeping that of B constant. The difference in optical path length between the two beams converging at M will change, and in general there will no longer be an intensity maximum at M. The situation at M is now described by

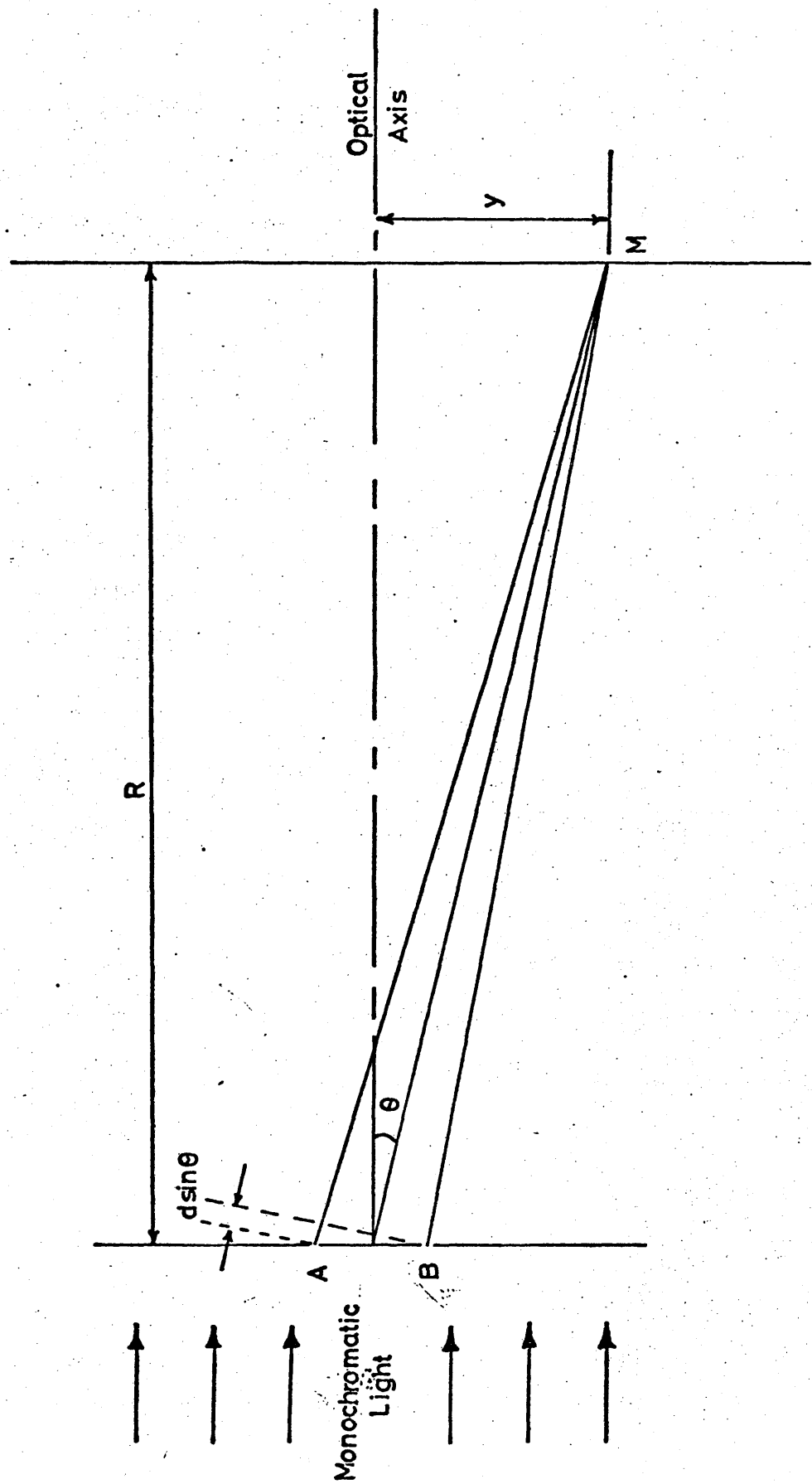

Fig 4.2

$$d \sin\theta + l(n_A - n_B) + l\Delta n_A = (m + \Delta m)\lambda \qquad m = 1, 2, \ldots \qquad (4.10)$$

where Δm is an increment in m, not necessarily integer. The product, $\lambda\Delta m$, is a measure of the displacement of the intensity maximum originally at M. Equations (4.9) and (4.10) combine to give

$$l\Delta n_A = \lambda\Delta m \qquad (4.11)$$

Thus by measuring the displacement of the Rayleigh interference pattern the change in refractive index of sample A can be estimated. Since the wavelength, λ , is constant, Δm, the number of "fringe shifts" in the interference pattern between any two points can be taken as a direct measure of the difference in refractive index between those two points.

If the change in refractive index at A is caused by placing solutions of different concentrations, C_A, at A, equation (4.11) becomes

$$l.p.\Delta C_A = \lambda\Delta m \qquad (4.12)$$

where p is a constant if, as is true for most electrolyte solutions, refractive index is a linear function of concentration. Thus the shift in the interference pattern is directly proportional to the change in concentration.

4.4.2 A Simple Rayleigh Interferometer The basic form of the Rayleigh interferometer after the model of Phillpot and Cook[51] is shown in Fig. 4.3. Monochromatic light from the point source P is focussed by lens L onto the screen. The mask M is inserted into the light beam and cells C and C^1 are placed in front of the slits. In the absence

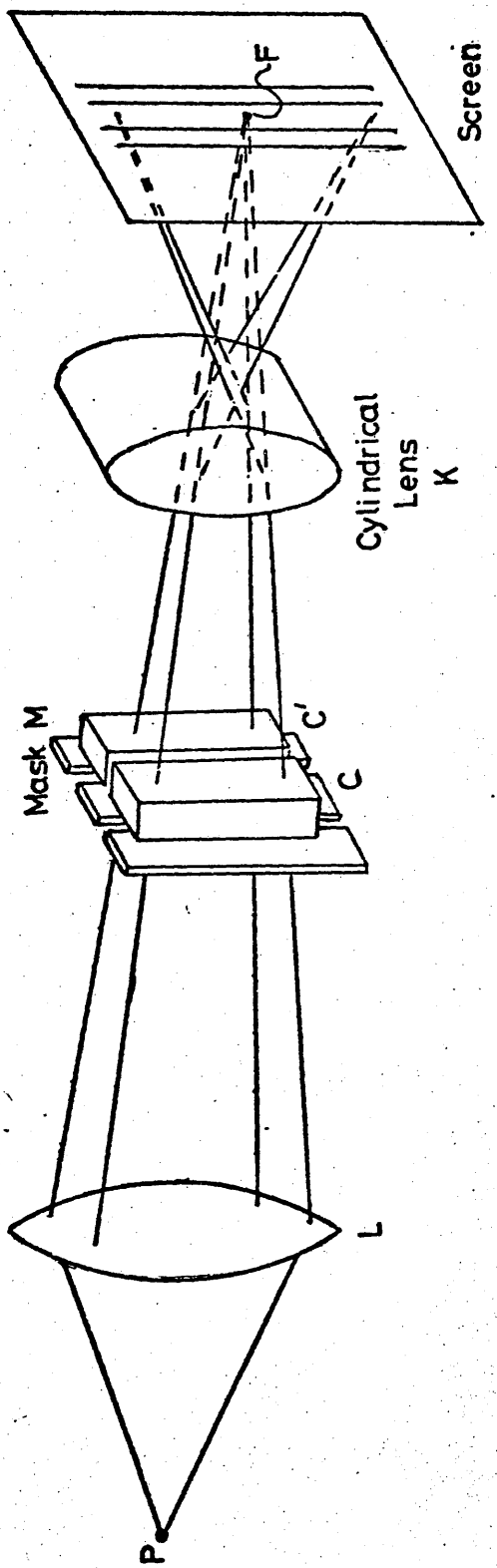

Fig. 4.3

of the cylindrical lens K the interference pattern produced will be focussed in a small image centred at point F. The cylindrical lens spreads this image cut in a vertical direction without distorting it in the horizontal direction[51,55]. If cell C contains a solution in which there is a one dimensional concentration gradient and C^1 contains a uniform reference solution this arrangement will produce a direct map of the refractive index gradient in C as the interference pattern is shifted by varying amounts by the varying refractive index in C.

The system described above produces a rather narrow pattern. A much broader and brighter pattern results if a multipoint source is used[56]. If the points are properly spaced to reinforce one another the effect is to superimpose the m'th fringe of one pattern on the less intense (m + 1)th fringe of the adjacent pattern, and the still less intense (m + 2)th fringe of the next pattern, etc.

4.4.3 Precision of the Method The precision of this method can be easily estimated. The sodium D line was used as a light source, therefore λ is 589 nm, p for most electrolyte solutions is of the order of 10^{-2} l mol $^{-1}$, and the pathlength used was 2.5 cm. Substitution of those values in equation (4.12) shows that one fringe shift corresponds to a concentration change of approximately 2×10^{-3} mol l^{-1}. Fringe shifts can be estimated easily to $\frac{1}{10}$ fringe, thus giving a precision of 2×10^{-4} mol l^{-1} in Δ C.

4.5 Experimental Apparatus and Technique

4.5.1 Apparatus Experimental measurements of diffusivity were made using a commercially available electrophoresis apparatus viz the

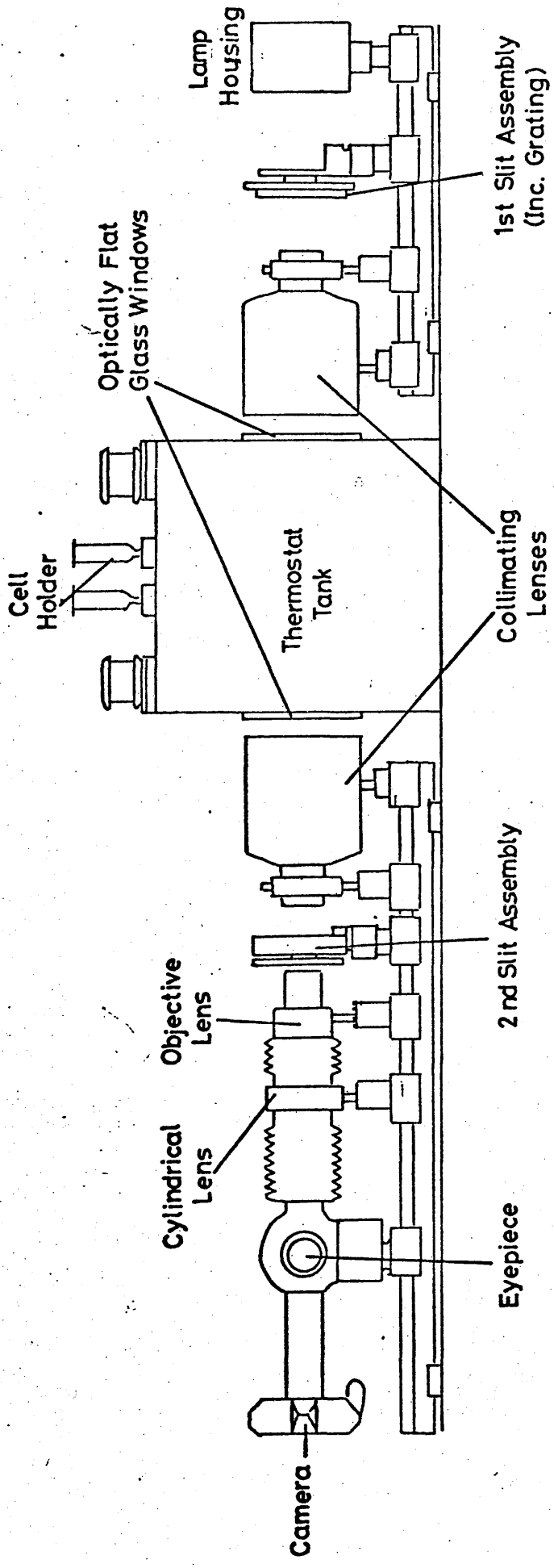

M.S.E. Model D Diffusion Apparatus

Fig 4.4

MSE Electrophoresis apparatus model D, purchased from Measuring & Scientific Equipment ltd. The apparatus offers a choice of a Schlieren or a Rayleigh optical system, and therefore the exact optical arrangement is slightly different from that of the simple Rayleigh interferometer described above, although the end result is the same. The optical arrangement of the machine is shown in Fig. 4.4.

Monochromatic light from the sodium lamp is passed through a condenser lens, and the resulting beam deflected along the optical path by the mirror. This beam is passed through a diffraction grating which acts as a multiple point source of light. The beam then passes through a collimating lens and a plane window into the thermostat bath. In the bath are the optical cell and slit assemblies, and after passing through these the beam passes out of the bath and through another collimating lens and is brought to focus by an objective lens onto the film plane of a 35 mm camera. A cylindrical lens between the objective lens and the camera spreads the image vertically. A movable mirror allows the final image to be observed through the eyepiece for focussing and visual estimation of the progress of diffusion.

4.5.2 Optical Cell Assembly and Holder The optical cell assembly, shown in Figs. 4.5 and 4.6 is basically a standard Tiselius cell, and is separated into three main sections, top, centre, and bottom, which fit together by means of flat ground glass plates. The middle section consists of two vertical, parallelopiped channels or limbs held together by two horizontal flat ground glass plates. The two narrow vertical faces of each limb are optically flat and parallel. On one

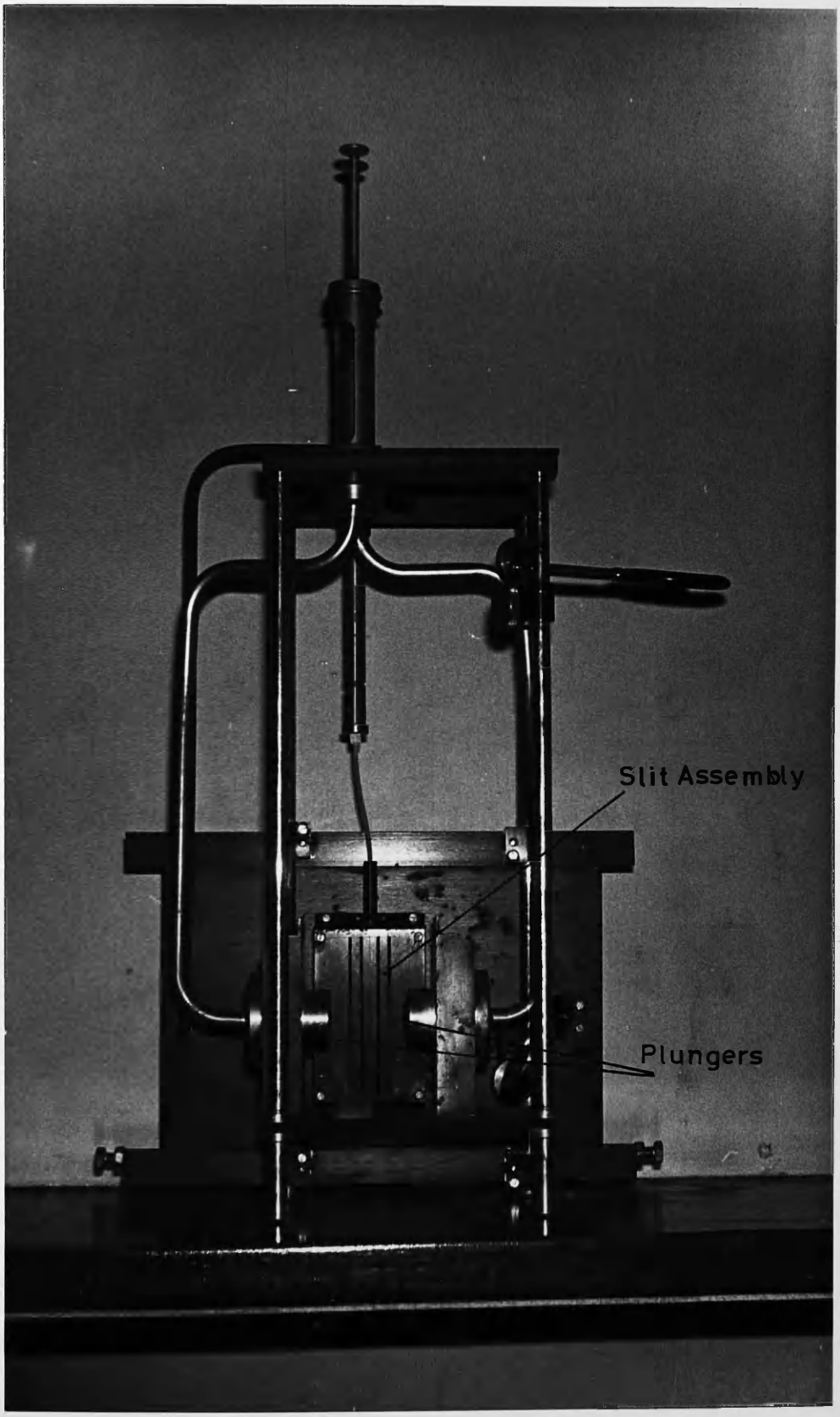

Fig 4.5

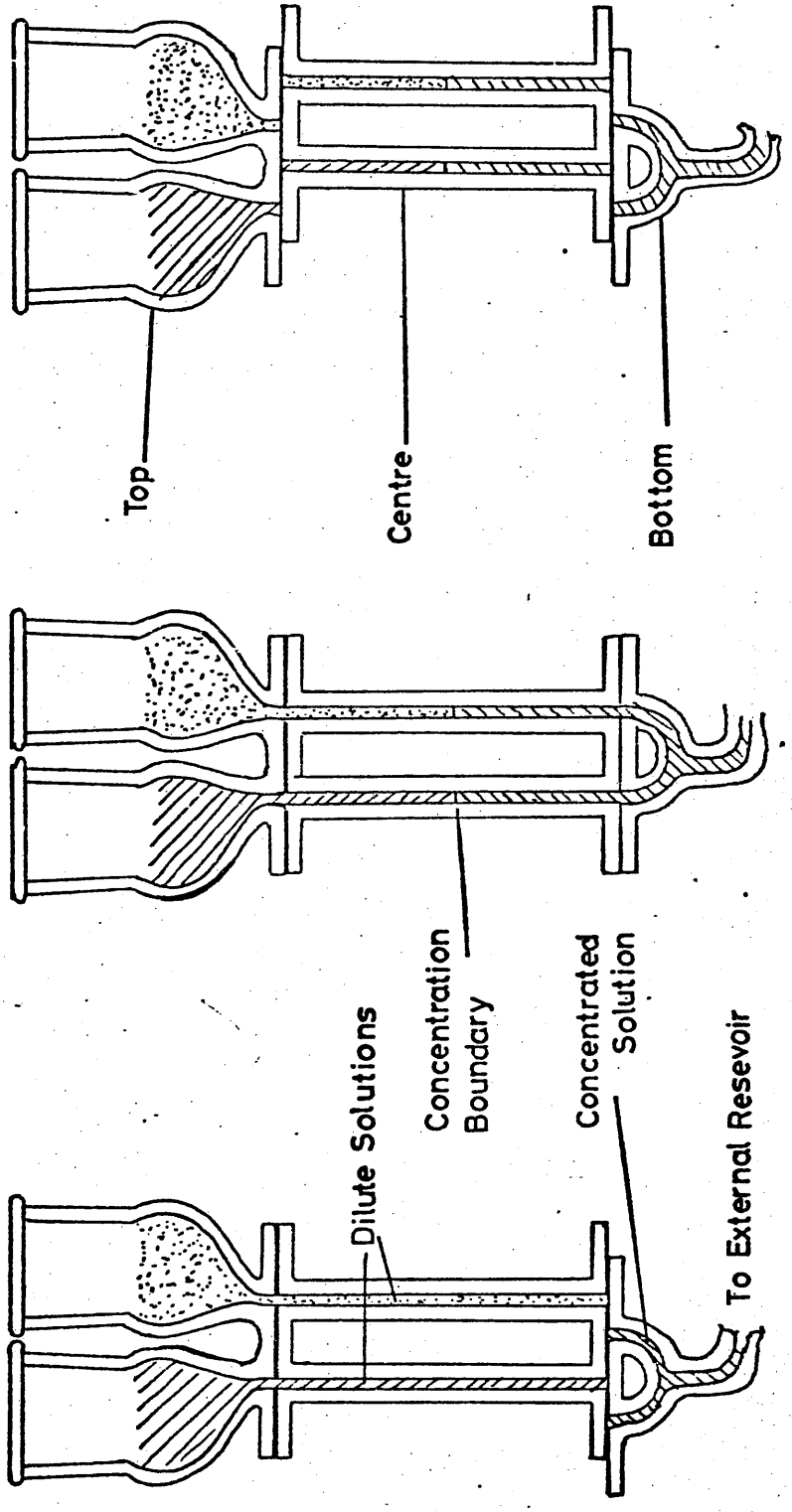
Top
Centre
Bottom
C
Concentration Boundary
Concentrated Solution
B
Dilute Solutions
To External Resevoir
A

Fig. 4.6

of the faces of each limb are etched two fine horizontal lines, approx. .02 mm thick, exactly $\frac{1}{6}$ of the total cell height from the top and bottom of the limb. The bottom section consists of a U tube held in a flat ground glass plate. The tips of the U tube channel are set to be able to connect exactly the two limbs of the middle portion. A connection is set into the bottom of the U tube to allow solution to be led in from an external reservoir via a flexible connecting tube. The top section consists of a flat ground glass plate supporting a reservoir above each limb. Each reservoir was closed by a teflon stopcock.

The optical cell assembly is held in a metal supporting framework shown in Fig. (4.5). This support has a system of plungers which are used to displace the centre section of the cell sideways to isolate it from the top and bottom sections. There is also an assembly on the cell holder consisting of four vertical slits in a metal plate. Those slits can be blocked off in any combination by a selector mechanism to produce the beams of light through the cell limb and surrounding solution which produce the interference pattern. The slit assembly can be shifted laterally to keep it in line with centre section of the cell. The cell assembly is supported in a large thermostat bath of distilled water maintained at a constant temperature to $\pm$ 0.002^{o}C by means of a thermostat controlled by a mercury toluene regulator.

The Rayleigh pattern is produced by interference between a beam of light passing through the cell limb and a reference beam passing through the liquid in the thermostat tank.

If the difference in refractive index between the solution in the cell and the liquid in the tank is too great an indistinct pattern is produced due to the slight inhomogeneity of the sodium light source[52]. The pattern may be sharpened by matching the optical path lengths of the two beams. This was done by adding ethylene glycol to the bath water to increase its refractive index.

4.5.3 Setting Up a Run The glass parts of the cell were cleaned in Decon 75 solution, well rinsed with distilled water, and dried after rinsing with Analar acetone. The ground glass surfaces were cleansed of grease by wiping with a tissue soaked in cyclohexane. The ground glass surfaces of the three sections were lightly smeared with a light silicone grease, pressed together, and slid to and fro until no air bubbles remained trapped in the grease between the ground glass plates. The glass assembly was then mounted in the cell holder and the flexible tube of the external reservoir attached to the bottom of the U tube. The plungers were tested to make sure that the centre section of the cell was free to move.

The centre section was pushed to the right thus closing off the tops of the U tube. The external reservoir was then filled with degassed test solution. The centre section was moved back to open the tops of the U tube and solution allowed to flow gently into the U tube by opening the stopcock in the external reservoir. Solution was allowed to flow until the U tube was full and solution had started to flow into the centre section. The centre section was slid back to close off the U tube again, and the small amount of solution remaining in the limbs of the centre section with-drawn with a syringe.

The limbs of the centre section and their associated reservoirs were then filled with solutions whose concentrations were slightly less than the solution in the external reservoir, each solution having been degassed and having a slightly different concentration (Fig. 4.6A). The exact values of the three concentrations did not need to be known.

The cell and holder were then placed in the thermostat tank and positioned so that the cell lay in the optical path of the machine, and left for some hours until thermal equilibrium was obtained. Three photographs of the Rayleigh pattern produced by each limb of the cell were taken. These Rayleigh patterns should consist of parallel vertical straight lines, and any deviation was assumed to be caused by imperfections in the optical faces of the limbs and corrected for when measuring the experimental films. The stop-cocks in the three reservoirs were closed and the centre section of the glass cell slid to the left so that the channels of all three parts of the cell were aligned (Fig. 4.6B). The slit assembly was also shifted to the left to keep it in alignment with the cell limbs. This produced a sharp concentration boundary in the limbs at the junction of the bottom and centre portions of the glass cell.

These boundaries were then shifted, one at a time, until they were in the middle of the limbs of the centre section, as observed with the crosswires in the eyepiece. The stopcock on the left hand reservoir was opened, that of the right hand reservoir being kept shut. The stopcock of the external reservoir was then opened gently and the boundary in the left hand limb of the cell allowed to rise slowly.

This was followed by observing the Schlieren pattern in the eyepiece. The Schlieren pattern, which gives the gradient of refractive index in the solution, was found more useful for setting the boundary as it consisted of a sharp peak. When the peak was centred on the crosswire in the eyepiece the stopcocks on the external and left hand reservoirs were closed. The process was repeated in the right hand limb. At this stage the boundaries could be sharpened, if required, by inserting a fine syringe needle into the centre of the concentration boundary and gently with-drawing about 5 ml of solution from the boundary region. Normally this was not necessary. The centre section of the cell was displaced to the left, thus closing the limbs at the top and bottom (Fig. 4.6C), the slit assembly moved into position, and the timer started. The conditions for restricted diffusion were fulfilled when the concentration gradient reached the ends of the limb, and measurements could then be started. This normally took about 2 days. A typical run took about twelve days from setting up the boundary to the end of the run, and normally two pictures of the Rayleigh pattern were taken per day in each limb.

4.5.4 Analysis of Solutions At the end of a run the cell in its holder was removed from the thermostat bath, rinsed with distilled water, and allowed to dry. The top reservoirs were emptied and dried with paper tissues to remove any last drops of solution. With the centre section held in position the top section was slid over to open the tops of the limbs. The solution in each limb was well mixed with a clean dry syringe, and then transferred, using the syringe, to a clean, dry, weighed flask. The concentration of the mixed solution

corresponded to the concentration which would be attained after infinite time, and is the one to which the measured diffusion coefficient corresponds. The flask plus solution was weighed, and reweighed after the solution had been diluted with distilled water. The concentration of this solution was determined by titration with E.D.T.A. solution in the normal way, and the concentration of the solution in the limb calculated.

4.5.5 Measurement of the Films Each exposure of the film gave a picture of the refractive index profile of the solution in a limb of the cell at a specific time. Typical examples of the pictures obtained at the beginning, middle, and calibration of the cell are shown in Figs. (4.7), (4.8) and (4.9). The measurement required from the films is the net displacement undergone by a fringe between the two reference lines, A and B, etched on the cell, given by $w\Delta m^1$ where w is the width of one fringe and Δm^1 is the number of fringe widths by which the m'th fringe is displaced on going from line A to line B. w will be a constant of the apparatus.

The films were measured using a Nikon Model 6C profile projection microscope. This instrument had a stage whose lateral and longitudinal movements could be measured by vernier scales capable of reading to 0.001 mm. The film was sandwiched between two sheets of optically flat glass and placed on the microscope stage. Using the crosswires in the centre of the screen the left hand reference line A on the film was made perpendicular to the longitudinal drive direction of the stage. The crosswires were central on a position where the top of a dark fringe crossed the reference line, and the width of 25 fringes

Fig 4.7

Initial Concentration Gradient

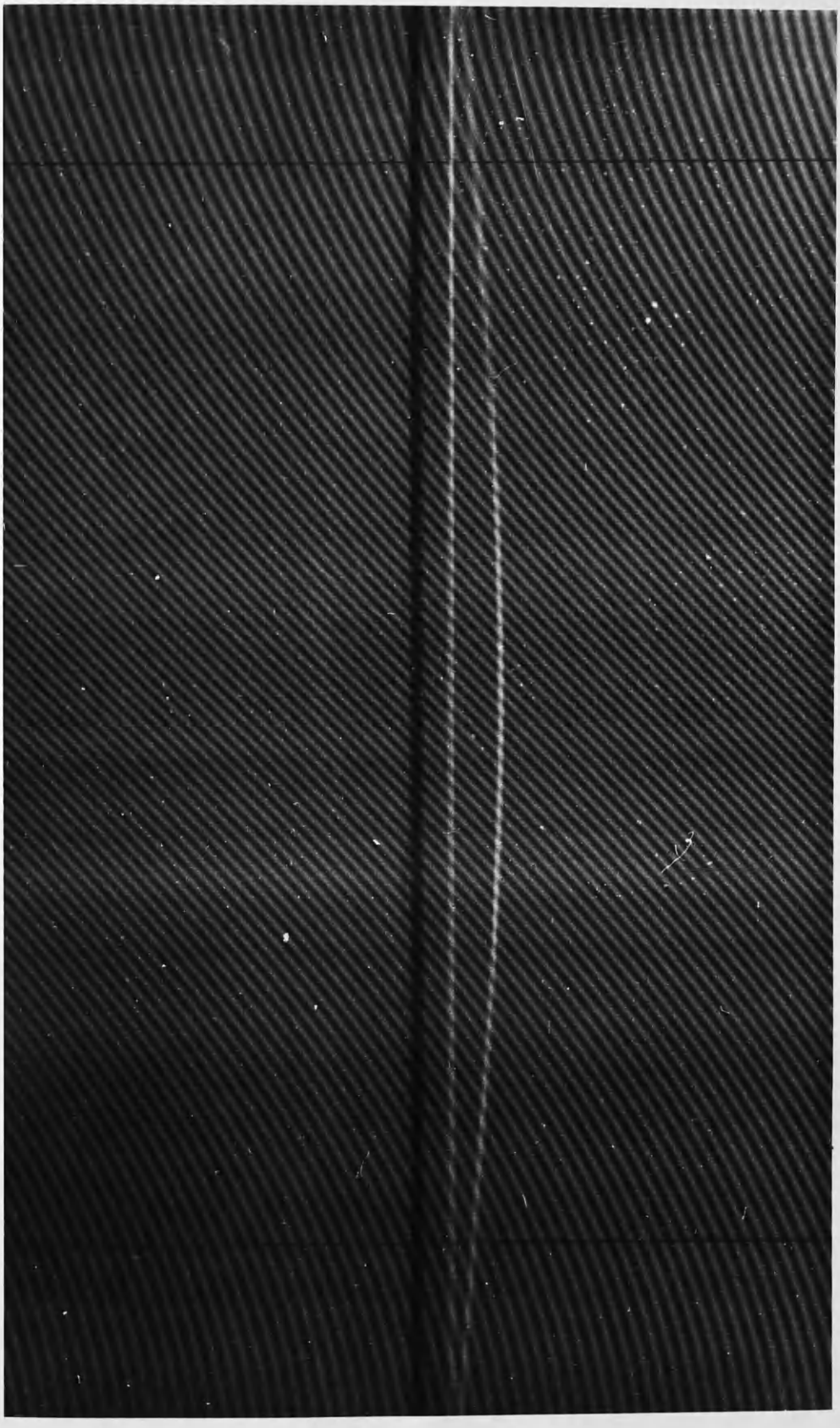

Fig 4.8

Final Concencentration Gradient

Fig 4.9

Calibration

measured by displacing the microscope stage in the lateral direction. This gave a measure of the average width of a fringe, w. This varied slightly from frame to frame having a standard deviation of around 0.5% over all the films measured. The deviation in duplicate measurements of the same frame was never greater than 0.2%.

The crosswires were again centred on the intersection of a fringe top with reference line A and the stage moved in a longitudinal direction until reference line B was reached. The number of fringes crossed while doing this was noted. This procedure was equivalent to moving the stage laterally from this position and counting the number of fringes crossed until the original fringe was reached. The residual fraction of a fringe crossed, but not counted, was estimated by displacing the stage laterally to the top of the next fringe top and measuring the displacement. This, divided by the average width of a fringe, gave the remaining fraction of a fringe, which was added to the integral total to give Δm^1.

The calibration pictures taken at the start of each run were always measured first. With an optically perfect system these frames would show no deflection of the fringe pattern, i.e. Δm^1 would be zero, but in practice a constant shift of about half a fringe was observed. This was ascribed to optical imperfections in the glass cell, and the experimental results were corrected for it. The standard deviation of twelve measurements of this correction factor was taken as representative of the accuracy with which Δm^1 could be estimated. This deviation was never greater than 0.1 of a fringe and was usually much smaller. As the value of Δm^1 during a run changed typically from

around 40 to around 20 this precision corresponds to about 0.3% in a single measurement.

4.6 Calculation of the Diffusion Coefficient It was shown above that Δm^1 is directly proportional to the difference in the refractive indices of the solution at points A and B in the cell ($\Delta n = n_A - n_B$). The quantity required for substitution in equation (4.7) is the concentration difference between those two points, Δc, and it remains to be shown that Δc is directly proportional to Δn for the two systems studied. To do this the refractive index of aqueous solutions of zinc chloride and zinc perchlorate was measured as a function of concentration over the whole concentration range studied using an Abbé refractometer. All measurements were carried out at a constant temperature of 25°C. The results are shown in Fig. (4.10) as plots of refractive index against molarity.

It is obvious from Fig. (4.10) that for these salts the refractive index of an aqueous solution is not directly proportional to molarity, and therefore we cannot simply write $\Delta c = A \Delta n$. Harned has shown however,[47,57] that such a relation will still be true provided the quantity measured is a symmetrical function of concentration. That this is the case for the two salts studied is shown by the results in table (4.1). The first column shows values of $C_1 - C_2$ centred about a mean concentration of $(C_1 + C_2)/2$, the second column shows the corresponding value of $n_1 - n_2$, and the third column shows the value of the quotient $(C_1 - C_2)/(n_1 - n_2)$. The constancy of the values in the third column at each mean concentration is proof of the relation $\Delta c = A\Delta n$.

Substitution of this relation into equation (4.7) gives :-

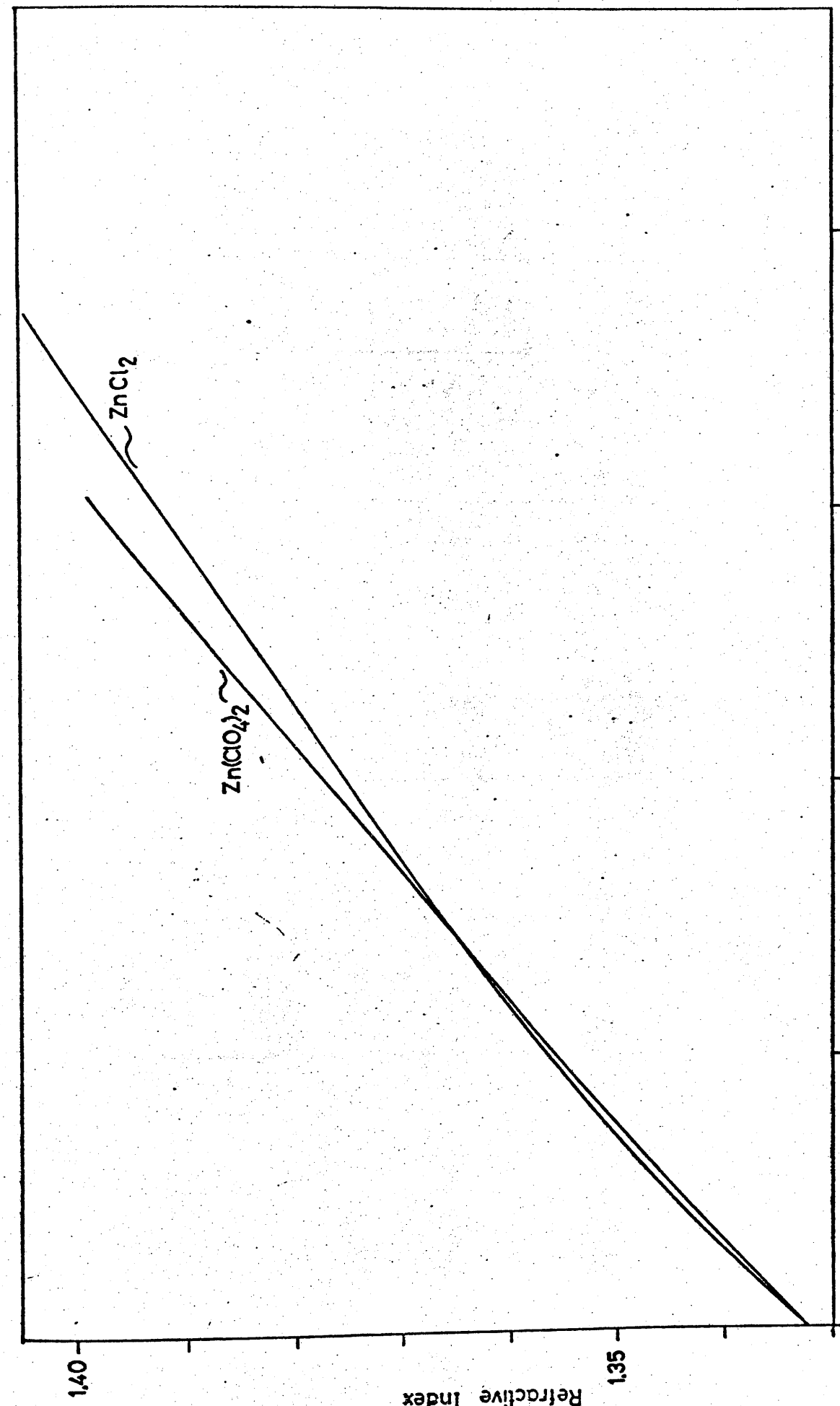

Fig. 4.10

Table 4.1

Salt	$\frac{C_1 + C_2}{2}$	$C_1 - C_2$	$n_1 - n_2$	$c_1 - c_2 / n_1 - n_2$
$ZnCl_2$	1.0	1.0	0.0207	0.0207
	1.0	0.5	0.0104	0.0207
$ZnCl_2$	2.0	1.0	0.0178	0.0178
	2.0	0.5	0.0088	0.0176
$ZnCl_2$	3.0	1.0	0.0173	0.0173
	3.0	0.5	0.0088	0.0172
$Zn(ClO_4)_2$	1.0	1.0	0.0222	0.0222
	1.0	0.5	0.0112	0.0224
$Zn(ClO_4)_2$	2.0	1.0	0.0217	0.0217
	2.0	0.5	0.0109	0.0218

$$\ln(\Delta n) = B^{II} - \ln A - D\left(\frac{\pi}{a}\right)^2 \qquad (4.13)$$

and since Δn is directly proportional to Δm^1 we have :-

$$\ln(\Delta m^1) = B^{III} - D\left(\frac{\pi}{a}\right)^2 \qquad (4.14)$$

Thus a plot of $\log(\Delta m^1)$ against time should give a straight line of slope $-2.303D\left(\frac{\pi}{a}\right)^2$. Table 4.2 gives a typical set of results for one limb of a run. The measured value of Δm^1 was corrected, the logarithm taken, and the value plotted against time to give the straight line graph shown in Fig. (4.11). A computer programme written to perform most of those calculations is reproduced in the Appendix. This programme read in as pairs of Δm^1 and time, and then read in the correction factor. It then calculated the natural logarithm of the corrected value of Δm^1 and produced a straight line fit of this against time by the method of least squares. The programme then checked if any of the experimental points deviated too far from the least squares line, rejected any that did, and repeated the calculation with those remaining. The programme then calculated and printed out the value of the diffusion coefficient.

Most of the deviant points were found to lie at the beginning or the end of a run. A deviation at the beginning of a run was considered to be caused by the elapsed time being too short to allow the higher terms of equation (4.8) to become negligible, and deviation at the end of a run was considered to be caused by the onset of convection currents in the cell because the density gradient was too low to overcome the effects of vibration.

4.7 Results The experimental results are shown in table 4.3 for zinc chloride and zinc perchlorate. In table 4.4 are given the

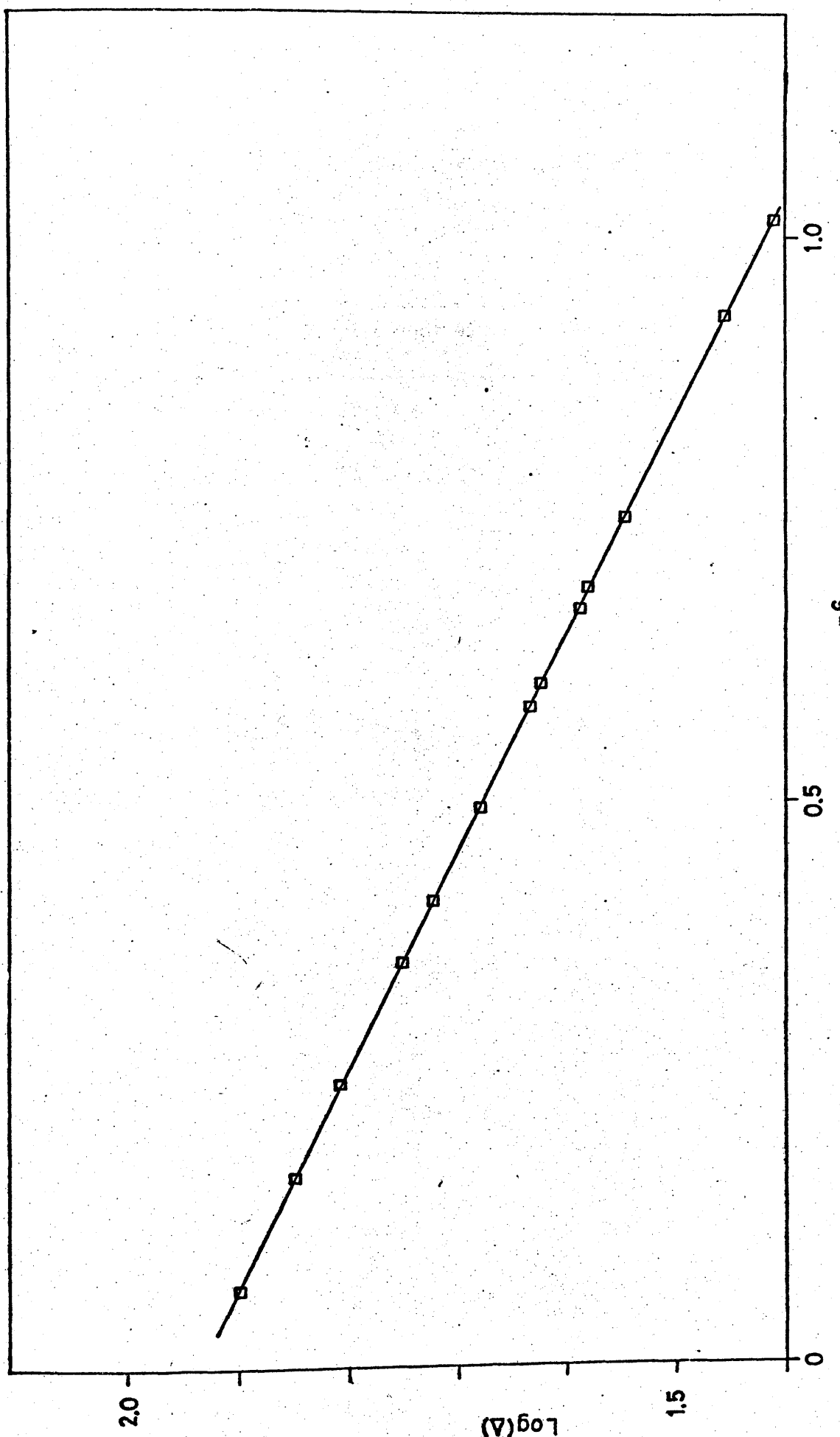

Fig. 4.11

Table 4.2 Analysis of a Typical Diffusion Run with Zinc Chloride

Displacement of Fringe Pattern with zero concentration gradient = 0.25 ± .05 fringe

Time (secs)	Displacement of Pattern (Δ)	log Δ
74100	78.94	1.8973
252600	64.11	1.8069
363350	56.32	1.7507
415900	52.74	1.7221
498100	47.85	1.6799
587950	43.11	1.6346
607460	42.12	1.6245
674550	38.86	1.5895
692200	38.08	1.5807
754400	35.22	1.5468
932600	28.51	1.4550
1016950	25.90	1.4133

Molarity of final Solution = .17484 M

Diffusion Coefficient $D = 1.01803 \times 10^{-5} \text{ cm}^2 \text{s}^{-1}$

Table 4.3 Experimental Diffusion Coefficients

Zinc Chloride		Zinc Perchlorate	
Molarity	D x 10^5 cm^2 s^{-1}	Molarity	D x 10^5 cm^2 s^{-1}
0	1.209	0	
.0499	1.048	.0255	1.046
.1748	1.018	.0416	1.054
.2477	1.005	.0823	1.030
.2796	1.002	.0915	1.034
.3254	.995	.1908	1.085
.6137	.979	.3525	1.119
.7442	.967	.3632	1.127
.7651	.975	.6198	1.214
.9096	.971	.6426	1.222
1.2829	1.007	1.5136	1.493
1.3115	1.012	1.5677	1.507
1.8114	1.042	2.1701	1.574
1.8313	1.050	2.2175	1.564
2.3569	1.127	2.5495	1.539
2.9948	1.206	3.0727	1.328
3.0946	1.204	3.1705	1.347
3.4419	1.248		
3.9067	1.271		

Table 4.4 Coefficients of Least Squares curve fit Expressions of D v $\sqrt{C}$

	Coefficients					
	a_0	a_1	a_2	a_3	a_4	a_5
$ZnCl_2$ 0.0-1.5 M	1.21034	-1.32779	3.91632	-6.17783	4.65707	-1.29486
$ZnCl_2$ 1.2-3.9 M	2.39104	-3.164110	2.240799	-0.468191	-	-
$Zn(ClO_4)_2$ .03-3.15 M	1.1157	-0.705702	1.831215	-1.511311	-0.882843	-0.260420

coefficients of the least squares curve fit of the diffusion coefficient against the square root of molarity for both salts. The standard deviation of the results is 0.5% in each case.

Chapter 5

The Measurement of Transference Numbers and Potentiometric Measurements

5.1 Measurement of Transference Numbers

The measurement of transference numbers is an essential part of an irreversible thermodynamic analysis. The transference number represents one of the three independent transport properties required for the calculation of mobility or frictional coefficients when the Onsager reciprocal relations are assumed. Furthermore the identity or otherwise of the cell emf transference number with the Hittorf (or moving boundary) transference number provides a test of these relations[13,14,15]. There are three major techniques for measuring transference numbers, and as they have all been described comprehensively elsewhere[58,59,60,61] only a brief summary will be given.

5.1.1 Moving Boundary Methods[58,59,60,61] In these methods a sharp boundary between two electrolyte solutions is formed in a narrow tube. The two solutions must possess a common ion, and the two non-common ions should have significantly differing mobilities. If an electrical current is now passed the unequal mobilities of the non-common ions will cause the boundary to move along the tube. The volume by which the boundary is displaced by the passage of a known quantity of electricity is simply related to the transference number of the more mobile of the non-common ions. The main disadvantage of the technique is that a frame of reference correction is required. The movement of the boundary is measured relative to the experimental apparatus, while the transference number is normally required on a

solvent fixed reference frame. This correction becomes progressively larger and more uncertain as the concentration of the solutions studied increases.

5.1.2 Concentration Cell emf Method[58,59,61] The basis of this method is that the emf of a concentration cell with transport is a function of the transference numbers of the ion constituents in the solutions concerned. The method requires that electrodes can be found which are reversible to at least one of the ionic species in solution, and that activity coefficient data are available as a function of concentration for the electrolyte concerned. There is no limit to the concentration range which can be studied as long as suitable electrodes are available.

5.1.3 The Hittorf Method[58,59,61] This is the oldest of the techniques for measuring transference numbers. A measured quantity of electricity is passed through the solution concerned and the change in concentration in the regions near the electrodes determined. The electrodes need not behave reversibly to the constituent ions; but they should be capable of passing a fairly heavy current without excessive heating or gas evolution. Any concentration range from 0.01 Molar upwards can be studied.

5.1.4 Selection of Methods In chapter (2) it was shown that transference numbers measured by the Hittorf or moving boundary methods, t_1^h, and transference numbers measured by the cell emf method, t_1^c, are identical only when the Onsager reciprocal relations are valid. The ORR can only be proved theoretically under the limiting conditions of vanishingly small thermodynamic forces, and must therefore

be verified experimentally. Consequently two of the three techniques outlined above must be used. As the moving boundary method becomes unreliable at the concentrations studied here the two methods chosen were the cell emf and Hittorf methods.

5.1.5 Selection of Zinc Salts for Study The primary objective of this thesis is to compare the transport properties of zinc chloride solutions, which show heavy ion complexing, with those of another zinc salt in which complexing is absent. The most suitable choice for this second salt would appear to be zinc nitrate, as Raman studies[62] have shown complexing to be absent from its solutions. Unfortunately it was found impossible to produce electrodes that would behave reversibly in zinc nitrate solutions, or even pass a current without excessive gas evolution. It was, therefore, not possible to measure transference numbers in zinc nitrate solutions. For this reason zinc perchlorate was studied instead. There is no direct evidence for the absence of complexing in solutions of this salt, but as the perchlorate ion is generally considered to be an extremely poor ligand complexing was assumed to be absent.

Transference number data are available in the literature for both zinc chloride and zinc perchlorate. Harris and Parton[63] measured the cell transference number of zinc chloride in the concentration range 0.5 - 12 mol Kg^{-1} of solvent, and Stokes and Levien[64] measured t_1^c for zinc perchlorate in the concentration range 0.1 - 4.0 mol Kg^{-1} of solvent. In addition a few early measurements of t_1^h at 18°C by Hittorf[65,66] are also available for zinc chloride. The experimental work consisted of determining the Hittorf transference

numbers of zinc chloride and zinc perchlorate solutions in the concentration range 0.1 - 4 mol Kg^{-1} of solvent, and of determining the cell emf transference numbers of zinc chloride solutions in this concentration range. This duplication of the published work[63] over a large section of the concentration range was seen as a useful verification of earlier data, particularly since the preparation of zinc chloride shows certain variations from one study to another.

5.2 Measurement of the Hittorf Transference Number

5.2.1 Apparatus The Hittorf cell used was of a similar design to that introduced by MacInnes and Dole[67] and used recently by Pikal and Miller[68,69]. A photograph of the cell in its holder is shown in Fig. 5.1. The cell was constructed of 10 mm bore pyrex tubing in two sections coupled together by a B14 Quickfit joint. The assembled cell could be separated into three compartments using two large bore stopcocks A and B. Each of the electrode compartments had a volume of approximately 25 cm^3 and the volume of the whole cell was approximately 100 cm^3.

For the analysis of a Hittorf experiment it is essential that the concentration changes produced are confined to the two electrode compartments, and for this reason every precaution was taken to prevent thermal and gravitational convection currents within the cell. The cell was bent in several places to break up any such currents and the barrels of the stopcocks were made hollow to allow cooling water to circulate through them and prevent any local Joule heating. The cell was held rigidly in a special holder and was

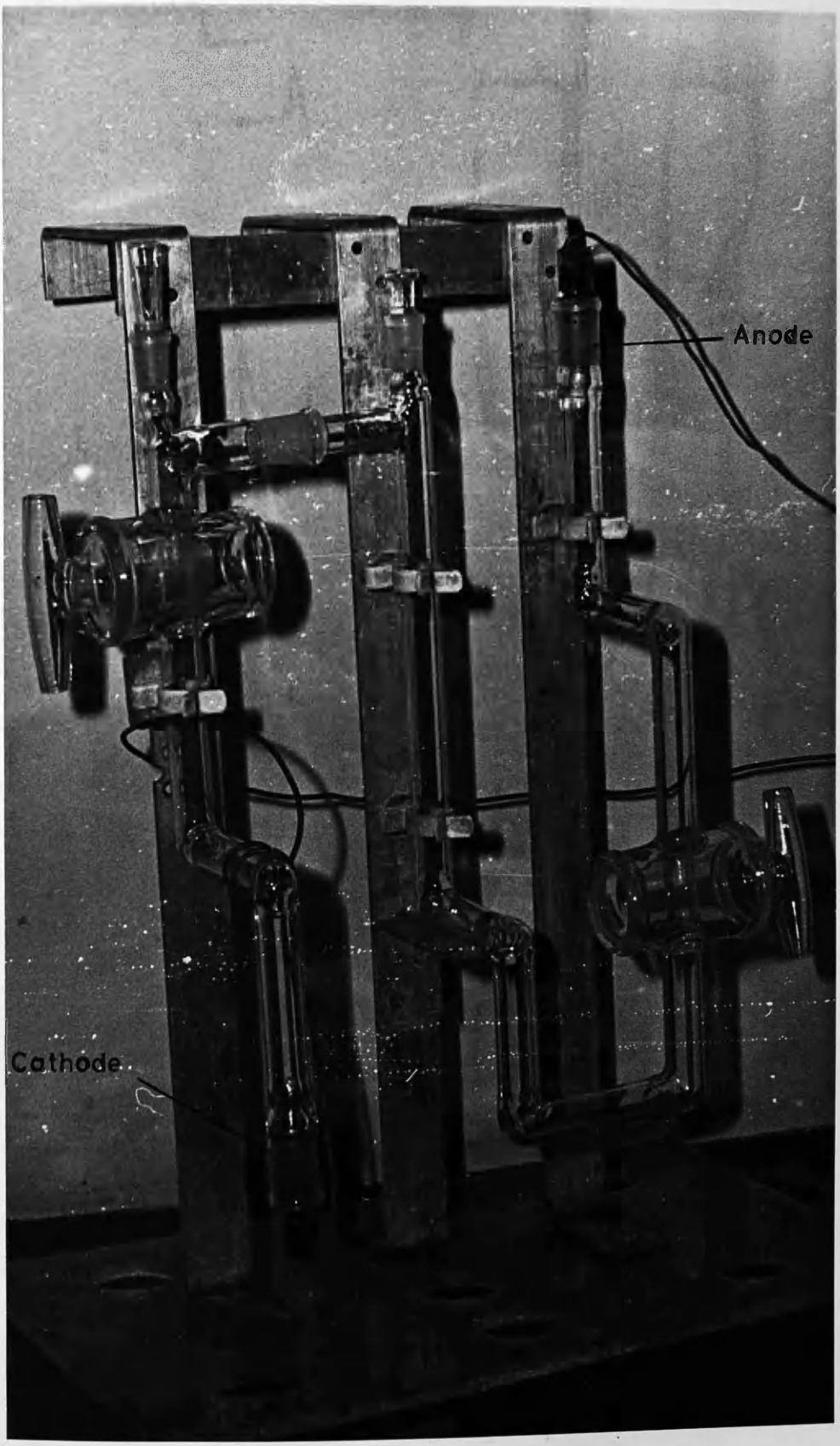

Fig 5.1

Hittorf Cell

immersed in a water bath maintained at 25 ± .005°C as described in section 3.4.3. To minimise vibration the water tank was placed on rubber pads, and the thermostat stirrer motor was supported on a separate stand, also sitting on rubber pads, which did not touch the water tank. Finally, to avoid density mixing, the polarity of the electrodes was arranged such that the anode (round which the concentration is expected to increase) was situated at the bottom of the cell, and the cathode at the top.

5.2.2 Electrodes Both electrodes consisted of short lengths of spectroscopically-pure zinc rod sealed into a B14/20 Quickfit cone with Araldite. Before each run they were cleaned by dipping them into strong nitric acid for a few minutes to remove any possible oxide film, and finally rinsed with distilled water, and dried with a clean tissue. During the preliminary runs with zinc chloride solutions using electrodes treated in this way it was noted that there was substantial gas evolution at both cathode and anode. It was also noted that a white film, presumably of zinc oxide or oxychloride, formed on the anode, and that after passing current for 15 hours or more the solution around the anode started to become cloudy due to precipitation of zinc oxychloride. These side reactions were greatly reduced by using amalgamated electrodes. These were prepared by dipping the cleaned electrodes into dilute mercuric chloride solution for a few minutes, rinsing with distilled water, and polishing gently with a clean tissue. Electrodes treated in this way were virtually free from side reactions provided the electrolysis was not carried on for too long.

5.2.3 Current Supply A Solartron P.S.U. AS1413 current source was used to supply a constant current to the cell. This instrument had an output voltage of 40V, and was capable of supplying to the cell currents of either 5.8 or 15.8 mA constant to ± 0.1%. Both values are safely under the maximum current values recommended by Pikal and Miller[68]. The current was monitored when entering and leaving the cell by measuring the potential drop across two 10 ohm standard resistors placed in series with the cell. No leakage of current from the cell to the thermostat tank was found.

5.2.4 Experimental Method The two parts of the cell, with the electrodes in position, were weighed clean and dry. The test solution was swept clear of dissolved oxygen by passing nitrogen gas through it for about 30 minutes. The cell was assembled in its holder, filled with solution, and left in the thermostat tank for one hour to allow thermal equilibrium to be attained. The electrodes were then connected to the current source and the current switched on at a noted time. The duration of a run was anything from five to fifteen hours depending on the current used and the amount of electrolysis possible before side reactions at the electrodes became troublesome (see section 5.2.7 for more details). In any case the concentration change in the electrode compartments was restricted to a maximum of ± 10% to minimise the risk of concentration changes outwith the two electrode compartments.

At the end of the experiment the current was switched off, and the total elapsed time noted. The electrode compartments were then isolated by closing the two stopcocks, A and B. The cell was

then removed from the thermostat bath and the exterior cleaned and dried. Three samples of solution were taken from the central section of the cell, one from the region close to the anode compartment, one from close to the cathode compartment, and one from the centre region. The electrode compartments were each weighed with their contents, after which the contents of each compartment were thoroughly mixed and transferred to clean, dry, stoppered flasks to await analysis. The weights of the electrode compartments were corrected for the weight of zinc transferred from the anode to the cathode during electrolysis, and the weights of solution in each compartment at the end of the run calculated.

5.2.5 Analysis of Solutions This was carried out, as described in Section (3.2.2), by triplicate E.D.T.A. titration of weighed samples of solution. The concentrations of the three samples from the central portion of the cell were determined first. Any discrepancy in those three concentrations was taken as an indication that concentration changes during the run had not been confined to the electrode compartments, and that the experiment must be discarded. When the concentrations of the three samples agreed within the expected experimental error (0.07% or less) they were averaged. The concentrations of the samples from the anode and cathode compartments were then determined in a similar manner.

5.2.6 Calculation of the Transference Number From the definition of transference number[58] the number of millicoulombs carried by the zinc species in solution is $t_+ I \tau$, where I is the current in mA and τ is the time of the run in seconds. Therefore the amount of zinc

ion constituent transferred from the anode compartment to the cathode compartment is $t_+ \frac{I\tau}{2F}$ mmol. At the same time $\frac{I\tau}{2F}$ mmoles of zinc are added to the solution in the anode compartment, and removed from the solution in the cathode compartment, as a result of the electrode reactions. Therefore the change in the amounts of zinc ion constituent in the anode and cathode compartments respectively are given by :-

$$\Delta n_{anode} = (1 - t_+) \cdot \frac{I\tau}{2F} \qquad (5.1a)$$

$$\Delta n_{cathode} = (t_+ - 1) \cdot \frac{I\tau}{2F} \qquad (5.1b)$$

Those changes must be calculated with respect to a constant mass of solvent to ensure that the resulting transference number is referred to a solvent fixed frame of reference. If the average concentration of the solution in the electrode compartment at the end of a run is m_f mol kg^{-1} of solution, and the weight of this solution is W g, the amount of zinc present is $m_f W$ mmol, and this is associated with $W(1 - 10^3 m_f M_s)$ gms of solvent, where M_s is the molecular weight of the solute. At the start of the run the concentration of the solution in the electrode compartment was m_i mol Kg^{-1}, from which it can be shown that the amount of zinc ion constituent associated with one gram of solvent was $m_i/(1 - 10^{-3} m_i M_s)$ mmoles. Therefore :-

$$\Delta n = m_f W - m_i W \frac{(1 - 10^{-3} m_f M_s)}{(1 - 10^{-3} m_i M_s)} \qquad (5.2)$$

$$= \frac{W}{(1 - 10^{-3} m_i M_s)} \cdot (m_f - m_i)$$

Δn is positive for the anode compartment and negative for

the cathode compartment. Combining equations (5.1) and (5.2) gives

$$(1 - t_+) = t_- = \frac{2F}{I\tau} \cdot \frac{W}{(1 - 10^{-3} m_i M_s)} \left| m_f - m_i \right| \qquad (5.3)$$

where t_- is the transference number of the negative ion constituent. Transference numbers were calculated from the experimental results using equation (5.3), with m_i as the average concentration of the solution in the centre compartment, and m_f as the concentration of the mixed solution in either the anode or cathode compartments.

5.2.7 Results The results of the experiments performed with zinc chloride and zinc perchlorate solutions are summarised in tables (5.1) and (5.2) respectively. In these tables the first column gives the molarity of the solution concerned, and the next five columns give the concentrations, in mol Kg^{-1}, of respectively the centre, cathode centre, anode centre, anode, and cathode solutions. The seventh and eighth columns give respectively the weights of solution in the anode and cathode compartments at the end of the run, and the ninth gives the value of the factor $\frac{2F}{I\tau}$ which represents the total amount of electrolysis which has taken place. The final three columns give the transference numbers calculated from the results at the anode and cathode compartments, and the average value, respectively. The results are estimated to have an accuracy of $\pm$ .01 in the average value, the bulk of this error arising in the analysis of the solutions.

The accuracy obtainable by the Hittorf method, even for ideal systems, is limited by the basic factor that the end result depends on a small difference between two relatively large concentrations. The special problems associated with the aqueous solutions

Table 5.1 Experimental Hittorf Transference Numbers for Zinc Chloride

M molarity	m_c	m_{cc}	m_{ac} mols Kg^{-1}	m_a	m_c	W_A gms	W_C gms	$\frac{2F}{I\Upsilon}$ mmoles^{-1}	t_{+a}	t_{+c}	t_{+av}
.15769	.15514	.15528	.15507	.17635	.13577	26.507	28.593	1.13711	.347	.336	.342
.42303	.40395	.40386	.40399	.30417	.50261	28.242	28.218	.23189	.316	.309	.313
.62459	.58378	.58371	.58395	.67860	.48742	25.640	25.116	.27340	.278	.281	.279
.87973	.80205	.80175	.80224	.86745	.73884	29.419	30.256	.35476	.225	.239	.232
1.36069	1.18748	1.18734	-	-	1.18741	-	31.522	.51882	-	.118	.118
2.02064	1.66933	1.66936	1.66853	1.72170	1.61880	31.985	33.720	.46557	- .015	- .022	- .018
2.49453	1.98620	1.98557	1.98667	2.05098	1.92206	33.121	34.054	.37069	- .091	- .109	- .100
2.74507	2.14468	2.14612	-	-	2.08276	-	34.495	.37285	-	- .132	- .132
3.36780	2.51660	2.51678	2.51657	2.57265	2.46229	35.681	36.524	.40614	- .235	- .227	- .231

N.B. m denotes concentration in units of mol Kg^{-1} of solution

Table 5.2 Experimental Hittorf transference numbers for Zinc Perchlorate

Mc molarity	m_c	m_{CC}	m_{AC}	m_A	m_C	W_A	W_C	$\frac{2F}{I\Upsilon}$	t_{+A}	t_{+C}	t_{+av}
			mols Kg^{-1}			gms	gms	$mmoles^{-1}$			
.09730	.095703	-	.095727	.111073	-	26.499	-	1.42207	.406	-	.406
.32225	.30376	.30343	.30391	.32985	.27946	27.835	28.430	.81540	.360	.384	.372
.46084	.42331	.42332	.42372	.51449	.33280	28.838	28.912	.21693	.362	.359	.361
.57431	.51735	.51739	.51646	.55073	.48511	29.161	30.074	.56954	.358	.360	.359
1.01539	.84904	.84857	.84996	-	.77614	-	31.701	.22247	-	.336	.336
1.0408	.86642	.86646	.86722	.89117	.84332	31.402	32.043	.67053	.329	.349	.339
1.15571	.94532	.94536	.94478	-	.90913	-	32.783	.38021	-	.325	.325
1.4636	1.14200	1.14269	1.14220	1.17517	1.11028	33.645	34.190	.43526	.308	.320	.314
1.9656	1.42740	1.42900	1.42770	1.45199	1.40480	36.279	37.146	.50543	.287	.307	.297
2.4247	1.65823	1.65803	-	-	1.63754	-	39.095	.50173	-	.279	.279

N.B. m denotes concentration in mol Kg^{-1} of solution

of the zinc salts make the situation even less satisfactory. The maximum concentration change which could be obtained in the electrode compartments before side reactions at the electrodes began to occur was limited to 10% for the more dilute solutions, falling to 3% for the more concentrated solutions. The formation of an oxide or oxychloride coating on the anode was usually the first side reaction to occur and was the more serious as it markedly affected the results. Gas evolution at the cathode only occurred in a few cases and produced no measurable effect on the results provided it was not excessive. In a few cases in tables (5.1) and (5.2) results are reported only from the cathode compartment. In each of these runs there was a light deposit formed on the anode, but no side reaction at the cathode. In only one run, with the most dilute solution used, was there substantial gas evolution at the cathode and no side reaction at the anode. This was probably caused by the concentration of zinc in the immediate neighbourhood of the cathode becoming so low that the reduction of hydrogen ions in the solution became the favoured reaction.

Potentiometric Measurements on Zinc Chloride Solutions - Measurement of the Concentration Cell Transference Number

5.3.1 Theory The relationship between the potentials developed in concentration cells with and without transport (cell A and cell B with emf's E_A and E_B respectively) is given by equation (5.4) which is derived from equation (2.53)

$$E_A = \int_{\alpha}^{\beta} t_i^c \, dE_B$$

where the integration is from the anode, α, through the cell to the cathode, β, and t_i^c is the local cation transference number. The two types of concentration cell can be written :-

$Ag/AgCl\ ZnCl_{2\ aq}\ (C_2) \quad \underset{LJ}{\|} \quad ZnCl_{2\ aq}\ (C_1)\ AgCl/Ag$ cell A

$Ag/AgCl\ ZnCl_{2\ aq}\ (C_2)\ Zn/ZnHg\ ZnCl_{2\ aq}\ (C_1)\ AgCl/Ag$ cell B

$$C_1 < C_2$$

If C_1 is kept constant and C_2 is varied the cell transference number at concentration C_2 is given by equation (5.5)[58,59]

$$t_i^c = \frac{dE_A}{dE_B} \qquad (5.5)$$

The emf of the cell without transference, E_B, is most conveniently obtained by combining the emf's of cells of the form of cell C.

$Zn/ZnHg \quad ZnCl_2\ (C) \quad AgCl/Ag$ cell C

The anion cell transference number, t_2^c, can be obtained in a similar fashion, using cells D and E, with emf's E_D and E_E respectively.

$Zn/ZnHg\ \ ZnCl_2(C_1) \quad \underset{LJ}{\|} \quad ZnCl_2(C_2)\ \ ZnHg/Zn$ cell D

$Zn/ZnHg\ \ ZnCl_2(C_1)\ \ Ag/AgCl\ \ ZnCl_2(C_2)\ \ ZnHg/Zn$ cell E

The emf of cell E is again obtained by combining the emf's of two cells of type C, and is seen to be equal to E_B. The anion transference number is therefore given by

$$t_2^c = \frac{dE_D}{dE_B} \qquad (5.6)$$

The first step in the measurement of the cell transference number is therefore the measurements of the emf's of cells of types A, C and/or D with C_1 kept constant and C_2 varied through the desired concentration range. Unfortunately if the difference between C_1 and C_2 becomes too large the heat of mixing at the liquid junction introduces unacceptably large errors into E_A and E_D[70]. This difficulty is avoided by covering the concentration range in a stepwise fashion, and using the additivity of cell potentials. Thus for cells 1, 2, and 3

$Zn/ZnHg \quad ZnCl_2(C_1) \| \; ZnCl_2(C_2) \quad ZnHg/Zn$	cell 1
$Zn/ZnHg \quad ZnCl_2(C_2) \| \; ZnCl_2(C_3) \quad ZnHg/Zn$	cell 2
$Zn/ZnHg \quad ZnCl_2(C_1) \| \; ZnCl_2(C_3) \quad ZnHg/Zn$	cell 3

the emf's are related by equation (5.7)

$$E_1 + E_2 = E_3 \qquad (5.7)$$

5.3.2 Experimental Apparatus and Measurements

5.3.2.1 Glass Cell The glass cell used was based on the design of Pikal and Miller[68], and is shown in Fig. 5.2. The cell consisted of two halves, each consisting of four interconnecting electrode compartments, joined by a 120° three way stopcock, C. The third opening of stopcock C was connected to an open tube used in filling the cell. Stopcocks A and B were used for filling the cell.

Two zinc amalgam electrodes and two silver-silver chloride electrodes were placed in each half of the cell. Side 1 of the cell was filled with the more dilute solution and side 2 with the more concentrated, and the liquid junction formed inside stopcock C.

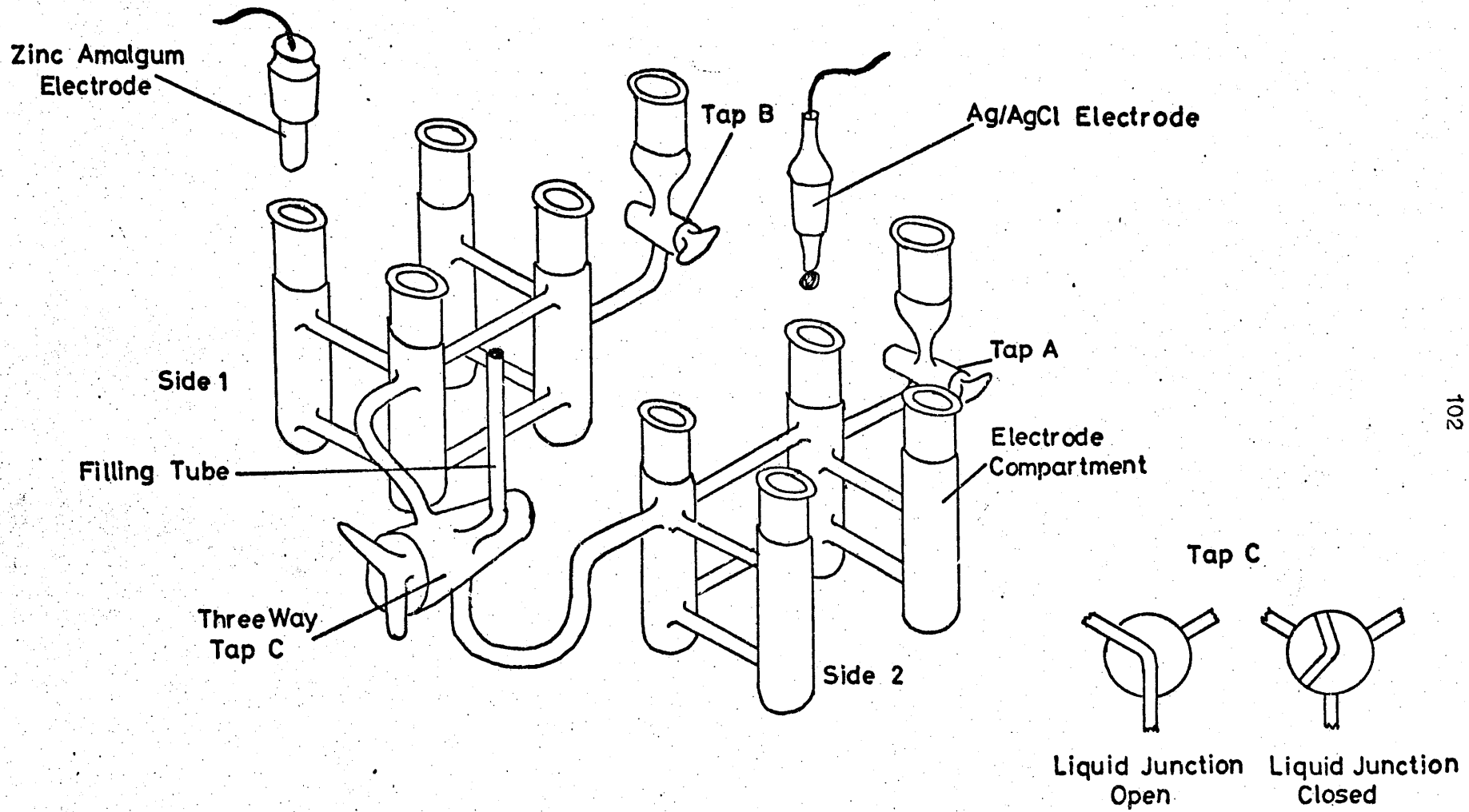

Concentration Cell

Fig. '5.2

In this way the liquid junction was stabilised against gravity mixing by having the denser solution at a lower level. Using this arrangement four separate electrochemical cells were formed. Each half of the glass cell contained a cell of type C, and cells of type A and D were formed across the liquid junction.

5.3.3.2 Preparation of Electrodes Zinc electrodes[63] were prepared by sealing short lengths of spectroscopically-pure zinc rod into B 14/20 Quickfit cones with Araldite epoxy resin. The electrodes were filed smooth, cleaned in strong nitric acid for a few minutes, and then anodised with a large current for a short time. This procedure removed all remaining surface 'roughness'. At this stage the electrodes were dark grey in colour and had bias potentials of approximately 1 mV in dilute zinc chloride solution. These electrodes were lightly amalgamated by immersing them in a solution of mercuric chloride for a few minutes until an even black coat of amalgam formed over them. They were then well rinsed with distilled water and gently polished with a clean dry paper tissue. The electrodes were now bright and silvery and had stable bias potentials, in the absence of oxygen, of less than 0.02 mV. Before each experiment the electrodes were cleaned with nitric acid, and re-amalgamated, before being quickly transferred to the concentration cell, where they were kept under an atmosphere of nitrogen.

The silver-silver chloride electrodes were of the thermo-electrolytic type, and were prepared as recommended by Ives and Janz[71]. A length of platinum wire was sealed into the end of a B 14/20 air leak, twisted into a coil, and cleaned by flaming with ethanol. The

wire was coated with a paste of spectroscopically pure silver oxide in conductivity water and allowed to air dry. The electrode was then roasted in an oven for one hour at 400°C to decompose the oxide to sintered silver metal. The process was repeated twice more to ensure complete coverage of the platinum wire. The electrodes were then anodised for two hours at a potential of 2 V and a current of 2.5 mA per electrode using 0.1 M hydrochloric acid as electrolyte. After ageing for one week the electrodes had stable bias potentials of less than 0.02 mV. When not in use they were stored in dilute hydrochloric acid solution in darkened vessels.

5.3.2.3 Degassing the Solutions and Filling the Cell

The test solutions were prepared by dilution from concentrated stock solutions and analysed by E.D.T.A. titration. The oxygen sensitivity of the zinc amalgam electrodes made it necessary to remove all dissolved air from the solutions by sweeping out with nitrogen. The apparatus for doing this without changing the concentrations of the solutions, and for filling the glass cell under a nitrogen atmosphere, is shown in Fig. 5.3. Cylinder nitrogen was purified by passing through concentrated sulphuric acid, distilled water, concentrated sodium hydroxide solution, sofnolite, and two lots of distilled water. The purified gas could then be fed to any combination of four degassing lines (Fig. 5.3). Each of these lines consisted of three Dreschel bottles containing samples of the solution to be degassed. On passing through the first two bottles of solution the purified nitrogen became saturated with water vapour of the same activity as that of the water in the solution. This prevented any

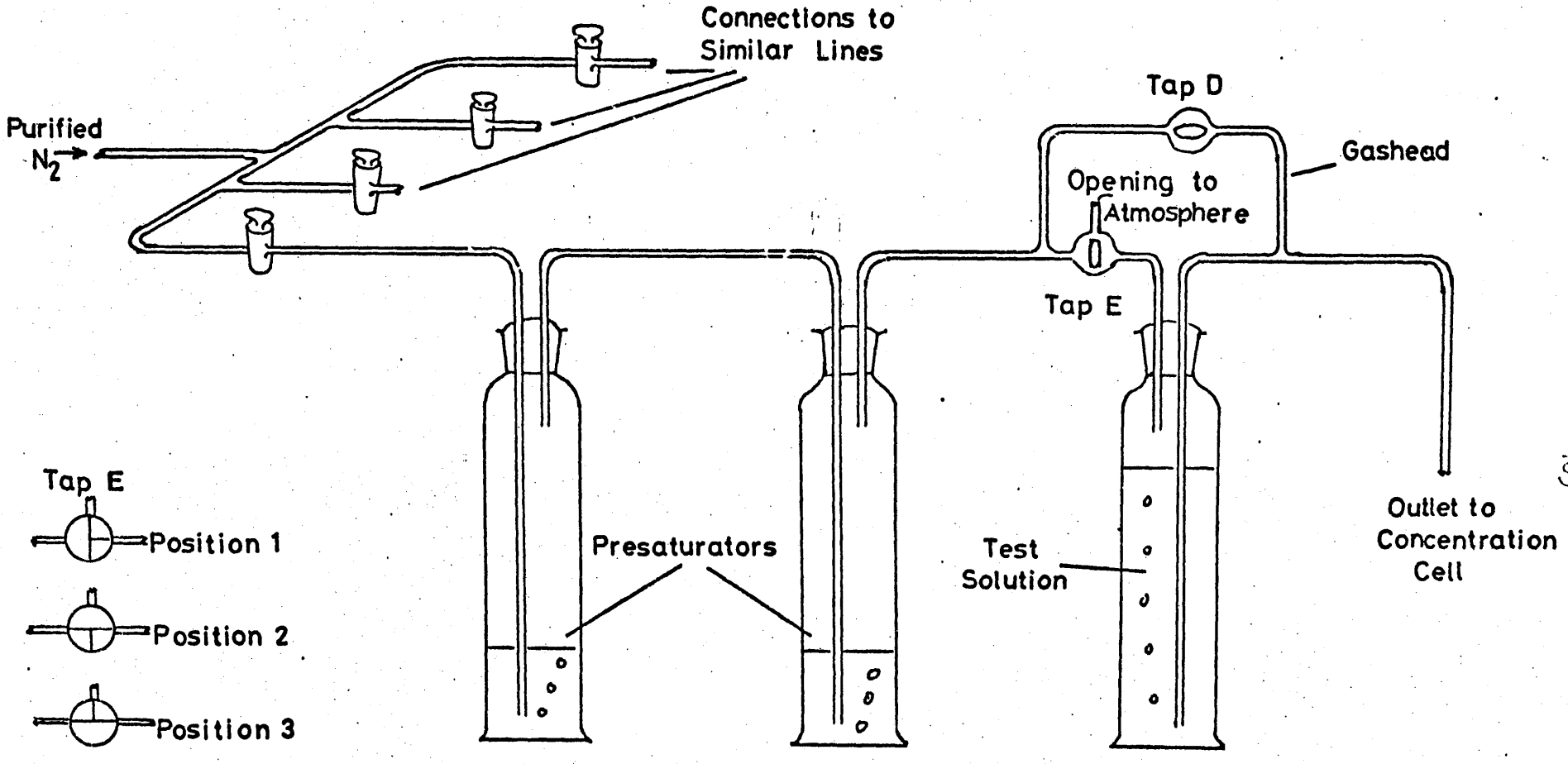

Degassing Line

Fig 5.3

concentration changes occurring in the test solution in the third Dreschel bottle whilst it was being saturated with nitrogen. The final reservoir was fitted with a gashead, which allowed the test solution to be degassed and then dispensed to the concentration cell in the absence of oxygen.

Two degassing lines were used to set up each concentration cell. Purified nitrogen was passed through each solution for half an hour by closing the outlet tube of the gashead, opening tap D, and opening tap E to position 1 to allow the nitrogen to escape into the atmosphere (Fig. 5.3). The outlet tube of the degassing line containing the concentrated solution was then connected to inlet A of the concentration cell. Tap A was opened and tap C was turned to connect side 1 of the concentration cell to the atmosphere (Fig. 5.3). Tap E was turned to position 2. This arrangement allowed nitrogen to pass through the concentration cell and displace the atmospheric oxygen. After a few minutes the electrodes were inserted with the nitrogen still flowing. Tap D was then closed whereupon the gas pressure forced the solution out of the Dreschel bottle, through the outlet tube, and into side 1 of the concentration cell. When the cell was full and free of gas bubbles taps C and A on the cell were closed, and tap E was turned to position 3 to allow the nitrogen to escape to the atmosphere. The procedure was repeated to fill side 2 of the cell with dilute solution from the other degassing line. The cell was then placed in a water thermostat bath whose temperature was regulated to $25^{\circ}C \pm .005^{\circ}C$ and left for an hour to equilibrate.

5.3.2.4 Measurement of the emf's of the Electrochemical Cells

All the potential measurements were made using a Solartron

LM 87 digital voltmeter to a precision of 0.01 mV. As each electrode was duplicated four readings for each emf value were obtained. These four readings were checked to ensure that they agreed within the uncertainty introduced by the bias potentials ($\pm$ .02 mV) and then averaged. In addition the bias potentials of the common electrodes in each solution were checked to ensure that they remained within the acceptable limit. In this way the effect of the bias potentials was at least partly eliminated. In a separate experiment the bias potentials were checked across stopcock C with the same solution in each side of the cell, and were found to be normal.

Potential readings were taken every half hour until they were steady, showing that the electrodes had fully equilibrated with the surrounding solution. This usually happened about four hours after filling the cell. Four sets of readings were then taken over the next two hours, and these values averaged to give the reported emf's. A few runs which were left in the thermostat overnight confirmed that the potentials remained constant within $\pm$ .02 mV at the steady values obtained after a few hours. To minimise diffusion in the liquid junction, stopcock C was only opened when potential readings were actually being taken.

5.3.3 Results The results of the experimental measurements are given in table 5.3, where C_1 and C_2 are the molarities of the solutions in side 1 and side 2 of the cell respectively, E_{C1} and E_{C2} are the emf's of the cells of type C formed in side 1 and side 2 of the glass cell respectively, and E_A^1 and E_D^1 are the emf's of the concentration cells with transference of type A and D respectively. The maximum error in

Table 5.3 Results of potential measurements on Zinc Chloride Solutions

Cell	C_1 mol dm^{-3}	C_2 mol dm^{-3}	E_{C1}	E_{C2}	E_D^1	E_A^1
1	.09877	.42966	1.08136	1.03229	.03220	+ .01685
2	.09971	.21586	1.08151	1.05577	.016724	+ .009037
3	.21554	.43042	1.05578	1.03248	.015399	+ .007898
4	.43422	.74053	1.03233	1.01589	.011599	+ .004872
5	.09788	.25299	1.08143	1.05066	.019874	+ .010905
6	.25116	.43982	1.05071	1.03243	.012275	+ .006018
7	.43385	1.02886	1.03242	1.00573	.019441	+ .007272
8	.74412	1.82970	1.015779	.987252	.023793	+ .004752
9	1.02687	1.81039	1.005639	.987427	.015953	+ .002258
10	1.03820	2.00157	1.005748	.983608	.019552	+ .002609
11	1.82396	2.00143	.987184	.983691	.003435	+ .000086
12	1.82059	2.52408	.987366	.974901	.013874	- .001406
13	2.00665	2.52873	.983524	.974821	.010404	- .001663
14	2.01482	2.98123	.983662	.966708	.019845	- .002891
15	2.54098	2.99870	.974706	.966562	.009531	- .001296
16	2.99053	3.56828	.966723	.955260	.012243	- .000815
17	3.54960	4.44964	.955440	.937913	.023662	- .006060
18	3.00066	4.44508	.966425	.937653	.035938	- .007083
19	.044143	.097078	1.107394	1.081569	.016080	+ .009724
20	1.92445	2.49354	.983383	.974971	.009393	- .000984
21	2.50726	2.97774	.974958	.966398	.009735	- .001148
22	2.98528	3.40550	.966193	.958504	.009273	- .001580

Table 5.3 (cont.)

Cell	C_1 mol dm^{-3}	C_2 mol dm^{-3}	E_{C1}	E_{C2}	E_D^1	E_A^1
23	3.39928	3.63169	.958565	.954133	.005496	- .001057
24	.020869	.099804	1.129957	1.082350	.031499	+ .016100
25	3.65605	3.72739	.953980	.952588	.002347	+ .000955
26	1.35849	2.01556	.997299	.983920	.012714	+ .000673
27	1.36351	2.02185	.997133	.983535	.012578	+ .001020
28	2.01981	2.54603	.983839	.974880	.010165	- .001183
29	1.35494	2.02527	.997701	.983721	.013043	+ .000948
30	.86390	1.35675	1.011339	.997724	.011156	+ .002463
31	1.35706	1.36569	.997452	.997277	.000025	+ .000133
32	.86415	1.36158	1.011333	.997303	.011345	+ .002676
33	.69421	1.35911	1.018026	.997328	.016261	+ .004466
34	.69450	.86394	1.018121	1.011225	.004974	+ .001934
35	.44066	.69540	1.032100	1.018038	.010026	+ .004116
36	.44141	.86365	1.031950	1.011251	.014959	+ .005887

the emf's reported in table 5.3 is expected to be $\pm$ .02 mV. This determined primarily by the magnitude of the bias potentials between pairs of electrodes used.

Using equation (5.4) and choosing the 0.09836 M solution as the reference, table 5.4 was produced from the data in table 5.3. In table 5.4 C is the concentration denoted by C_2 in section (5.3.1), E_C is the emf of the cell of type C containing this concentration of solution, and E_A, E_B and E_C are the emf's of cells of type A, B and C respectively in which C_1 = 0.09836 M and C_2 = C. T_1 and T_2 are the integral transference numbers defined by equations (5.8)

$$T_1 = \frac{E_A}{E_B} \qquad (5.8a)$$

$$T_2 = \frac{E_D}{E_B} \qquad (5.8b)$$

Whenever there was more than one way to combine the data in table 5.3 all possible combinations were averaged. The emf's in table 5.4 are expected to have an uncertainty of $\pm$ .08 mV, and the concentrations an accuracy of 0.2%.

5.3.4 Calculation of Transference Numbers Transference numbers were obtained from the potential measurements by evaluation of the differentials in equations (5.5) and (5.6). Several analytical methods are available for this purpose. The most obvious is to obtain polynomial expressions of the form

$$y = \sum_{i=0}^{n} a_i x^i \qquad i = 1, 2 \ldots 5$$

between E_A and E_B, and E_D and E_B, by the method of least squares, and

Table 5.4 emf's of Zinc Chloride Concentration Cells with dilute solution of .09836 Mol dm^{-3}

C mol dm^{-3}	E_C	E_D	E_A	E_B	T_1	T_2
.020869	1.129957	- .031499	- .016100	- .048490	.33203	.64960
.044143	1.107394	- .016080	- .009724	- .025927	.37505	.62020
.09836	1.081467	0	0	0	-	-
.21570	1.055775	.016724	.009037	.025692	.35174	.65094
.25208	1.050685	.019874	.010905	.030782	.35427	.64564
.43459	1.032390	.032157	.016903	.049080	.34440	.65546
.69470	1.018062	.042214	.021010	.063405	.33136	.66578
.74233	1.015835	.043756	.021775	.065632	.33177	.66669
.86391	1.011287	.047146	.022859	.070180	.32572	.67179
1.03131	1.005706	.051598	.024175	.075761	.31910	.68106
1.35625	.997626	.058267	.025307	.083841	.30185	.69497
1.36168	.997268	.058516	.025535	.084199	.30327	.69563
1.82116	.987307	.067550	.026480	.094160	.28122	.71740
2.00926	.983604	.071068	.026675	.097863	.27257	.72620
2.02021	.983827	.071270	.026232	.097640	.26066	.72993
2.52492	.974853	.081448	.025043	.106594	.23494	.76410
2.98151	.966296	.091183	.023895	.115171	.20747	.79172
2.99278	.966605	.090946	.023811	.114862	.20730	.79178
3.40239	.958535	.100456	.022315	.122932	.18152	.81717
3.55894	.955350	.103189	.023051	.126117	.18277	.81820
3.63169	.954133	.105952	.021264	.127334	.16699	.83208
4.44736	.937783	.126866	.016887	.143684	.11753	.88295

Table 5.5 Coefficients of Curve Fit Polynomials of Potential Measurements on Zinc Chloride Solutions

Fit	a_0	a_1	a_2	a_3	a_4	a_5
E_D v E_B - 0.05 V : - 0.06 V	0.000262	0.631785	- 0.0534551	8.189898	-	-
E_D v E_B 0.05 V : 0.14 V	0.016831	0.0533332	5.695713	- 5.066991	-	-
E_Av E_B - 0.05 V : 0.06 V	- 0.000304	0.367491	0.260517	-11.62264	-	-
E_Av E_B 0.05 V : 0.14 V	- 0.015136	0.887446	- 5.103338	3.278092	-	-
ln (C) v E_B - .05 V : 0.07 V	- 2.314729	30.48875	-17.03441	315.18583	-	-
C v E_B 0.06 : 0.14	- 1.074049	16.55036	157.81060	-	-	-
T_+ v E_B	0.332373	0.815566	1.148625	-270.84934	1046.1093	-
T_- v E_B	0.669557	- 0.750755	- 5.571925	321.84132	-1212.7433	-

simply differentiate those. This was done and the coefficients of the polynomials obtained are shown in table 5.5. However the results of the differentiation were totally unsatisfactory. The transference numbers obtained showed enormous variations over quite small concentration ranges, and the agreement between t_1^c obtained from equation (5.5) and t_2^c obtained from equation (5.6) was extremely poor. No good reason could be found for these variations, as the polynomial expressions reproduced the experimental data within the expected accuracy.

Far more satisfactory results were obtained when the differentials were evaluated by the method of Rutledge[58,72]. This method enables the derivative of a differentiable function, y, of x to be obtained at evenly spaced values of x. A fourth degree polynomial is used as a differentiating tool and applied successively to sets of five different points of data, (x_{-2},y_{-2}), (x_{-1},y_{-1}), (x_0,y_0), (x_1,y_1), and (x_2,y_2), where the x values are separated by equal intervals, h. It is not required that the polynomial should adequately represent the data as a whole. The values of the derivatives at x_{-1}, x_0, and x_1 are given by equation (5.9)

$$\frac{dy}{dx} = \frac{1}{12h} \left(C_{-2}y_{-2} + C_{-1}y_{-1} + C_0y_0 + C_1y_1 + C_2y_2\right) \qquad (5.9)$$

The values of the coefficients are given in table 5.6

	C_{-2}	C_{-1}	C_0	C_1	C_2
x_{-1}	-3	-10	18	-6	1
x_0	1	18	0	8	-1
x_1	-1	6	-18	10	3

Table 5.6 Coefficients of Rutledge Function

When more than five experimental points are available the process can be repeated stepwise along the data to give three values for the derivative at each point, except for the points at the extreme end of the data.

A computer programme was written in Algol to perform this calculation, and is reproduced in the Appendix. Equally spaced values of E_B were chosen and the corresponding values of E_D calculated from the least squares curve fit polynomial. Using equation (5.8) t_2^c was calculated at each value of E_B. The concentrations to which these values of E_B corresponded were then calculated from a least squares curve fit polynomial of concentration against E_B. The calculations were repeated using E_B and E_A to calculate the corresponding values of t_1^c. The transference numbers obtained by this method depended slightly upon the degree of the curve fit polynomial between E_B and E_A or E_D. The most self consistent results were obtained using third degree fits between E_D and E_B and between E_A and E_B. Unfortunately above 2.6 mol dm^{-3} the answers were still discordant.

Pikal and Miller[68] have described another method of obtaining t_1^c and t_2^c using the integral transference numbers defined by equations (5.7). Differentiating equations (5.8a) and (5.8b) with respect to E_B gives equations (5.10a) and (5.10b)

$$t_1^c = T_1 + E_B \frac{\partial T_1}{\partial E_B} \qquad (5.10a)$$

$$t_2^c = T_2 + E_B \frac{\partial T_2}{\partial E_B} \qquad (5.10b)$$

The differentials in equations (5.9) were evaluated from polynomial curve fits of T_1 and T_2 against E_B (see table 5.5 for coefficients) using the methods described above, the most self-consistent results being given by the fourth degree polynomials. This method proved to be much better in the higher concentration range; below 2.4 M the agreement between t_1^c and $(1 - t_2^c)$ was poor.

5.3.5 Results In table 5.7 the 'best' values of t_1^c and $(1-t_2^c)$ are listed along with the average value of t_1^c. The experimental error, based on the accuracy of the potential measurements, is probably $\pm$ .003 in the dilute solutions, rising to $\pm$ .010 in the more concentrated areas. The values below 2.6 M were obtained by the Rutledge method and those above 2.4 M by Pikal and Miller's method. The results are graphed against molarity in Fig. (5.4). Also included in Fig. (5.4) are the experimental results obtained by the Hittorf method, and the literature data of Harris and Parton[63] and Hittorf[65,66]. Two conclusions can be drawn from Fig. (5.4). Firstly there is approximate agreement of the present work with the published data which is better at higher concentrations, and secondly the cell and Hittorf transference numbers also agree within the expected experimental error. This implies that the Onsager Reciprocal relations are valid. Fig. (5.5) shows a plot of the cell transference numbers of Stokes and Levien[64] for zinc perchlorate against molarity, and for comparison the Hittorf data obtained from this work. Again the two sets of transference numbers agree within experimental error, implying the validity of the ORR for this salt also. A more direct test of the ORR will be given for both salts in chapter 6.

Table 5.7 Cell emf Transference numbers for Zinc Chloride

Concentration mol dm^{-1}	t_1 from cell D	t_1 from cell A	t_1 Average
0.0	-	-	.409
.2236	.353	.356	.355
.3030	.339	.339	.339
.4120	.319	.315	.317
.4814	.307	.300	.304
.6316	.280	.275	.277
.8193	.233	.230	.232
1.0148	.187	.186	.187
1.2148	.145	.143	.144
1.4294	.097	.100	.098
1.6490	.053	.057	.055
1.8761	.010	.015	.013
2.1111	- .032	- .027	- .029
2.3541	- .073	- .068	- .070
2.6049	- .114	- .108	- .111
2.4083 *	- .078	- .071	- .075
2.6560 *	- .127	- .118	- .123
2.9163 *	- .174	- .164	- .169
3.1845 *	- .218	- .209	- .214
3.4605 *	- .258	- .252	- .255
3.7445 *	- .294	- .290	- .292

* These values were obtained from equation (5.10).

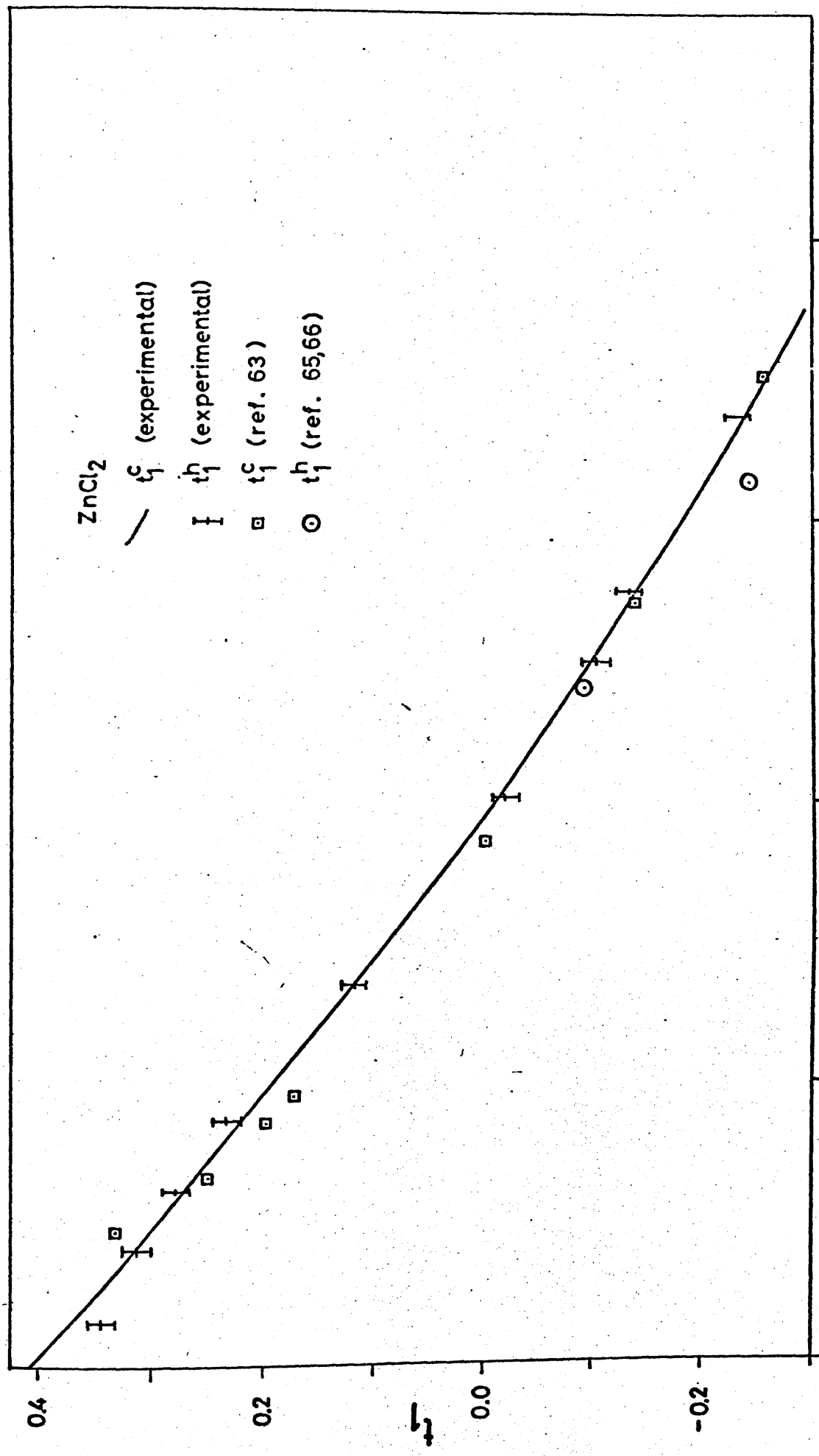
ZnCl2
t_1^c (experimental)
t_1^h (experimental)
t_1^c (ref. 63)
t_1^h (ref. 65,66)
t_1
0.4
0.2
0.0
-0.2
0
1
2
3
4
Molarity

Fig. 54

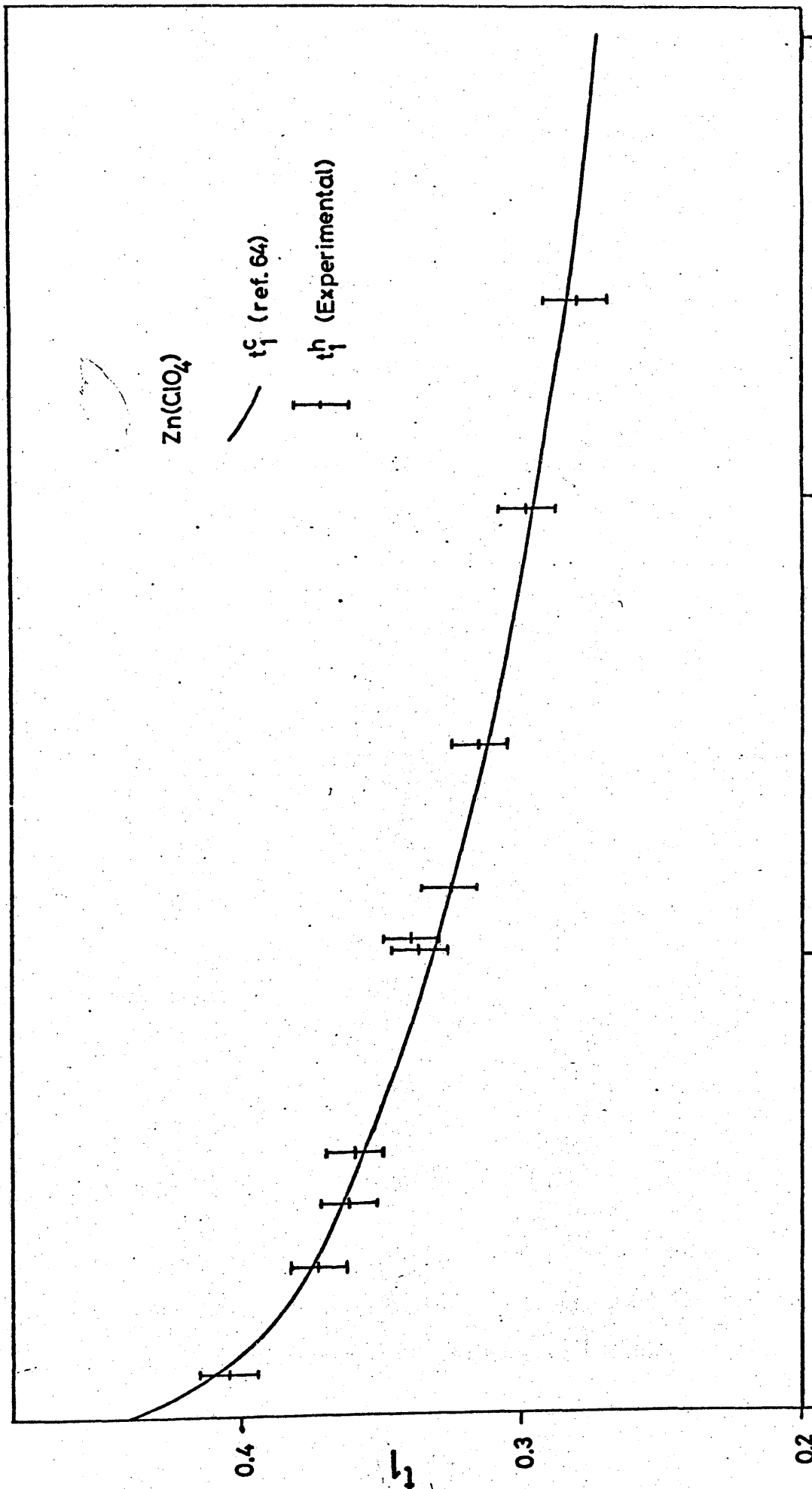

Fig 5.5

5.3.6 Calculation of Activity Coefficients from the Potentiometric Data The emf of a cell of type C is given by equation (5.11)

$$E_c = E^o - \frac{RT}{2F} \ln 4\, m_{12}^3\, \gamma_{\pm}^3 \qquad (5.11)$$

where m_{12} is the molality of the solution in the cell, $\gamma_{\pm}$ is the mean molal activity coefficient, and E^o is the standard electrode potential. Equation (5.11) can be used, in conjunction with the potentiometric measurements made above, to calculate values of the activity coefficient at various concentrations, provided the standard electrode potential can be estimated. Several values for this parameter are available in the literature although the agreement between them is rather poor[63,73,74,75]. However in a parallel study in this laboratory Dunsmore, Lutfullah and Paterson[76] have carried out precise measurements of the emf's of cells of type C containing very dilute zinc chloride solutions, and from these have derived a value for E^o of 0.98409 ± .02 mV. This value was used for the calculation of activity coefficients for two reasons. Firstly, Lutfullah has obtained emf values at concentrations far lower than previously reported using electrodes of the type described in section (5.3.3.2) thus making the extrapolation technique used to estimate E^o more accurate, and secondly Lutfullah used zinc chloride solutions which were identical to those used in this work.

The values of $\gamma_{\pm}$ calculated from the potentials listed in table 5.4 are given in table 5.8. The expected accuracy, based on the experimental errors in E_c and m_{12}, is ± 2.5%. In Fig. (5.6) values of $\gamma_{\pm}$ from table 5.8, and from the literature[59,63,73] are

Table 5.8 Mean Molal Activity Coefficient of Zinc Chloride calculated from emf Results

Molarity	Molality	E_C	$\gamma_{\pm}$
0.09836	0.09862	1.08147	.511
0.2157	0.2159	1.05578	.454
0.4346	0.4398	1.03239	.409
0.6947	0.7085	1.01806	.368
1.0313	1.0632	1.00571	.338
1.3617	1.4200	0.99727	.315
2.0093	2.1477	0.98360	.297
2.0202	2.1604	0.98383	.294
2.5249	2.7580	0.97485	.290
2.9928	3,3386	0.96661	.297
3.6317	4.1718	0.95413	.328

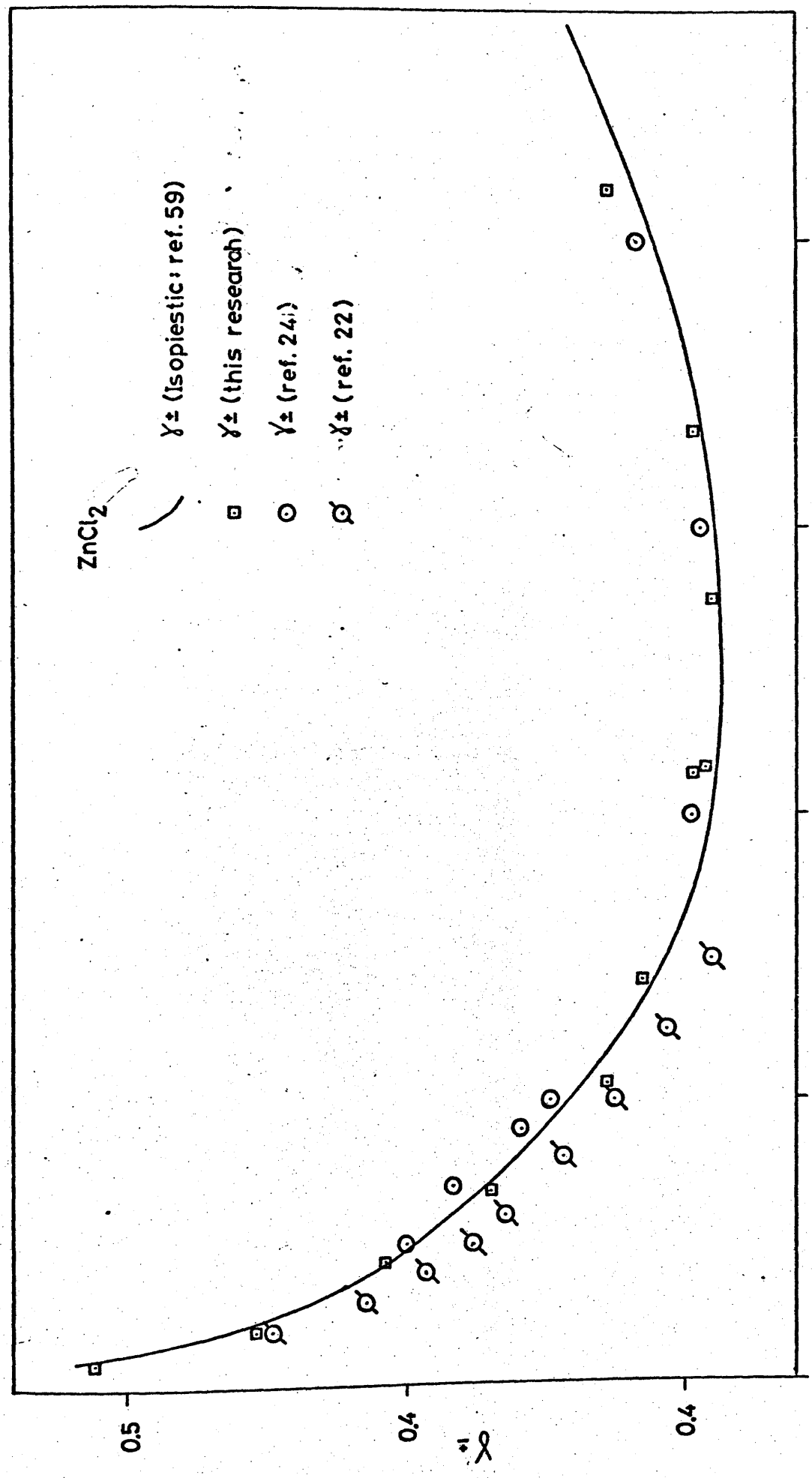
$ZnCl_2$
γ± (isopiestic; ref. 59)
γ± (this research)
γ± (ref. 24)
γ± (ref. 22)
0.5
0.4
0.4
γ±
0
1
2
3
4
Molarity

Fig. 5.6

plotted against molality. The results of the present study agree, within the estimated errors, with those of Harris and Parton[63], and the isopiestic data of Robinson and Stokes[59]. Scatchard and Tefft's[73] values appear to be somewhat low, especially at higher concentrations.

Chapter 6

Results and Discussion of The Irreversible Thermodynamic Analysis

6.1 Calculation of the Irreversible Thermodynamic Coefficients

This was done using the theory discussed in Chapter 2. The mobility coefficients were calculated using equation (2.64) and the frictional coefficients were obtained by matrix inversion using equations (2.64), (2.65) and (2.66). The experimental data required were values of equivalent conductivity, Λ, cation transference number, t_1, volume fixed diffusion coefficient, D_v, and the activity term, $(1 + \frac{\partial \ln \gamma_\pm}{\partial \ln m})$, along with the solution density to allow interconversion between the molar and molal concentration scales. The calculations were performed for zinc chloride and zinc perchlorate solutions.

6.1.1 Data for Zinc Chloride Values of Λ and D_v were calculated at round number concentrations using curve fit polynomials of the experimental data reported in Chapters 3 and 4 respectively. The uncertainty in the smoothed values was estimated to be $\pm$ 0.05% for Λ and $\pm$ 0.3% for D_v. The limiting values for each at infinite dilution were calculated using the limiting ionic conductances, λ_i^o, given by Robinson & Stokes[31]. Cell emf transference numbers, t_1^c, were obtained at round number concentrations from a large scale plot of the experimental t_1^c data reported in chapter 6. Since the Hittorf and emf transference numbers were equal within experimental error the O.R.R. were assumed. This assumption will be justified in section (6.2). The uncertainty in t_1^c is estimated to be $\pm$ .007. The value of t_1 at infinite dilution

was calculated from the limiting equivalent conductivities. The solution densities used were the data reported in chapter 3 and have an estimated uncertainty of ± 0.01%.

The activity term was calculated from the isopiestic activity coefficient data of Robinson and Stokes[31]. Using this data curve fit polynomials of ln ($\gamma_{\pm}$) as a function of molality were obtained and differentiated by the method of Rutledge[72] Section (5.3.4) . The coefficients of the curve fit polynomials are given in table 6.1. The uncertainty in the activity term is estimated to be ± 0.5%.

6.1.2 Data for Zinc Perchlorate Values of Λ and D_v were obtained from the data given in chapters 3 and 4 as described above and have uncertainties of ± .05% and ± .3% respectively. The transference numbers used were the cell emf values reported by Stokes & Levien[64], which these authors estimate to have an uncertainty of ± 0.002. As for zinc chloride the t_1^h values reported in chapter 6 and the t_1^c values were found to coincide within experimental error. The solution densities used were those reported in chapter 3 and had an uncertainty of ± .01%. The activity term was calculated in the same way as for zinc chloride using the activity coefficient data of Robinson & Stokes[31]. The coefficients of the curve fit polynomials between ln($\gamma_{\pm}$) and molality are given in table 6.1.

6.1.3 Results of Calculations The calculations were carried out by a computer using an Algol programme reproduced in the appendix. The results for zinc chloride and zinc perchlorate are given in tables 6.2 and 6.3 respectively. In table 6.4 the results of a similar analysis on barium chloride by Miller[9a] are reported. Also given in tables 6.2,

Table 6.1 Coefficients of Curve Fit Polynomials between $\ln\gamma_{\pm}$ and molality for Zinc Chloride and Zinc Perchlorate

	a_o	a_1	a_2	a_3	a_4	a_5
Zinc Chloride 0.0 - 0.2 m	-0.001941	-44.85305	1758.212	-32651.44	253510.9	-645418.7
Zinc Chloride 0.3 - 5.0 m	-0.685284	-0.561454	0.191802	-0.027493	0.0017624	-
Zinc Perchlorate 0.1 - 1.2 m	-0.538632	-0.491337	1.401362	-0.460680	-	-
Zinc Perchlorate 1.0 - 4.0 m	-0.095851	0.968917	0.430310	0.637674	-0.037420	-

Table 6.2 Zinc Chloride - Irreversible Thermodynamic Parameters

C mol dm^{-3}	m mol Kg^{-1}	Λ $cm^2 ohm^{-1} equiv^{-1}$	t_1	$10^5 D_v$ $cm^2 s^{-1}$	$1 + \frac{\partial \ln \gamma_\pm}{\partial \ln m}$
0.0	0.0	129.15	0.410	1.2090	1.0000
0.1	0.1004	89.31	0.385	1.0310	0.9508
0.2	0.2012	80.43	0.362	1.0051	0.9092
0.3	0.3024	73.33	0.340	0.9930	0.8650
0.4	0.4042	67.77	0.319	0.9862	0.8287
0.5	0.5066	62.56	0.297	0.9822	0.8004
0.6	0.6095	57.89	0.279	0.9801	0.7803
0.7	0.7130	53.72	0.256	0.9794	0.7771
0.8	0.8173	49.98	0.235	0.9801	0.7515
0.9	0.9223	46.64	0.214	0.9820	0.7451
1.0	1.0279	43.65	0.193	0.9850	0.7412
1.5	1.5601	32.74	0.084	1.0159	0.7928
2.0	2.1348	25.91	-0.009	1.0701	0.8872
2.5	2.7278	21.09	-0.094	1.1401	1.0304
3.0	3.3521	17.48	-0.176	1.2013	1.2057
3.5	1.1430	14.67	-0.252	1.2478	1.4182

N	L_{11}/N $\times 10^{12}$	L_{12}/N $\times 10^{12}$	L_{22}/N $\times 10^{12}$	$C_1 R_{11}$ $\times 10^{-11}$	$C_2 R_{22}$ $\times 10^{-11}$
0.0	1.396	0.000	8.080	3.582	1.238
0.4472	1.084	0.332	6.544	4.679	1.551
0.6325	1.026	0.489	6.490	5.053	1.598
0.7746	1.000	0.660	6.518	5.361	1.644
0.8944	0.985	0.809	6.575	5.647	1.692
1.0000	0.974	0.950	6.623	5.970	1.756
1.0954	0.966	1.064	6.612	6.293	1.839
1.1832	0.942	1.146	6.584	6.732	1.927
1.2649	0.950	1.270	6.647	7.065	2.020
1.3416	0.944	1.351	6.640	7.478	2.126
1.4142	0.937	1.422	6.628	7.909	2.237
1.7321	0.868	1.587	6.396	10.559	2.865
2.0000	0.811	1.635	6.078	13.462	3.594
2.2361	0.749	1.605	5.688	16.870	4.444
2.4494	0.684	1.534	5.275	20.978	5.442
2.6458	0.617	1.433	4.838	25.932	6.616

N	C_0	$-C_2 R_{12}$ $\times 10^{-11}$	$-C_0 R_{10}$ $\times 10^{-11}$	$-C_0 R_{20}$ $\times 10^{-11}$	$C_0^2 R_{00}/N$ $\times 10^{-11}$
0.0	55.345	0.0	3.582	1.2376	3.028
0.4472	55.185	0.461	4.218	1.3204	3.414
0.6325	55.185	0.762	4.291	1.2173	3.363
0.7746	55.061	1.086	4.275	1.1012	3.239
0.8944	54.932	1.390	4.257	0.9970	3.126
1.0000	54.791	1.712	4.258	0.8994	3.028
1.0954	54.645	2.026	4.267	0.8256	2.959
1.1832	54.494	2.343	4.389	0.7551	2.950
1.2649	54.337	2.700	4.365	0.6704	2.853
1.3416	54.168	3.044	4.435	0.6037	2.821
1.4142	54.001	3.395	4.515	0.5398	2.793
1.7321	53.061	5.242	5.317	0.2438	2.902
2.0000	52.003	7.243	6.220	-0.0277	3.082
2.2361	50.869	9.520	7.350	-0.3158	3.359
2.4494	49.679	12.198	8.780	-0.6570	3.732
2.6458	48.478	15.359	10.573	-1.064	4.222

Table 6.3 Zinc Perchlorate - Irreversible Thermodynamic Parameters

C mol dm^{-1}	m mol Kg^{-1}	Λ $cm^2 ohm^{-1} equiv^{-1}$	t_1	$10^5 D_v$ $cm^2 s^{-1}$	$1 + \frac{\partial \ln \gamma_\pm}{\partial \ln m}$
0.0	0.0	120.16	0.439	1.1821	1.0000
0.1	0.1009	87.57	0.409	1.0357	0.9790
0.2	0.2032	81.65	0.389	1.0617	1.0010
0.3	0.3070	77.65	0.377	1.0966	1.0250
0.4	0.4122	74.52	0.368	1.1342	1.1193
0.5	0.5189	71.66	0.360	1.1752	1.3231
0.6	0.6271	68.99	0.359	1.2104	1.4492
0.7	0.7369	66.45	0.348	1.2476	1.5804
0.8	0.8485	64.03	0.342	1.2838	1.7184
0.9	0.9617	61.73	0.337	1.3187	1.8645
1.0	L.0766	59.52	0.332	1.3521	2.0195
1.5	1.6801	49.21	0.311	1.4903	2.9271
2.0	2.3368	39.67	0.294	1.5635	3.9891
2.5	3.0569	30.83	0.280	1.5480	5.1099
3.0	3.8512	22.78	0.271	1.4198	6.3585

N	l_{11}/N x 10^{12}	l_{12}/N x 10^{12}	l_{22}/N x 10^{12}	$C_1 R_{11}$ x 10^{-11}	$C_2 R_{22}$ x 10^{-11}
0.0	1.407	0.0	7.241	3.530	1.381
0.4472	1.105	0.286	6.130	4.582	1.651
0.6325	1.045	0.384	6.127	4.898	1.671
0.7746	0.982	0.392	5.980	5.228	1.717
0.8944	0.915	0.356	5.771	5.602	1.776
1.0000	0.847	0.308	5.541	6.028	1.842
1.0954	0.794	0.276	5.338	6.415	1.908
1.1832	0.747	0.252	5.157	6.807	1.972
1.2649	0.703	0.231	4.987	7.218	2.036
1.3416	0.664	0.210	4.816	7.639	2.105
1.4142	0.626	0.191	4.653	8.085	2.176
1.7321	0.470	0.1184	3.878	10.718	2.599
2.0000	0.356	0.0848	3.178	14.151	3.167
2.2361	0.269	0.0736	2.531	18.765	3.982
2.4494	0.195	0.0580	1.901	25.874	5.310

N	C_0	$-C_2 R_{12}$ x 10^{-11}	$-C_0 R_{10}$ x 10^{-11}	$-C_0 R_{20}$ x 10^{-11}	$C_0^2 R_{00}/N$ x 10^{-11}
0.0	55.345	0.0	3.530	1.381	3.146
0.4472	54.997	0.4274	4.154	1.438	3.515
0.6325	54.623	0.614	4.284	1.364	3.506
0.7746	54.250	0.686	4.542	1.374	3.645
0.8944	53.871	0.692	4.910	1.430	3.885
1.0000	53.493	0.670	5.358	1.507	4.186
1.0954	53.113	0.663	5.752	1.576	4.552
1.1832	52.728	0.665	6.142	1.639	4.710
1.2649	52.339	0.668	6.550	1.702	4.977
1.3416	51.949	0.668	6.971	1.772	5.257
1.4142	51.558	0.665	7.420	1.844	5.553
1.7321	49.558	0.655	10.064	2.271	8.303
2.0000	47.508	0.756	13.395	2.789	9.487
2.2361	45.397	1.091	17.674	3.437	12.273
2.4494	43.241	1.596	24.279	4.513	16.652

Table 6.4 Barium Chloride - Irreversible Thermodynamic Parameters

c	m	Eqv Cond	t+	$D(v)\times10^5$	$1+\frac{\partial \ln \gamma_\pm}{\partial \ln m}$
0.0000	0.00000	139.98	0.4546	1.3850	1.0000
0.0010	0.00100	132.11	0.4483	1.3200	0.9457
0.0050	0.00501	123.93	0.4419	1.2670	0.8998
0.0100	0.01003	119.03	0.4381	1.2390	0.8759
0.0500	0.05020	105.19	0.4249	1.1780	0.8295
0.1000	0.10060	98.56	0.4162	1.1600	0.8252
0.2000	0.20160	91.55	0.4036	1.1500	0.8415
0.5000	0.50760	80.50	0.3793	1.1610	0.9264
1.0000	1.02790	68.90	0.3527	1.1790	1.0980

N	$L_{11/N}$ x 10^{12}	$L_{12/N}$ x 10^{12}	$L_{12/N}$ x 10^{12}	C_1R_{11} x 10^{-11}	C_2R_{22} x 10^{-11}
0.0000	1.7080	0.0000	8.1969	2.9275	1.2200
0.0472	1.6514	0.1223	8.0726	3.0132	1.2402
0.1000	1.5965	0.2522	7.9328	3.1476	1.2670
0.1414	1.5645	0.3287	7.8406	3.2243	1.2867
0.3162	1.4648	0.5294	7.5559	3.5022	1.3578
0.4472	1.4036	0.6043	7.3884	3.6924	1.4029
0.6325	1.3193	0.6543	7.1728	3.9696	1.4602
1.0000	1.1536	0.6675	6.7015	4.5994	1.5835
1.4143	0.9521	0.5992	5.9884	5.6045	1.7821

N	C_0	$-C_2R_{12}$ x 10^{-11}	$-C_0R_{20}$ x 10^{-11}	$-C_0R_{20}$ x 10^{-11}	$-C_0{}^2R_{00/N}$ x 10^{-11}
0.0000	55.345	0.0000	2.9275	1.2240	2.6842
0.0472	55.343	0.0919	2.9393	1.1942	2.6639
0.1000	55.349	0.2001	2.9475	1.1669	2.6407
0.1414	55.316	0.2703	2.9540	1.1516	2.6286
0.3162	55.288	0.4907	3.0115	1.1125	2.6177
0.4472	55.179	0.6040	3.0884	1.1009	2.6451
0.6325	55.066	0.7242	3.2453	1.0981	2.7205
1.0000	54.678	0.9163	3.6831	1.1253	2.9669
1.4142	154.003	1.1216	4.4829	1.2213	2.5556

6.3 and 6.4 are the values of various coupling coefficients which will be discussed in a later section.

6.2 Validity of the Onsager Reciprocal Relations It was shown in chapter 2 that the cell emf and Hittorf transference numbers can only be identical if the ORR are true. Miller[13] has shown, however, that this does not necessarily mean that good experimental agreement between t_1^h and t_1^c provides a good test of the ORR. This is illustrated by equation (6.1).

$$\frac{t_1^h}{t_1^c} = \frac{Z_1 l_{11} + Z_2 l_{12}}{Z_1 l_{11} + Z_2 l_{21}} \qquad (6.1),$$

from which it is clear that a sensitive test of the ORR can only be obtained when l_{12} and l_{21} are large relative to l_{11}. This is, in general, only true in binary electrolyte solutions when there is a significant amount of ion paining. Two tests of the ORR on such systems have been published recently, by Miller and Pikal[14] for silver nitrate, and by McQuillan[15] for cadmium chloride, both of which show the ORR to be valid within $\pm$ 1%. It seems worthwhile, therefore, to add to these a test of the ORR for zinc chloride solutions, which provide another system where the cross coefficients l_{12} and l_{21} are large relative to the direct coefficients, l_{11}.

6.2.1 Equations for testing the ORR From equation (2.) equation (6.2) can be easily derived.

$$\frac{l_{21}}{l_{12}} = 1 - \left(\frac{\Lambda}{10^3 F^2 Z_1 Z_2}\right) \cdot \frac{(t_1^h - t_1^c)}{l_{12}/_N} \qquad (6.2)$$

The ratio $\frac{l_{21}}{l_{12}}$ should, of course, be unity if the ORR are true.

Miller[14] performed an error analysis on equation (6.2) and showed that the uncertainty in the ratio, $\frac{l_{21}}{l_{22}}$, was due almost entirely to the experimental uncertainties in the transference numbers, δt_1^h and δt_1^c. The uncertainty in $\frac{l_{21}}{l_{12}}$ is given by equation (6.3)

$$\delta\left(\frac{l_{21}}{l_{12}}\right) = \frac{\Lambda}{10^3 F^2 (l_{12}/_N)} \cdot (\delta t_1^h + \delta t_1^c) \qquad (6.3)$$

From these equations it is seen that the sensitivity of the test of the ORR is increased by a low value of Λ as well as a high value of l_{12}.

6.2.2 Results of the test for zinc chloride and zinc perchlorate The data used for insertion into equations (6.3) and (6.4) were obtained as follows. For each experimental value of t_1^h the corresponding value of t_1^c was read from a large scale plot and the value of Λ calculated from the relevant polynomial fit of the experimental data. The value of $l_{12/N}$ was obtained from a large scale plot of the data in tables 6.2 and 6.3. The results are shown in table 6.5 for zinc chloride and table 6.6 for zinc perchlorate.

Table 6.5 shows that for zinc chloride the ORR are clearly obeyed within the rather generous errors of $\pm$ 5% for the dilute solutions to $\pm$ 1% for the concentrated solutions. The results for zinc perchlorate in table 6.6 are less satisfactory. The ORR are obeyed within the experimental uncertainty, but this uncertainty is $\pm$ 15% for the dilute solutions rising to $\pm$ 30% for the concentrated ones. This occurs despite the fact that the experimental data are, if anything, more precise than those for zinc chloride. This finding thus bears out

Table 6.5 Onsager Reciprocal Relations for Zinc Chloride

Molarity	t_1^h	t_1^c	$l_{12}/_N$ x 10^{12}	$l_{12}/_{l_{21}}$	Error limit in ratio
0.4230	.313	.314	0.847	0.997	± 0.06
0.6246	.279	.272	1.099	1.019	± 0.04
0.8797	.232	.222	1.331	1.019	± 0.03
1.3607	.118	.119	1.568	0.999	± 0.01
2.0206	- .018	- .011	1.636	0.994	± 0.01
2.4945	- .100	- .096	1.598	0.997	± 0.01
2.7451	- .132	- .140	1.565	1.005	± 0.01
3.3678	- .231	- .239	1.464	1.005	± 0.01

Table 6.6 Onsager Reciprocal Relations for Zinc Perchlorate

Molarity	t_1^h	t_1^c	$l_{12}/_N$ x 10^{12}	$l_{12}/_{l_{21}}$	Error limit in ratio
0.0973	.406	.409	.385	0.963	± 0.15
0.3223	.372	.374	.455	0.982	± 0.15
0.4608	.361	.363	.350	0.978	± 0.17
0.5743	.355	.359	.287	0.948	± 0.22
1.0154	.336	.330	.190	1.100	± 0.25
1.0408	.339	.329	.185	1.170	± 0.25
1.1557	.325	.324	.164	1.018	± 0.26
1.4636	.314	.312	.122	1.044	± 0.27
1.9656	.297	.295	.089	1.049	± 0.27
2.4247	.279	.282	.076	0.932	± 0.28

Miller's[13,14] statement that a good agreement between t_1^h and t_1^c does not imply a good percentage test of the ORR, and is a consequence of the fact that for zinc perchlorate $l_{11} >> l_{12}$. However, since the overwhelming weight of experimental evidence is in favour of the ORR, and since there is no evidence to the contrary, they will be assumed for zinc perchlorate.

6.3.1 Evidence for Complexing in Aqueous Solutions of Zinc Salts

The principal aim of this thesis is to compare the transport properties of a salt which shows extensive self complexing in solution with those of a salt in which self complexing is absent. Zinc chloride was chosen as the self complexing salt and zinc perchlorate as the standard. It is, therefore, worthwhile to review the evidence for complex formation in zinc halides and the lack of it in other 2:1 zinc salts.

The first evidence for complex formation in zinc halides came from the early transference number measurements of Hittorf[66] which produced negative cation transference numbers at higher concentrations. These findings were confirmed by later workers who surveyed a wide concentration range of the zinc halides by the emf method[24,74-76]. Those results were explained by postulating the presence in solution of complexes of zinc and halide ions, X^-, of the form ZnX_n^{2-n}, where n can have a maximum value of 4. It was assumed that when the concentrations of the negatively charged zinc species, ZnX_3^- and ZnX_4^{2-}, were high enough more zinc ion constituent would be carried to the anode by anionic complexes than would be carried to the cathode by the positively charged species Zn^{2+} and $ZnCl^+$. Thus the cation transference number would become negative.

More evidence for complex formation in zinc halides was provided by the activity coefficient data for 2:1 salts which was largely provided by the work of Robinson, Stokes, and co-workers[31,77]. A comparison of plots of the variation of the mean molal activity coefficient, $\gamma_{\pm}$, with molal concentration showed that at higher concentrations the activity coefficients of the zinc halides were lower than would be expected. The assumption was that dissociated 2:1 zinc salts would have activity coefficients which would be very similar to those of analogous magnesium salts. This was found to be true of the perchlorates and nitrates[64], but not of the halides except in dilute solutions. The deviation was explained by the presence of complexes in the halide solutions which caused them to exhibit weak electrolyte behaviour in more concentrated solutions.

The presence of complexing in zinc halide solutions received its final confirmation from Raman spectroscopic studies[78-85]. The Raman spectra showed lines which could be unambiguously assigned to the covalently bonded complexes.

In contrast, there is no evidence of extensive complexing in solutions of zinc nitrate and zinc perchlorate. Raman studies have been undertaken on solutions of both salts[62,86] with completely negative results. The activity coefficients of both salts[77,64] and the transference numbers of zinc perchlorate[64], show 'normal' behaviour. There is, however, some conflicting evidence from electrical conductance studies that zinc perchlorate solutions are not entirely without ion association effects. Davies & Thomas[87] found no evidence for ion association. Dye, Faber and Karl[88] found anomalous behaviour in the

equivalent conductivity of zinc perchlorate solutions, but were reluctant to ascribe this to the formation of the ion pair, $ZnClO_4^+$, because they could not obtain a reproducible value for the association constant. Frei and Podlahova[89], on the other hand, quote a value of 4.5 ± 10^{-2} for the first association constant of zinc perchlorate.

There are, consequently, conflicting opinions upon the degree of dissociation of zinc perchlorate in aqueous solution. The indirect methods for estimating this, such as electrical conductivity and emf studies, depend entirely on the assumption that the properties of a dilute solution may be calculated from electrolyte theory. Deviations from theory may often suggest new, associated, species in solution. However the validity of such theories as the Onsager limiting law and the Debeye-Hückel limiting law is open to question in 2:1 electrolytes. It seems preferable, therefore, to favour the direct evidence which suggests that zinc perchlorate is not associated to any significant extent.

6.3.2 Review of the Experimental Results with Reference to Complex Formation in Zinc Chloride Solutions The experimental results, obtained as described in the preceding chapters, may now be reviewed. Special reference is made to the effect of self complexing by comparing the properties zinc chloride solutions with those of zinc perchlorate and zinc nitrate. In some cases data for barium chloride and calcium chloride are included for additional comparison.

6.3.2.1 Equivalent Conductivity The equivalent conductivities of zinc chloride, zinc perchlorate, and zinc nitrate were plotted in Fig (3.5) as a function of molar concentration. At low concentrations

the curves for the three salts follow a similar trend, but at higher concentrations the curve for zinc chloride falls considerably below those of zinc nitrate and zinc perchlorate. This may be explained by the formation of the neutral species, $ZnCl_2$, which reduces the number of charge carriers present in solution. At higher concentrations, however, the curve for zinc chloride approaches these of the two other salts. This probably occurs because the concentrations of the anionic complexes increase at the expense of the neutral complex, thus making more charge carrying species available.

6.3.2.2 Diffusion Coefficients The diffusion coefficients of zinc chloride and zinc perchlorate, obtained as described in chapter 4, are plotted against molar concentration in Fig (6.1). The diffusion coefficients of calcium chloride[90] and barium chloride[91] are also included for comparison. Fig (6.1) shows that the behaviour of the diffusion coefficient of zinc chloride is different from that of the other three salts. The curves for zinc perchlorate, calcium chloride, and barium chloride all have minima between 0.1 and 0.2 mol dm^{-3}, and the curves for calcium chloride and zinc perchlorate both show maxima at approximately 2.0 mol dm^{-3}. For zinc chloride, however, the minimum value of the diffusion coefficient occurs approximately 0.8 mol dm^{-3}, and a maximum value is not attained in the range of measurement.

The direct comparison of those coefficients is hindered by the fact that they are affected by variations in two factors, the activity term, $(1 + {}^{d\ln\gamma_\pm}/_{d\ln m})$, and the thermodynamic mobility of the salt, $\frac{\overline{M}}{C}$. The salt mobility, $\frac{\overline{M}}{C}$, is related to the measured diffusion coefficient by equation (2.58)

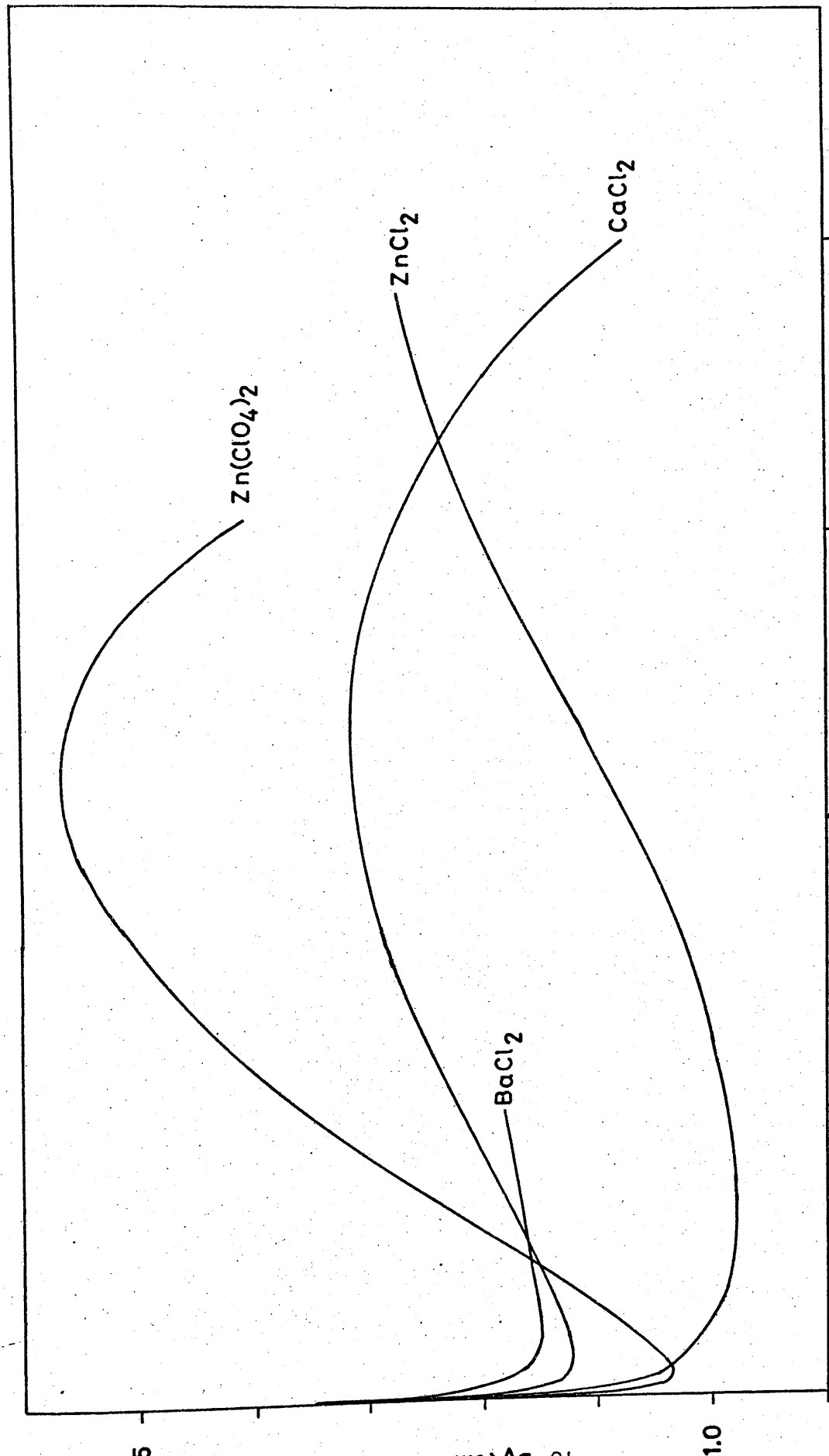

Fig 6.1

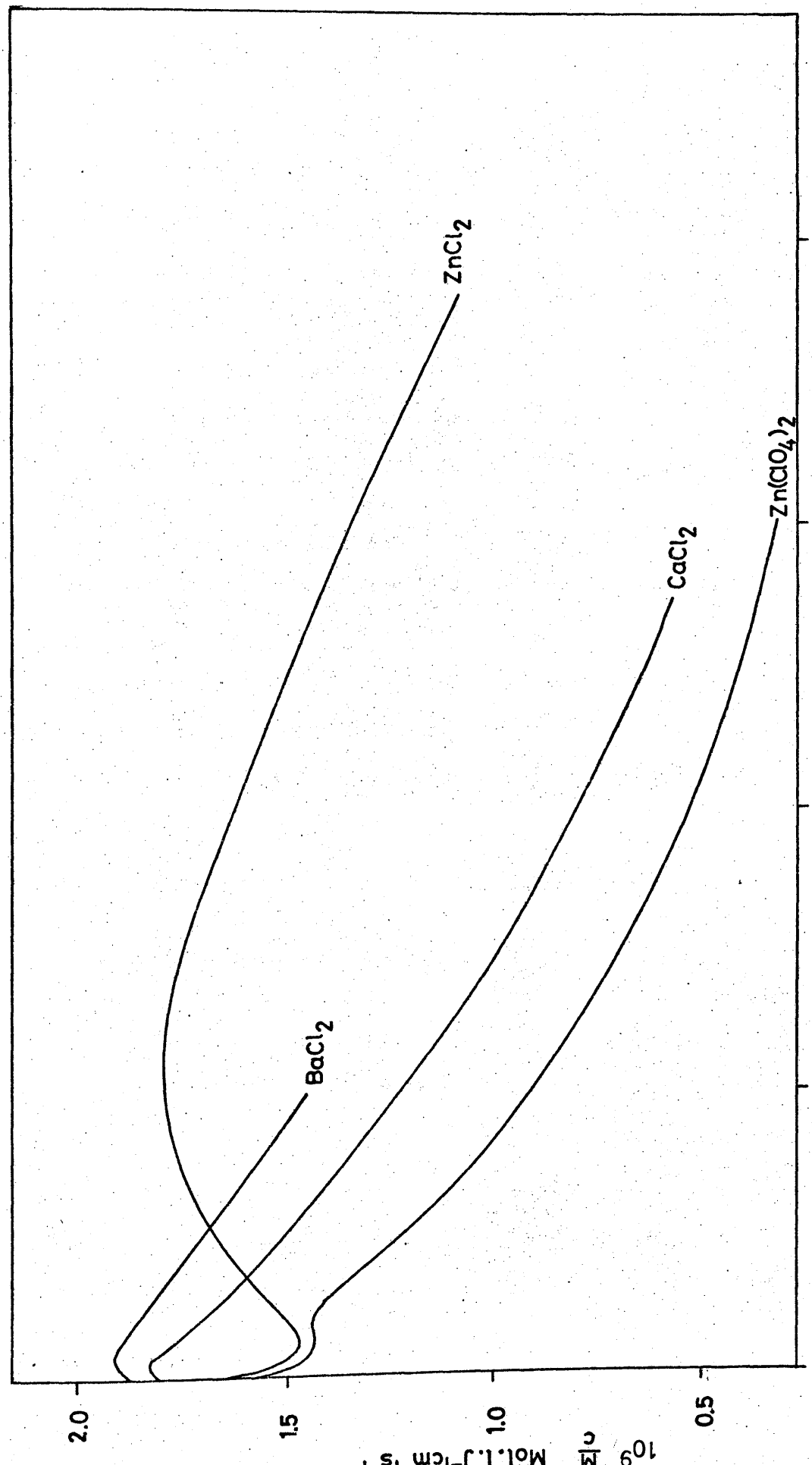
$10^9 \frac{\sigma}{M}$ Mol.l.J^{-1}cm^{-1}s^{-1}
2.0
1.5
1.0
0.5
0
1
2
3
4
Molarity
$ZnCl_2$
$CaCl_2$
$Zn(ClO_4)_2$
$BaCl_2$

Fig. 6.2

$$D_v = \frac{\overline{M}}{C} \cdot 10^3 rRT \quad (1 + \frac{\partial \ln \gamma_{\pm}}{\partial \ln m}) \qquad (2.58)$$

Values of $\frac{\overline{M}}{C}$ were calculated, using equation (2.58), for the four salts represented in Fig (6.1). These values, plotted against molal concentration in Fig (6.2), show more clearly the anomalous behaviour of zinc chloride. Above 0.2 mol dm^{-3} the curves of the three 'normal' salts fall smoothly in parallel with increasing concentration. The curve for zinc chloride however rises to a maximum at approximately 1.0 mol dm^{-3}, crossing the curves for calcium chloride and barium chloride.

6.3.2.3 Transference Numbers These were discussed in section (6.3.1). A comparison of Figs (5.4) and (5.5) shows that whereas the cation transference number for zinc perchlorate falls slightly with increasing concentration, that of zinc chloride becomes negative in solutions more concentrated than 2.0 mol dm^{-3}. This is undoubtedly due to the presence of negatively charged complexes in solution.

6.4 Discussion of the Irreversible Thermodynamic Parameters

6.4.1 The Mobility Coefficients The direct mobility coefficients, L_{ii}, define the flow of species i caused by a unit thermodynamic force on i when all other forces in the phenomenological equations are zero. The cross coefficients, L_{ij}, define the flow of species i caused by a unit thermodynamic force on species j when all other forces are zero. Both types of coefficient show a first order dependence on concentration. Consequently it is usual to discuss the function $L_{ij}/_N$, where N is the equivalent concentration, as the variations in these parameters now reflect changes in the environments of the ions.

At infinite dilution $L_{ii}/_N$ is directly related to the limiting equivalent conductivity of i, λ_i^o, by equation (6.4)

$$\left(\frac{L_{ii}}{N}\right)_{N\to 0} = \left(\frac{L_{ii}}{N}\right)^o = \frac{\lambda_i^o}{10^3 Z_i^2 F^2} \qquad (6.4)$$

$(L_{ii}/_N)$ is, therefore, solely a function of the interactions between i and the bulk solvent. At finite concentrations theoretical considerations [14,92] indicate that $L_{ii}/_N$ will be reduced by long range electrostatic ion-ion interactions, the relaxation effect, and by modifications to the bulk solvent caused by the presence of ions in solution. It is also expected that $L_{ii}/_N$ will be influenced by the presence of ion association or complexing [14, 92] and that the sign of this contribution will depend on the system considered.

The cross coefficients $L_{ij}/_N$ represent the interactions between species i and j. By definition they will be zero at infinite dilution. At finite concentrations the $L_{ij}/_N$ will be positive if i and j are of opposite sign and will consist of contributions from ion-solvent and ion-ion long range interactions. There will also be a large, positive contribution from any ion association or complexing which may be present [92].

6.4.1.1 <u>The Direct Coefficients</u> The coefficients $L_{11}/_N$ and $L_{22}/_N$ for zinc chloride, zinc perchlorate, and barium chloride are plotted against the square root of the equivalent concentration in Figs (6.3) and (6.4) respectively. On the y axes of Figs (6.3) and (6.4) scales of $Z_1^2(\underline{L_{11}})$ and $Z_2^2(\underline{L_{22}})$ are also marked to enable comparisons to be made between the coefficients for ions of differing valency types.

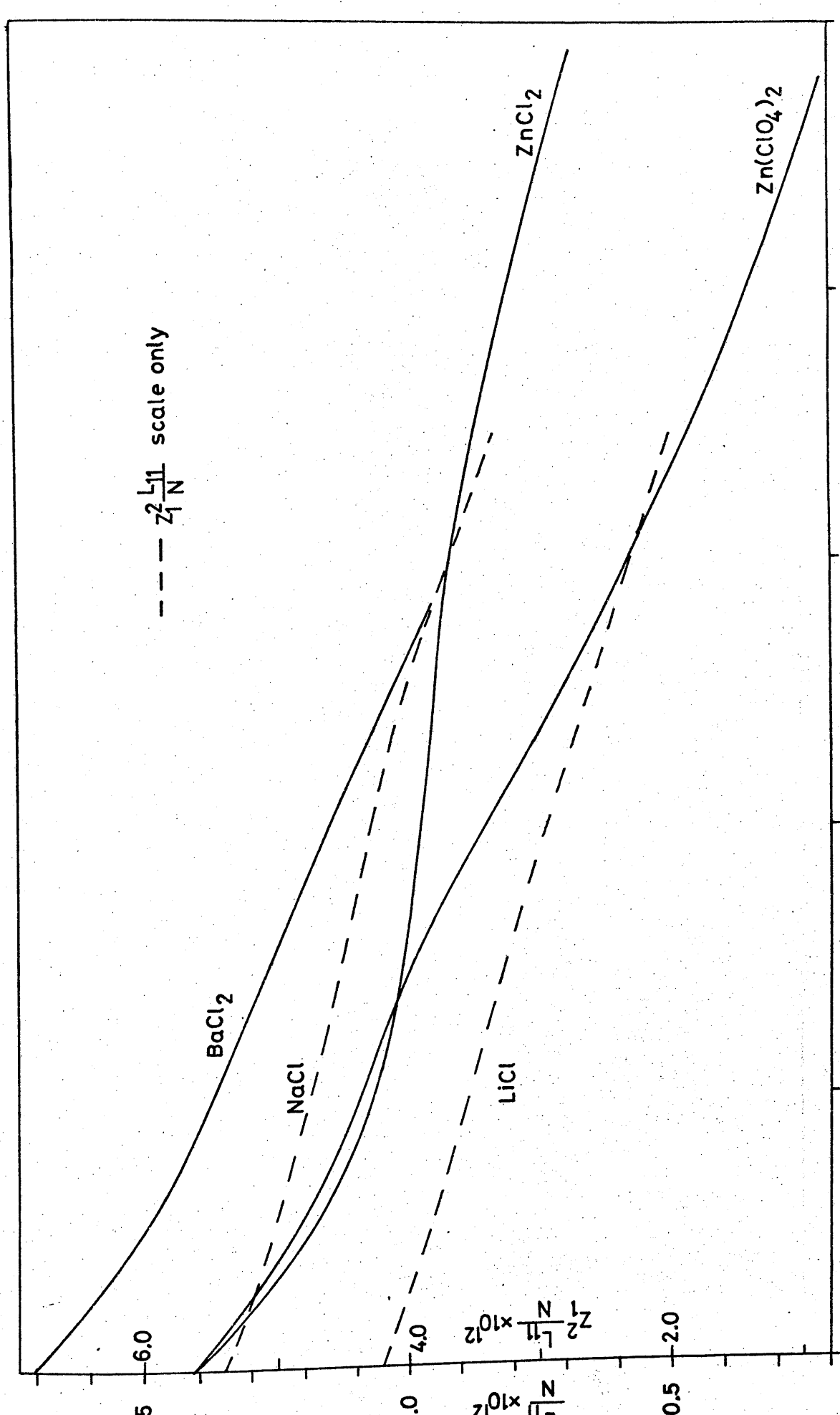
$ZnCl_2$
$Zn(ClO_4)_2$
$BaCl_2$
NaCl
LiCl
- - - $Z_1^2 \frac{L_{11}}{N}$ scale only
$\frac{L_{11}}{N} \times 10^{12}$
$Z_1^2 \frac{L_{11}}{N} \times 10^{12}$
$\sqrt{N}$
0
0.5
1.0
1.5
2.0
2.5
0.5
1.0
1.5
2.0
4.0
6.0

Fig 6.3

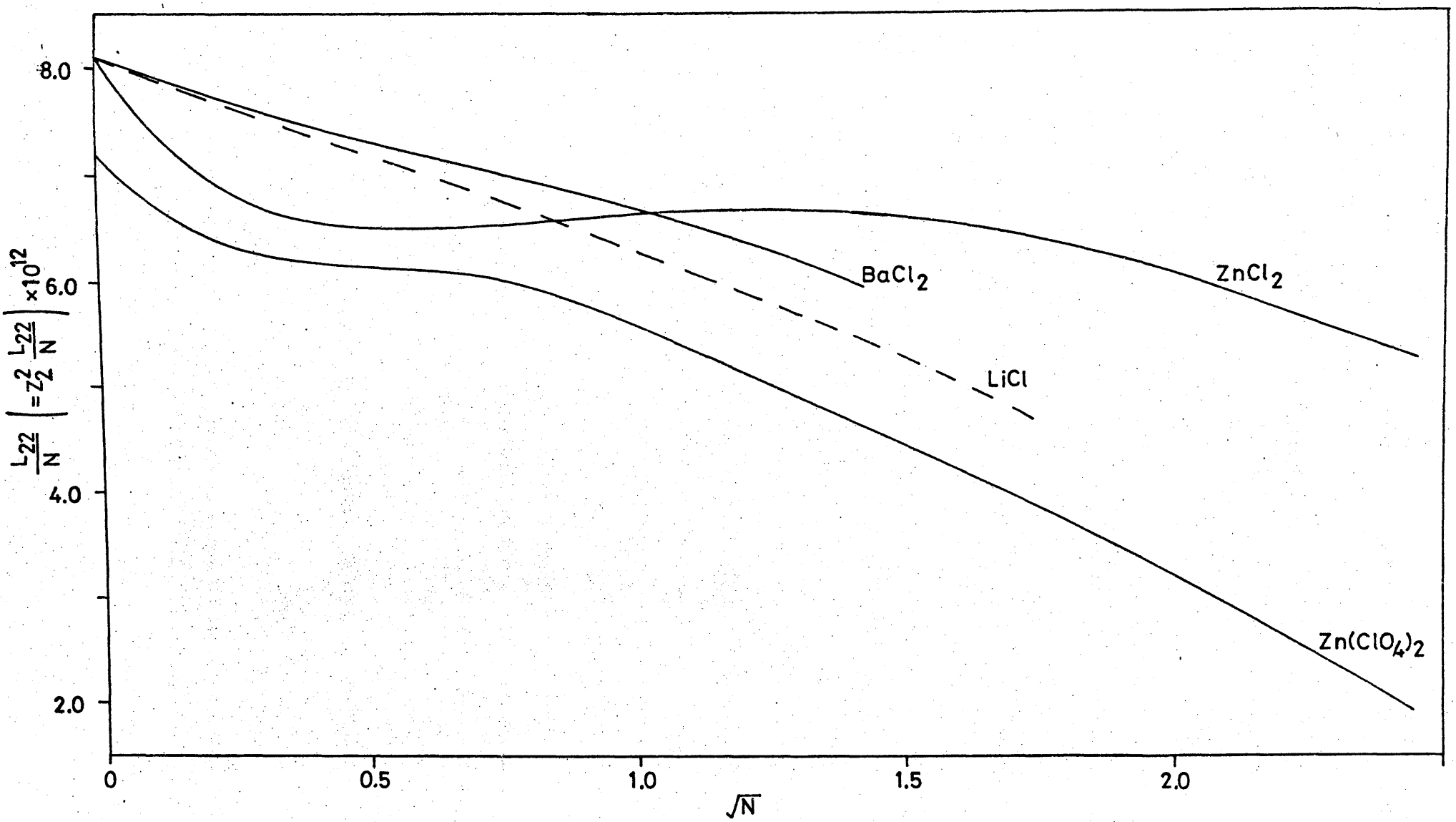
8.0
6.0
4.0
2.0
$\frac{L_{22}}{N}\left(=Z_2^2\frac{L_{22}}{N}\right)\times10^{12}$
0
0.5
1.0
1.5
2.0
$\sqrt{N}$
$BaCl_2$
$ZnCl_2$
LiCl
$Zn(ClO_4)_2$

Fig 6.4

This procedure was suggested by equation (6.4) and the usual practice of considering λ_i^o values when comparing the properties of different ions.

The value of L_{11}/N at infinite dilution is a function of the degree of solvation of the cation. As the smaller Zn^{2+} ion is more heavily solvated than the Ba^{2+} ion, $(\frac{L_{11}}{N})^o$ is lower for the zinc salts. This behaviour corresponds to that of the alkali halides[33,99] where the smallest ion, Li^+, has the lowest value of $(\frac{L_{11}}{N})^o$. As the electrolyte concentration is increased $\frac{L_{11}}{N}$ falls as a result of the negative contributions of the relaxation and electrophoretic effects mentioned above. For barium chloride and zinc perchlorate the curves of $\frac{L_{11}}{N}$ fall in an approximately parallel manner. For zinc chloride, however, the $\frac{L_{11}}{N}$ curve follows the zinc perchlorate curve closely until approximately 0.25 mol dm^{-3}, after which it falls less steeply. This is probably due to self-complexing. The positive deviation suggests that the complex or complexes formed have a higher mobility than the uncomplexed zinc ion[92]. It may also be noted that the curves of $Z_1^2(\frac{L_{11}}{N})$ for zinc perchlorate and barium chloride fall more steeply with increasing concentration than the corresponding curves for the alkali halides. This is shown in Fig (6.3) where values of $Z_1^2(\frac{L_{11}}{N})$ for lithium chloride and sodium chloride are plotted.

The variation of $\frac{L_{22}}{N}$ with concentration, shown in Fig (6.4) is mainly influenced by the effect of the cationic counter-ion on the solvent structure. As the electrolyte concentration increases $\frac{L_{22}}{N}$ for zinc perchlorate and barium chloride decreases as the increasing solvent structure and long range coulombic interactions reduce the ease with which the anion can move through the solution. The behaviour of $Z_2^2 L_{22}/N$ for

zinc perchlorate and barium chloride is similar to that of $Z_2^2 \frac{L_{22}}{N}$ for lithium chloride, as can be seen from Fig (6.4) where values for LiCl are included for comparison. Again zinc chloride solutions show different behaviour. Until approximately 0.25 mol dm^{-3} the curves of $\frac{L_{22}}{N}$ for zinc chloride and zinc perchlorate are roughly parallel, but above this concentration the curve for zinc chloride goes through a slight maximum before falling less steeply than the zinc perchlorate curve. As for $L_{11}/_N$ this behaviour may be ascribed to the presence of self-complexing in the more concentrated zinc chloride solutions. The similarity of $L_{11}/_N$ and $L_{22}/_N$ for zinc chloride and zinc perchlorate in dilute solutions implies that in these solutions self complexing of zinc chloride is not important.

6.4.1.2 <u>The Cross Coefficients</u> The coefficients $L_{12}/_N$ for zinc chloride, zinc perchlorate, and barium chloride are plotted against the square root of the equivalent concentration in Fig (6.5). By analogy with the direct coefficients the cross coefficients of salts of differing valence types are best compared using the function $|Z_1 Z_2| (\frac{L_{12}}{N})$. This scale is therefore also marked on the y axis of Fig (6.5).

The first observation from Fig (6.5) is that, as expected, $\frac{L_{12}}{N}$ for zinc chloride is very much greater at high concentrations than $\frac{L_{12}}{N}$ for zinc perchlorate or barium chloride. This is obviously the result of a large contribution to $\frac{L_{12}}{N}$ from the effects of self complexing. As for the direct coefficients the $\frac{L_{12}}{N}$ values for zinc chloride and zinc perchlorate are very similar below 0.25 mol dm^{-3}, implying that at low concentrations complex formation in zinc chloride solutions is not extensive. The $\frac{L_{12}}{N}$ curves for barium chloride and zinc perchlorate

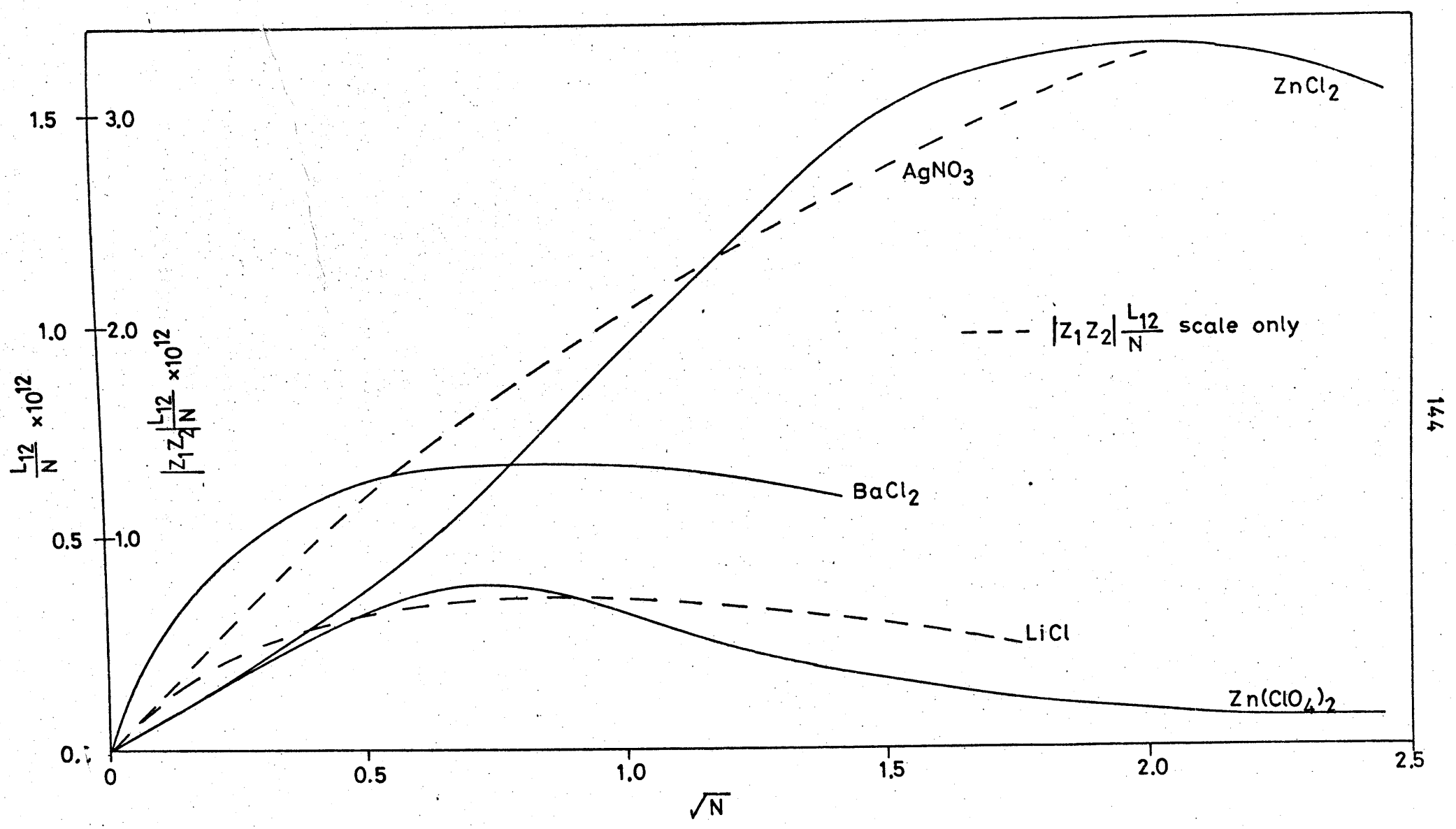
1.5
3.0
1.0
2.0
0.5
1.0
0.
$\frac{L_{12}}{N} \times 10^{12}$
$|Z_1Z_2|\frac{L_{12}}{N} \times 10^{12}$
$ZnCl_2$
$AgNO_3$
$BaCl_2$
LiCl
$Zn(ClO_4)_2$
$|Z_1Z_2|\frac{L_{12}}{N}$ scale only
0
0.5
1.0
1.5
2.0
2.5
$\sqrt{N}$

Fig 6.5

show similar trends, although $L_{12}/_N$ is always larger for the barium salt. A similar situation is found in the alkali chloride series where the salts with larger cations have larger values of $\frac{L_{12}}{N}$. Values of $|Z_1Z_2|\frac{L_{12}}{N}$ for lithium chloride and potassium chloride are plotted in Fig (6.5). The crystallographic radii of the Li^+ and Zn^{2+}, and the K^+ and Ba^{2+} ions respectively are similar. It can be seen from Fig (6.4) that so also are the values of $|Z_1Z_2|\frac{L_{12}}{N}$ for the corresponding salts.

Fig (6.5) also includes values of $|Z_1Z_2|\frac{L_{12}}{N}$ for silver nitrate, published by Miller and Pikal [14], which can be seen to be of comparable magnitude to the values for zinc chloride. It is well known that there is considerable ion-pairing in concentrated silver nitrate solutions which would be expected to lead to high values of $\frac{L_{12}}{N}$. From the data in Fig (6.5) it appears that self-complexing and ion-pairing provide similar contributions to $\frac{L_{12}}{N}$.

6.4.2 <u>The Frictional Coefficients</u> These are given by equation (2.38) which is obtained by matrix inversion of equation (2.21). Equation (2.28) defines the force on any species, i, in terms of the flows of all species in solution. The coefficients R_{ij} therefore represent the friction between species i and j. The frictional coefficient approach provides two main interpretive advantages over the mobility coefficient approach, both arising from the identity $\sum_{j=o}^{n} C_j R_{ij} = 0$. Firstly the coefficients are independent of the frame of reference chosen for the flows[9a], and secondly additional coefficients, R_{io}, are obtained which directly measure the friction between ion and solvent.

The significance of the R_{ik} coefficients is greatly clarified by the mechanistic interpretation of Spiegler[94] who considered the force

on ion i in solution, X_i, to be exactly balanced by the sum of all the frictional forces, $\tilde{x}_{ij}$, between i and all the other species in solution, equation (6.5)

$$X_i = \sum_{\substack{j=o \\ i=j}}^{n} - \tilde{x}_{ij} = \sum_{\substack{j=o \\ i=j}}^{n} f_{ij} \ (v_i - v_j) \qquad (6.5)$$

In equation (6.5) f_{ij} is the coefficient of kinetic friction between i and j and $(v_i - v_j)$ is the velocity of i relative to j.

The coefficient of kinetic friction, f_{ij}, can be identified with the frictional coefficients, R_{ij}, as follows. On a solvent fixed frame of reference, equation (2.28) becomes

$$\begin{aligned} X_1 &= R_{11}J_1 + R_{12}J_2 \\ X_2 &= R_{21}J_1 + R_{22}J_2 \end{aligned} \qquad (6.6)$$

Equation (2.29) is now used to eliminate R_{11} and R_{22}, giving equation (6.7)

$$\begin{aligned} X_1 &= R_{12}\left(\frac{C_2}{C_1} J_1 - J_2\right) - R_{10}\left(\frac{C_o}{C_1} J_o\right) \\ X_2 &= R_{21}\left(\frac{C_1}{C_2} J_2 - J_1\right) - R_{20}\left(\frac{C_o}{C_2} J_2\right) \end{aligned} \qquad (6.7)$$

Equation (2.18) is now used in equation (6.7) to give the flows, J_i, in terms of the velocities of the ions relative to the solvent, $(v_i - v_o)$, giving equations (6.8)

$$\begin{aligned} X_1 &= - C_2R_{12}(v_1 - v_2) - C_oR_{10}(v_1 - v_o) \\ X_2 &= - C_1R_{21}(v_2 - v_1) - C_oR_{20}(v_2 - v_o) \end{aligned} \qquad (6.8)$$

Inspection of equations (6.5) and (6.8) shows them to be

identical in all respects. The interpretation of the frictional coefficients is, therefore, that the term $-C_jR_{ij}$ represents the coefficient of kinetic friction, f_{ij}, between one mole of species i and the surrounding species j in one litre of solution. In comparing electrolytes of different valence types it is more useful to consider the function $\frac{-C_jR_{ij}}{|Z_i|}$ which represents the coefficient of kinetic friction between one equivalent of species i and the surrounding species j in one litre of solution.

6.4.4.1 The Direct Coefficients C_iR_{ii} On this model the direct coefficients, C_iR_{ii}, assume less importance than the cross coefficients, C_jR_{ij}, since they merely represent the sum of the frictional coefficients between one mole of species i and all other species in one litre of solution. The coefficients C_1R_{11} and C_2R_{22} are plotted for zinc chloride, zinc perchlorate and barium chloride in Figs (6.6) and (6.7) respectively. The magnitude and variation of C_1R_{11} and C_2R_{22} for all three salts is remarkably similar. For zinc chloride the major contribution in each case is provided by the cation-anion frictional term, whereas for zinc perchlorate and barium chloride the major contribution comes from the friction between ion and water in each case.

The identity, $\sum_{j=o}^{n} C_jR_{oj} = 0$, can be rearranged to give equation (6.7)

$$C_o^2 \frac{R_{oo}}{N} = \frac{-C_oR_{1o}}{|Z_1|} + \frac{-C_oR_{2o}}{|Z_2|} \qquad (6.7)$$

The function $C_o^2 \frac{R_{oo}}{N}$ therefore represents the total friction between ions and solvent in an electrolyte solution. This function is plotted

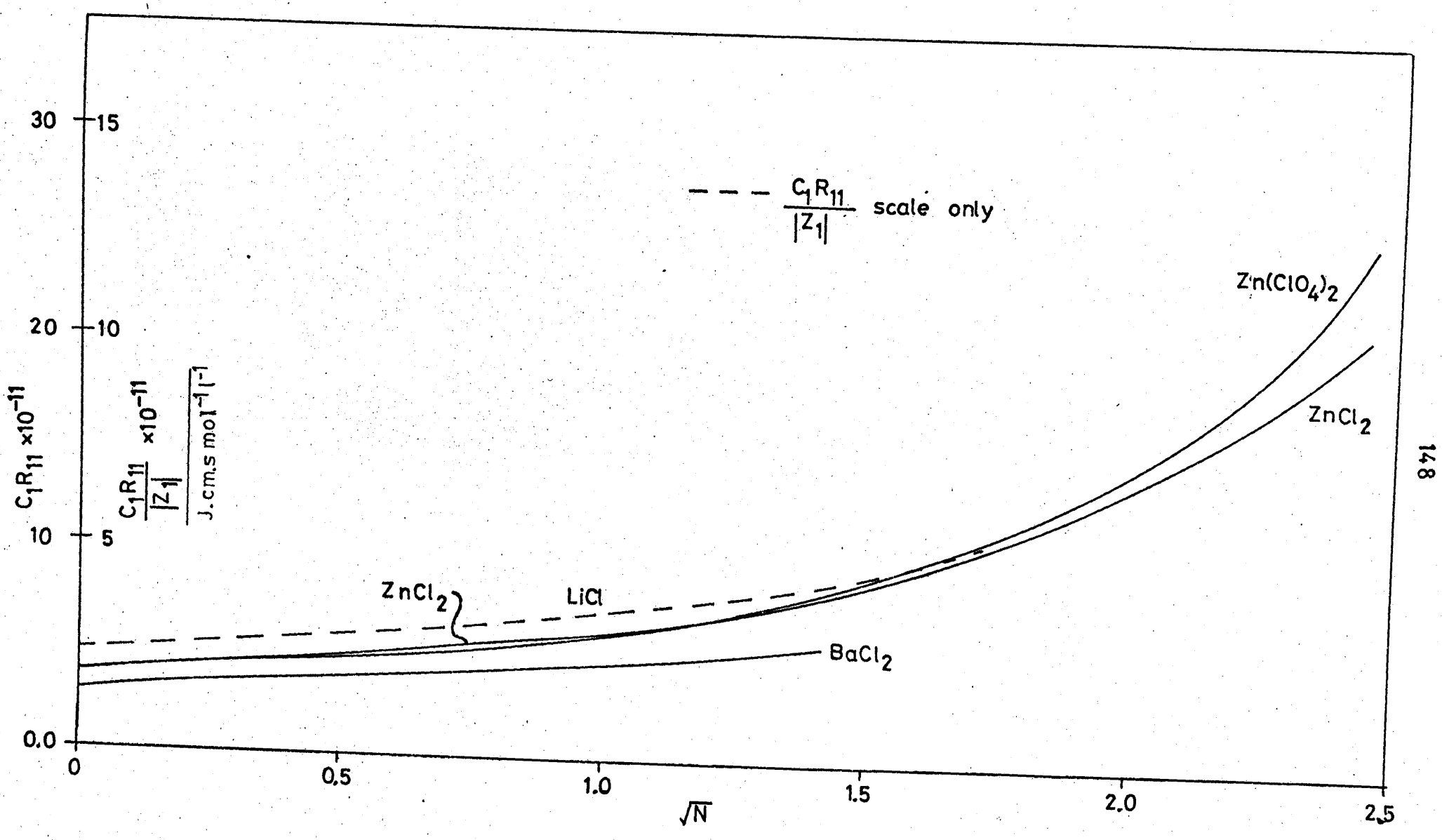
30
15
20
10
10
5
0.0
$C_1R_{11} \times 10^{-11}$
$\frac{C_1R_{11}}{|Z_1|} \times 10^{-11}$ J.cm.s mol^{-1} l^{-1}
$\frac{C_1R_{11}}{|Z_1|}$ scale only
$Zn(ClO_4)_2$
$ZnCl_2$
$ZnCl_2$
LiCl
$BaCl_2$
0
0.5
1.0
1.5
2.0
2.5
$\sqrt{N}$

Fig 6.6

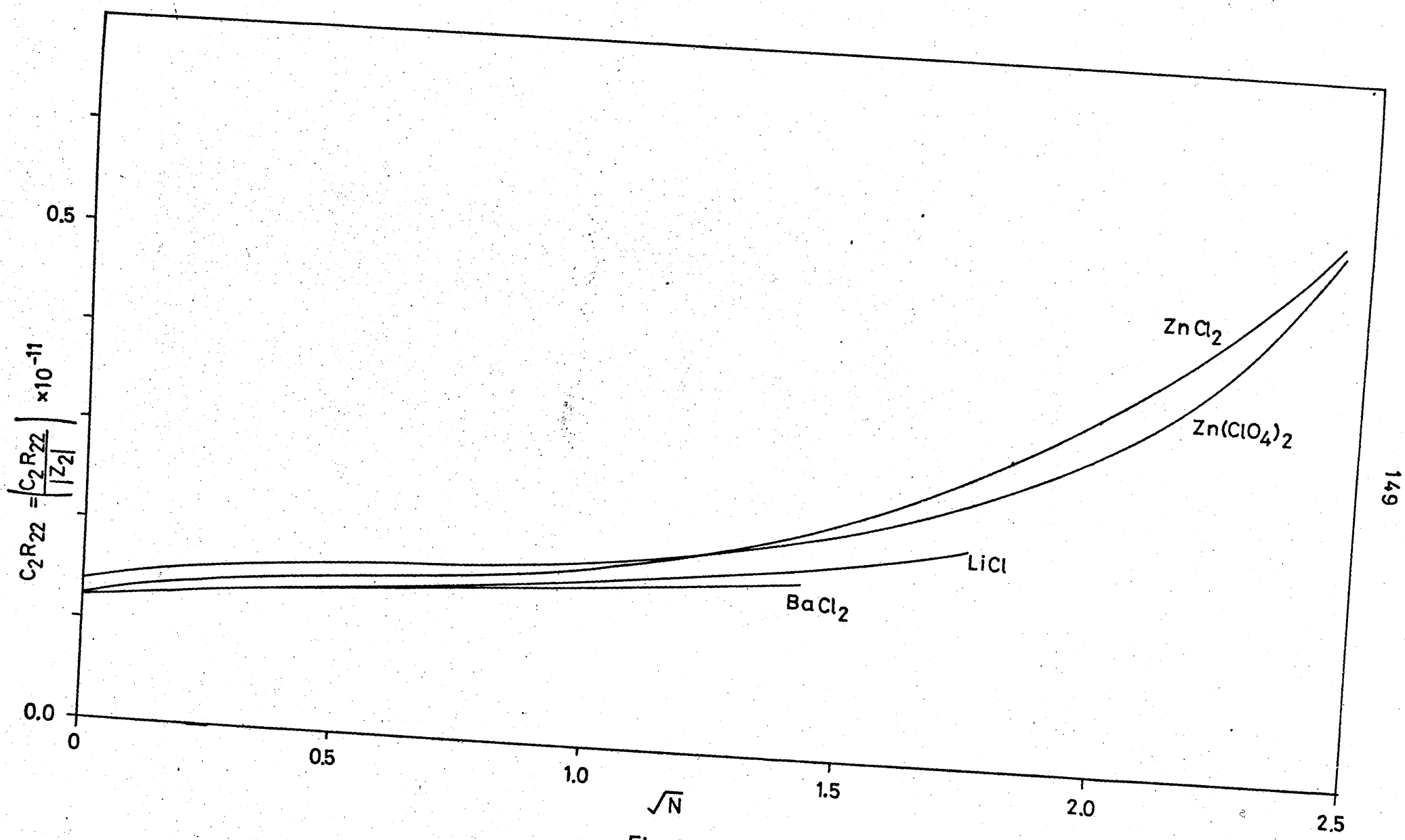
0.5
0.0
$C_2R_{22} = \left|\frac{C_2R_{22}}{|Z_2|}\right| \times 10^{-11}$
$ZnCl_2$
$Zn(ClO_4)_2$
LiCl
$BaCl_2$
0
0.5
1.0
1.5
2.0
2.5
$\sqrt{N}$

Fig. 6.7

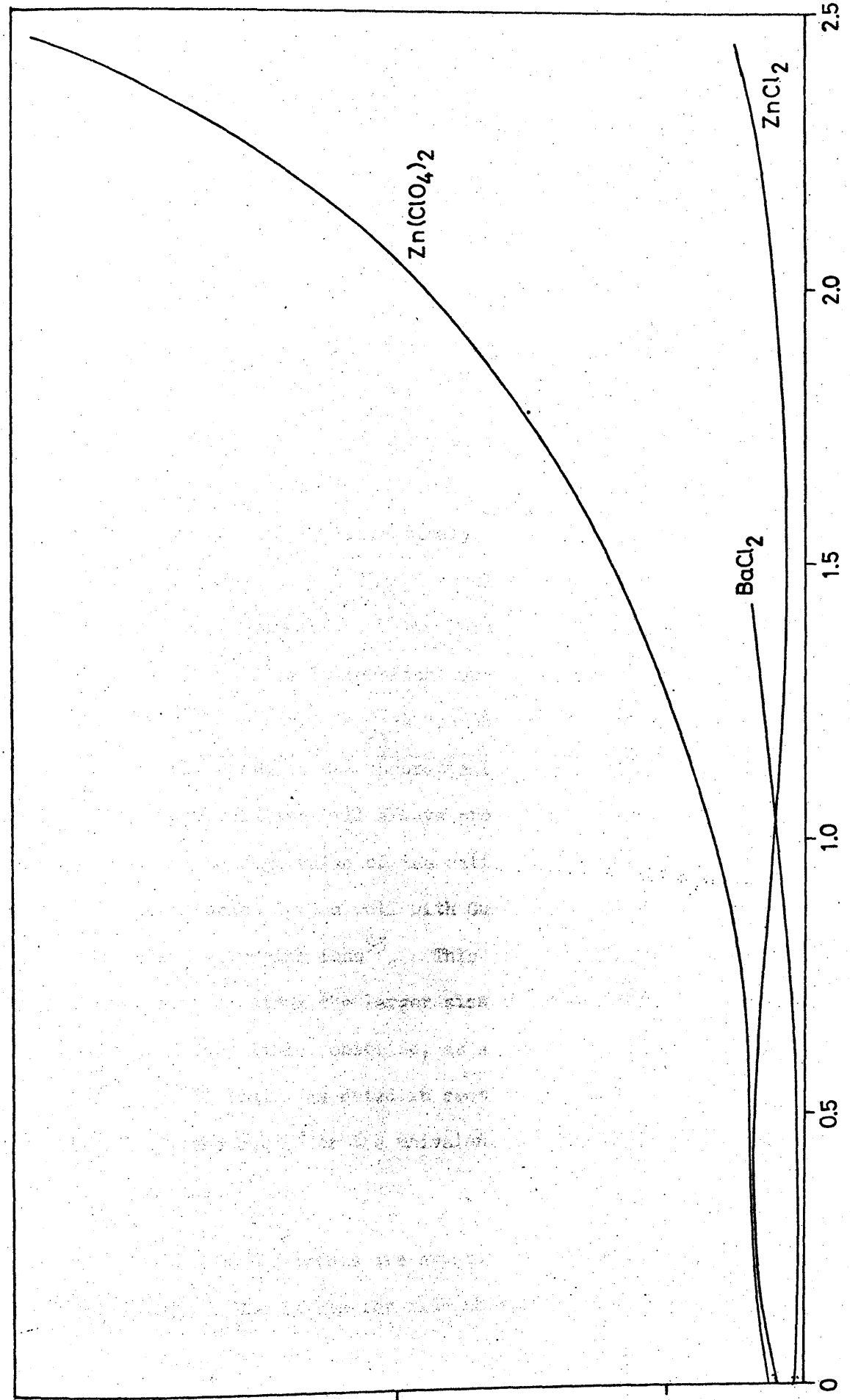
$Zn(ClO_4)_2$
$ZnCl_2$
$BaCl_2$
$\frac{C_0^2 R_{OO}}{N} \times 10^{-11}$
$\sqrt{N}$
0
0.5
1.0
1.5
2.0
2.5
5
10
15

Fig. 6.8

in Fig (6.8). The friction between ions and water is extremely large for zinc perchlorate, reflecting the high degree of solvation expected for this salt[33,93].

6.4.2.2 The Ion-solvent Frictional Coefficients $-C_0R_{10}/z_1$

The coefficients $-C_0R_{10}/|z_1|$ and $-C_0R_{20}/|z_2|$ represent the friction between one equivalent of ion constituent and the surrounding solvent in one litre of solution. They are plotted against $\sqrt{N}$ in Figs (6.9) and (6.10) respectively. The cation-water friction coefficient, $-C_0R_{10}/|z_1|$, increases with concentration for all the salts represented in Fig (6.9). The curves for zinc chloride and zinc perchlorate are virtually identical until approximately 0.25 mol dm^{-3} after which the curve for zinc perchlorate rises much more sharply. This result supports the theoretical analysis of Pikal[92] which predicts that ion association will always provide a negative contribution to $-C_0R_{10}$. The high value of the cation water frictional coefficient for zinc perchlorate agrees well with Gurney's concepts of order producing and order destroying ions[93]. This friction is smaller for barium chloride, reflecting the larger size of the bare Ba^{2+} ion, and larger initially for lithium chloride, as a result of the smaller radius of the bare Li^+ ion. As noted in section (6.4.1.1) when discussing $z_1^2 l_{11}/N$ the curve for the univalent cation, Li^+, is less steep than that for the bivalent cations.

Similar trends are apparent in the plots of $-C_0R_{20}/|z_2|$ in Fig (6.10). The curves for zinc chloride and zinc perchlorate once more show similar behaviour until 0.25 mol dm^{-3} after which they diverge.

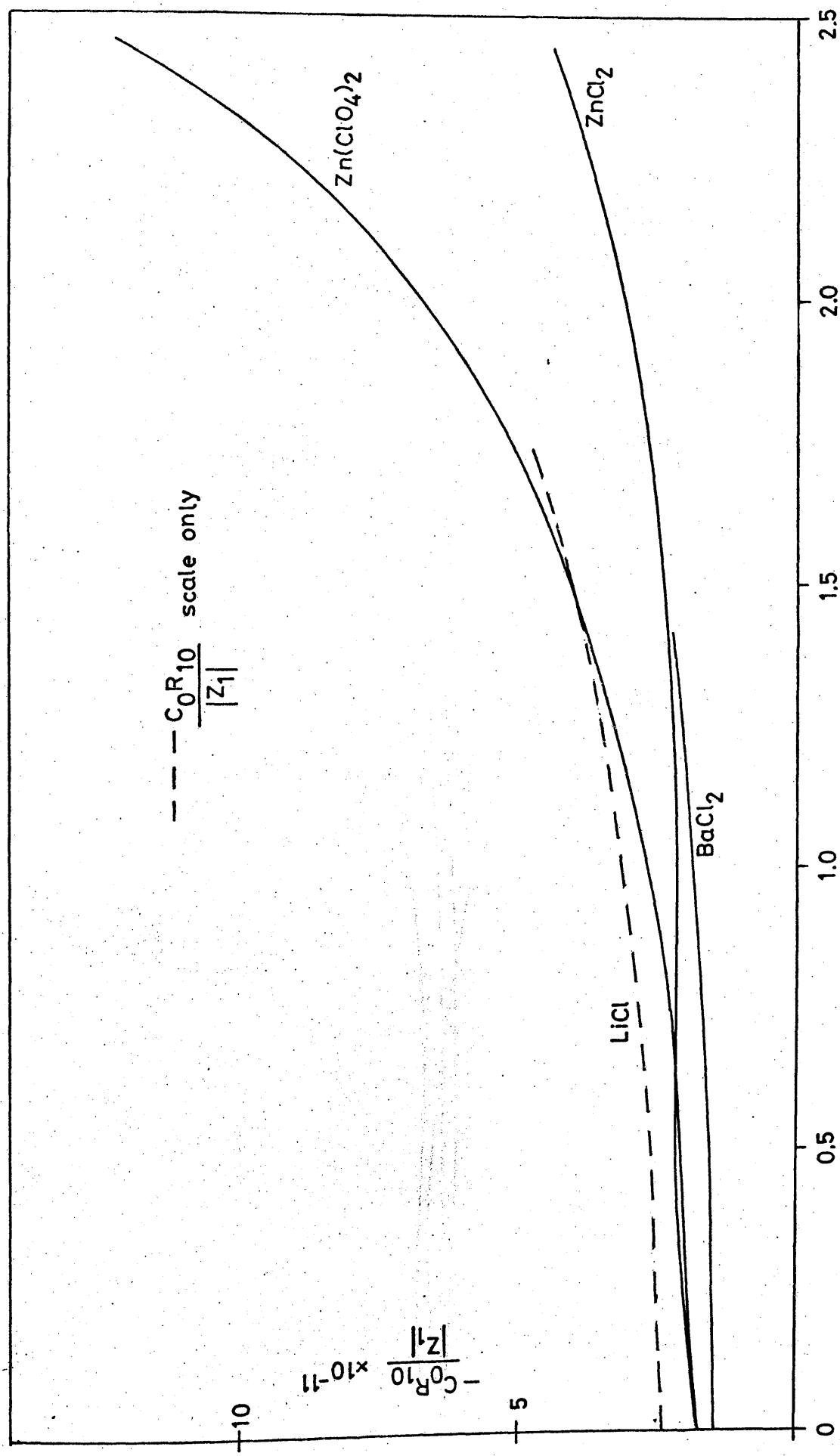
$Zn(ClO_4)_2$
$ZnCl_2$
LiCl
$BaCl_2$
$-\frac{C_0R_{10}}{|Z_1|}$ scale only
$-C_0R_{10}\times10^{-11}$
$-\frac{C_0R_{10}}{|Z_1|}\times10^{-11}$
20
10
0
10
5
0
2.5
2.0
1.5
1.0
0.5
0
$\sqrt{N}$

Fig. 6.9

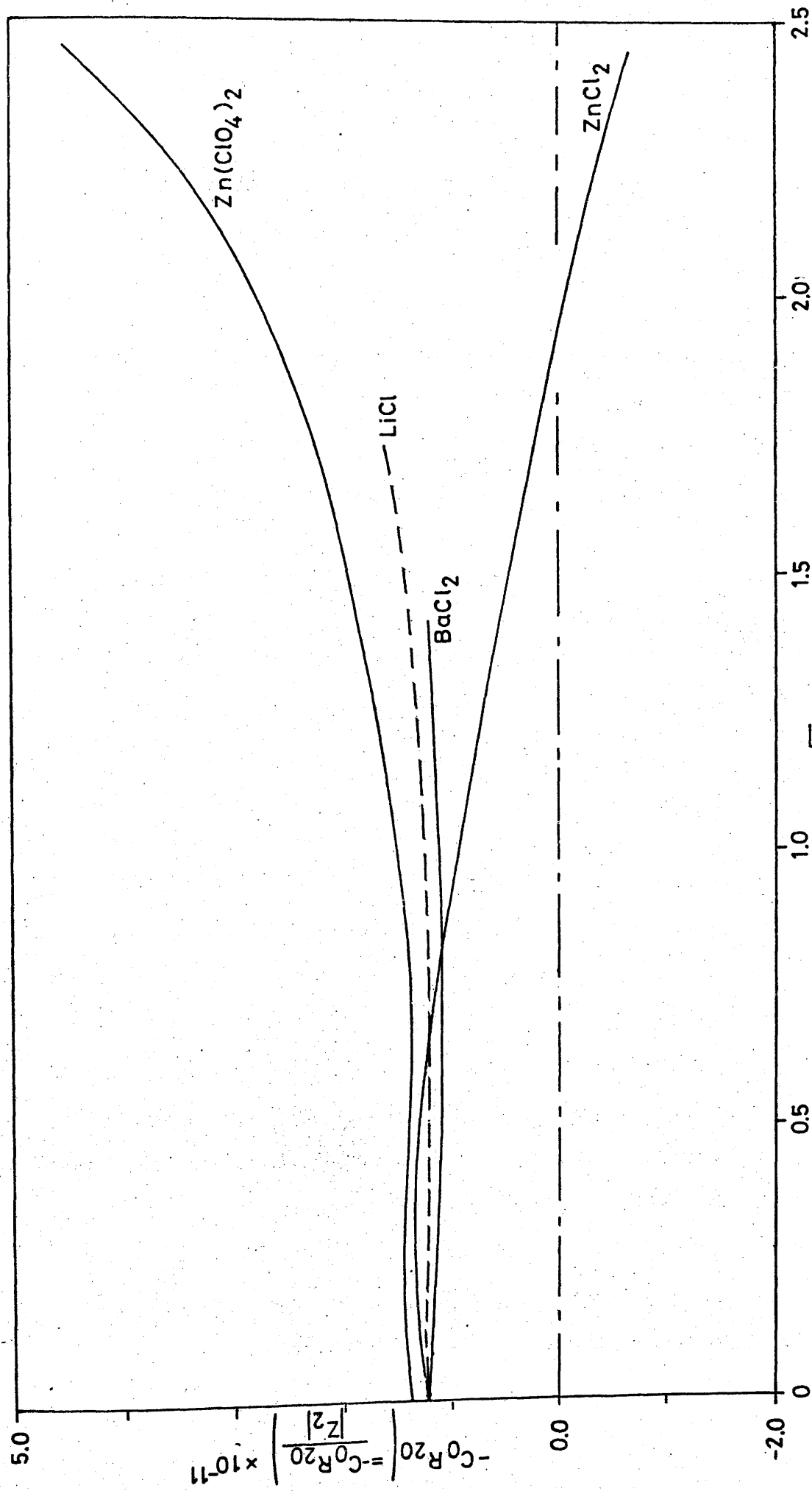
$Zn(ClO_4)_2$
LiCl
$BaCl_2$
$ZnCl_2$
$-C_o R_{20} \left(= \frac{-C_o R_{20}}{|Z_2|} \right) \times 10^{-11}$
5.0
0.0
-2.0
0
0.5
1.0
1.5
2.0
2.5
$\sqrt{N}$

Fig. 6.10

The anion-solvent friction coefficient continues to increase for zinc perchlorate, probably mainly as a result of the structuring effect of the cation on the solvent. A similar trend is apparent for barium chloride and lithium chloride.

In concentrated solutions of zinc chloride $-c_0R_{20}/|z_2|$ shows rather strange behaviour as it decreases steadily and eventually reverses sign and becomes negative. This presumably means that the negative ion association contribution[93] has become dominant. This sign reversal is a consequence of the sign reversal of the cation transference number, t_1, as can be seen from the expression for t_1 in terms of frictional coefficients, equation (6.8).

$$t_1 = \frac{(-c_0R_{20})/|z_2|}{(-c_0R_{10})/|z_1| + (-c_0R_{20})/|z_2|} \qquad (6.8)$$

6.4.2.3 The Cation-Anion Frictional coefficient $-c_2R_{12}/|z_1|$ This coefficient, plotted in Fig (6.11) against $\sqrt{N}$, represents the friction between one equivalent of cation constituent and the anion constituent contained in one litre of the surrounding solution. It is implied by the Onsager reciprocal relations that this is identical with the friction between one equivalent of anion constituent and the surrounding cation constituent in one litre of solution, $-c_1R_{21}/|z_1|$. As expected[33,14,95] this friction is much greater in the self complexed zinc chloride system than in the fully dissociated systems, zinc perchlorate, barium chloride, and lithium chloride. The cation-anion frictional coefficients for two other self complexing systems, cadmium chloride and cadmium iodide, are also plotted in Fig (6.11). The values for cadmium

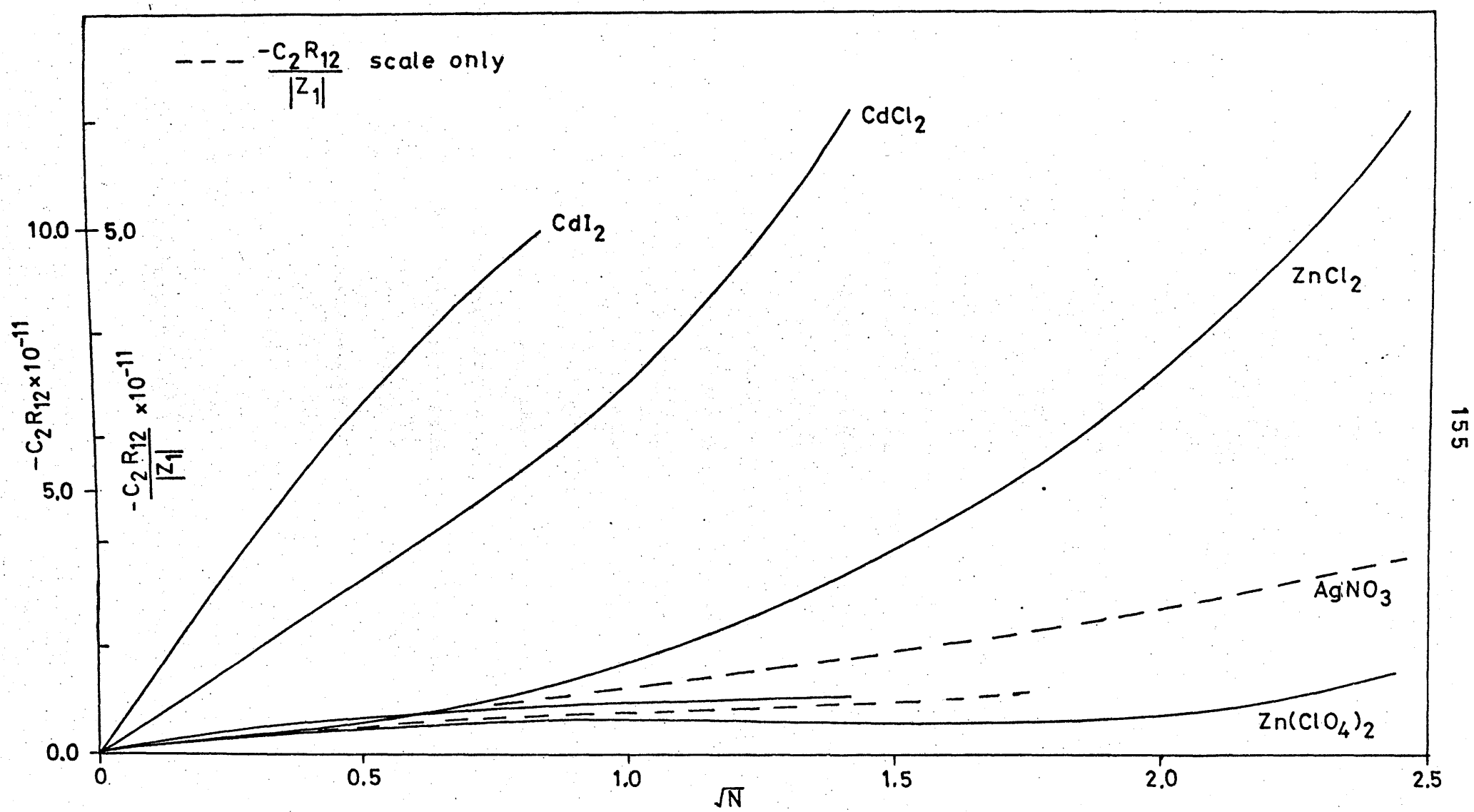
$-\frac{C_2R_{12}}{|Z_1|}$ scale only
$CdCl_2$
CdI_2
$ZnCl_2$
$AgNO_3$
$Zn(ClO_4)_2$
$-C_2R_{12}\times10^{-11}$
$-\frac{C_2R_{12}}{|Z_1|}\times10^{-11}$
10.0
5.0
5.0
0.0
0
0.5
1.0
1.5
2.0
2.5
$\sqrt{N}$

Fig. 6.11

chloride were calculated from mobility coefficient data published recently by McQuillan[15], and those for cadmium iodide are a private communication from Paterson and Anderson. In both cases the values are higher than those for zinc chloride at the same concentration. This behaviour might be expected as it is known that the equilibrium constants for the formation of the first complex, AX^+, are higher for the cadmium halides[96,97] than for zinc chloride[98-101].

Also included in Fig (6.11) are Miller and Pikal's[14] values for the cation-anion frictional coefficient of aqueous silver nitrate solutions. The curve for silver nitrate falls in the region between the curves for the completely dissociated systems such as zinc perchlorate and those for the self-complexing systems. This implies that the friction between cation and anion in the ion paired system, aqueous silver nitrate, is less than that between cation and anion in a self complexing system. This result might intuitively be expected since the interactions between cation and anion are obviously far stronger in a self-complexing system than in an ion-pairing system. This is not, however, reflected in the magnitude of $L_{12/N}$ which is similar for both zinc chloride and silver nitrate. It appears, therefore, that the frictional coefficient representation gives a far clearer indication of the magnitude of the interactions between different species than does the mobility coefficient representation.

6.5 Mobility coefficients of the Complex Species present in Zinc Chloride

It was shown in section (2.5) that in a self-complexing system the mobility coefficients of the ion-constituents, L_{ik}, given by

equation (2.21) can be expressed as combinations of the mobility coefficients of the complex species, l_{ik}, given by equation (2.71). The relations between the two sets of coefficients were given by equation (2.77) which can be written in expanded form as equations (6.9).

$$\frac{L_{11}}{N} = \frac{1}{N} \begin{bmatrix} l_{cc} & l_{c1} & l_{c2} & l_{c3} & l_{c4} \\ l_{1c} & l_{11} & l_{12} & l_{13} & l_{14} \\ l_{2c} & l_{21} & l_{22} & l_{23} & l_{24} \\ l_{3c} & l_{31} & l_{32} & l_{33} & l_{34} \\ l_{4c} & l_{41} & l_{42} & l_{43} & l_{44} \end{bmatrix} \quad I$$

$$\frac{L_{12}}{N} = \frac{L_{21}}{N} = \frac{1}{N} \begin{bmatrix} l_{c1} & 2l_{c2} & 3l_{c3} & 4l_{c4} & l_{cA} \\ l_{11} & 2l_{12} & 3l_{13} & 4l_{14} & l_{1A} \\ l_{21} & 2l_{22} & 3l_{23} & 4l_{24} & l_{2A} \\ l_{31} & 2l_{32} & 3l_{33} & 4l_{34} & l_{3A} \\ l_{41} & 2l_{42} & 3l_{43} & 4l_{44} & l_{4A} \end{bmatrix} \quad I \qquad (6.9)$$

$$\frac{L_{22}}{N} = \frac{1}{N} \begin{bmatrix} l_{11} & 2l_{12} & 3l_{13} & 4l_{14} & l_{1A} \\ 2l_{21} & 4l_{22} & 6l_{23} & 8l_{24} & 2l_{2A} \\ 3l_{31} & 6l_{32} & 9l_{33} & 12l_{34} & 3l_{3A} \\ 4l_{41} & 8l_{42} & 12l_{43} & 16l_{44} & 4l_{4A} \\ l_{A1} & 2l_{A2} & 3l_{A3} & 4l_{A4} & l_{AA} \end{bmatrix} \quad I$$

where I is the unit matrix.

Each term of the expanded matrices is divided by the total nomality, N. However the intrinsic mobility of a complex species, i, will be $\frac{l_{ii}}{c_i}$ and the interaction mobilities between two complex species,

i and k, will be $\frac{l_{ik}}{\sqrt{c_i c_k}}$ where c_i is the concentration of the complex species i. The relation between $\frac{l_{ik}}{N}$ and $\frac{l_{ik}}{\sqrt{c_i c_k}}$ is given by equation (6.10)

$$\frac{l_{ik}}{N} = \sqrt{y_i y_k} \; \frac{l_{ik}}{\sqrt{c_i c_k}} \qquad (6.10)$$

where $$y_i = \frac{c_i}{N} \qquad (6.11)$$

Equations (6.10) show that the contribution of a complex, i, to the mobility coefficients of the ion-constituents is governed by three factors, the intrinsic mobility of i, its interaction with other complex species, and the amount of ion constituent present in the form of complex i, y_i. Of the three contributions the last is likely to be the most important.

It would be extremely useful, therefore, if the concentrations of each complex species in zinc chloride solution could be estimated as a function of the total molarity. Unfortunately this is not possible at present, although work is in progress by Lutfullah, Dunsmore and Paterson to provide this data. Several sets of values are quoted in the literature of the stability constants for the formation of the complexes $ZnCl_n^{2-n}$ in aqueous zinc chloride solutions[98-101], but the agreement between them is extremely poor. An attempt was made to estimate the concentrations of the complexes using a computer programme, which had been proved to work for similar systems, but this was unsuccessful.

As no quantitative information is available it is only

possible to speculate in a qualitative way about the magnitudes of the $\frac{l_{ik}}{N}$ terms in equations (6.9) using experimental values of $\frac{l_{ik}}{\sqrt{c_i c_k}}$ for binary and ternary electrolyte solutions[9b,c], and Pikal's theoretical analysis[92], as guidelines. The intrinsic mobilities of the complexes, $\frac{l_{ii}}{c_i}$, may be expected to have positive values which fall slightly with increasing concentration, c_i. There is no experimental or theoretical evidence to suggest how the intrinsic mobility of the neutral complex, $\frac{l_{22}}{c_2}$, will behave, and it will therefore be assumed to follow a similar pattern. The coefficients representing interactions between different ionic complexes, $\frac{l_{ik}}{\sqrt{c_i c_k}}$ i,k = 2, will be zero for c_i or c_k =0 and may be expected to increase in absolute magnitude as c_i and/or c_k increase. Experimental data on ternary electrolyte systems[96] indicate that $\frac{l_{ik}}{\sqrt{c_i c_k}}$ will be positive if the i'th and k'th species have opposite charges and negative if they have like charges. It is impossible to predict how the terms representing interactions between the neutral complex, $ZnCl_2$, and the other species, k, in solution, $\frac{l_{2k}}{\sqrt{c_2 c_k}}$, will behave. However, it will probably be much smaller in magnitude than the $\frac{l_{ik}}{\sqrt{c_i c_k}}$ as there will be no contribution from culombic interactions. As stated above a major contribution to $\frac{l_{ik}}{N}$ is likely to come from the term $\sqrt{y_i y_k}$.

An attempt will now be made to interpret qualitatively the gross variations of $\frac{L_{11}}{N}$, $\frac{L_{22}}{N}$ and $\frac{L_{12}}{N}$ for zinc chloride using the ideas outlined above. Fig (6.3) shows that $\frac{L_{11}}{N}$ for zinc chloride is larger than might be expected in the concentration range where self-complexing is extensive. Equation (6.9) indicates that L_{11} contains only two terms which are expected to be negative, $l_{\alpha 1}$ and l_{34}. If it is

arbitrarily assumed that the sum of the direct mobilities, $\sum_{i=C,A,1}^{4} y_i \frac{l_{ii}}{c_i}$, corresponds approximately to the value $\frac{L_{11}}{N}$ would have in the absence of complex formation, the positive contribution of the effect of self-complexing to $\frac{L_{11}}{N}$ is explained if $\sum_{i=c,Al\ i=k}^{4} \sum_{k=C,A,1}^{4} \sqrt{y_i y_k}\ \frac{l_{ik}}{\sqrt{c_i c_k}}$ is positive. This will probably be the case in all but the more dilute solutions, where only the first complex is present, or in the most concentrated solutions where the third and fourth complexes will be predominant. The concentration range studied is probably not extensive enough to include the latter case, but the former case should be included, and in fact $\frac{L_{11}}{N}$ is lower for zinc chloride than for zinc perchlorate in the dilute range. An exactly similar agreement can be used to explain the fact that $\frac{L_{22}}{N}$ for zinc chloride is also increased by self complexing.

An examination of equation (6.9) shows that the expansion of L_{12} contains four negative terms, $l_{\alpha 1}$, $l_{3\beta}$, $l_{4\beta}$ and l_{34}, the last three of which are only likely to be important at fairly high concentrations of zinc ion constituent. Thus the net effect of self-complexing is to increase $\frac{L_{12}}{N}$. At lower concentrations, however, where only the first complex is important, this increase will be less than might be expected as a result of the negative contribution of the term $\sqrt{y_c y_1}\ \frac{l_{c1}}{\sqrt{c_c c_1}}$. At higher concentrations the negative terms involving $l_{3\beta}$, $l_{4\beta}$ and l_{34} will become larger in magnitude, and this is probably one of the reasons for the maximum in $\frac{L_{12}}{N}$ which occurs at approximately 2 mol dm^{-3} (Fig 6.5).

6.6 Conclusions Both the mobility coefficient and frictional coefficient formalisms have been discussed in this chapter. The choice of one or the other to represent the properties of an electrolyte system is very much a matter of personal preference since both have advantages and disadvantages for interpretative purposes. Although all the coefficients are affected by ion association or self-complexing the cross coefficients ${}^{1}_{12/N}$ and ${}_{2}R_{12/Z_1}$ are affected most directly. In this case the frictional approach seems preferable since the frictional coefficient reflects the presumed difference in degree of the interaction between Ag^{+} and NO_3^{-} from that between Zn^{2+} and Cl^{-} whereas the mobility coefficient does not. However if it is wished (in a self complexing system), to express the properties of the coefficients of the ion-constituents in terms of the coefficients of the individual complex species the mobility coefficient approach must be used. Such an analysis offers the prospect of calculating, in a semi-qualitative fashion, the experimentally measured mobility coefficients from values of the mobility coefficients of the individual complex species obtained from the theoretical expressions of Pikal[92].

The frictional and mobility coefficients for the fully dissociated 2:1 salts, zinc perchlorate and barium chloride, have been compared with those of the alkali chloride series on a charge corrected basis. There are close similarities between the two sets of electrolytes, especially between zinc perchlorate and lithium chloride and between barium chloride and potassium chloride. As these two comparisons are made between electrolytes with cations of similar crystallographic radii, this supports the proposal put forward by Gurney[93] that cation size is an important influence on the properties of an electrolyte solution.

Chapter 7

The Application of the Fuoss-Onsager Theory of Diffusinity to Associated Electrolytes

7.1 Introduction The Fuoss-Onsager theory[102] was developed to predict the limiting diffusion coefficient and the concentration dependence of the thermodynamic diffusion coefficient, $\overline{M}$, of electrolyte solutions. The limiting diffusion coefficient is correctly predicted, and Harned and coworkers proved[103], using the conductimetric method[47], that the concentration dependence of $\overline{M}$ in dilute aqueous solutions was also predicted correctly for 1.1 electrolytes. For 2.2 electrolytes[57], however, a considerable discrepancy was found between theory and experiment. Harned and Hudson attributed this to ion pair formation, and obtained good agreement between theory and experiment by introducing the mobility of the ion pair as an adjustable parameter.

Pikal[104] considered that a theory which predicts ion-ion electrostatic interactions should also be capable of predicting electrostatic ion-pairing, and analysed the failure of Fuoss-Onsager theory to do so. He produced an extension of the theory, by retaining more terms in the derivations, which produced terms attributable to ion pair formation. This theory was in good agreement with Harned and Hudson's results for zinc and magnesium sulphates, although it failed when applied to unsymmetrical electrolytes.

The approach adopted here is to consider that the original Fuoss-Onsager theory correctly predicts the diffusion coefficient of the free ions in solution and to show that for a range of 2:2 salts

this calculated diffusion coefficient is equivalent to the bulk diffusion coefficient at the same concentration.

7.2 Analysis of Harned's Results for Zinc and Magnesium Sulphates[57,104]

Harned and Hudson obtained their experimental results by using the conductimetric method to study restricted diffusion[47], the theory of which is discussed in chapter 4. They showed that the difference in electrical conductivity of two solutions, ΔL, was linearly proportional to the difference in their total salt concentrations, ΔC_s, and therefore that a plot of $\ln \Delta L_1$ (where ΔL_1 is the difference in electrical conductance of the solution in the diffusion cell at points a/6 and 5a/6) against time would give a straight line of gradient $-D_s(\frac{\pi}{a})^2$, where D_s is the differential diffusion coefficient of the salt.

It has been established[106] that in dilute solutions of partially associated electrolytes, classical conductance theories are valid provided the equivalent conductance is defined using the "true" ionic concentration ($C_{12} = \alpha C_s$, where α is the degree of dissociation). It is therefore to be expected that the specific conductances of zinc and magnesium sulphates will be proportional to C_{12}. That this is so can be seen from Fig (7.1) where the specific conductances of zinc and magnesium sulphates are plotted against C_{12} for each salt, calculated from the data of Owen & Gurry for $ZnSO_4$[107], and Dunsmore & James for $MgSO_4$[108]. For both salts the plot approximates closely to a straight line in the concentration range studied by Harned & Hudson. Therefore the conductance differences between the top and bottom of the diffusion cell, ΔL_1, are proportional to the differences in the ionic concentration,

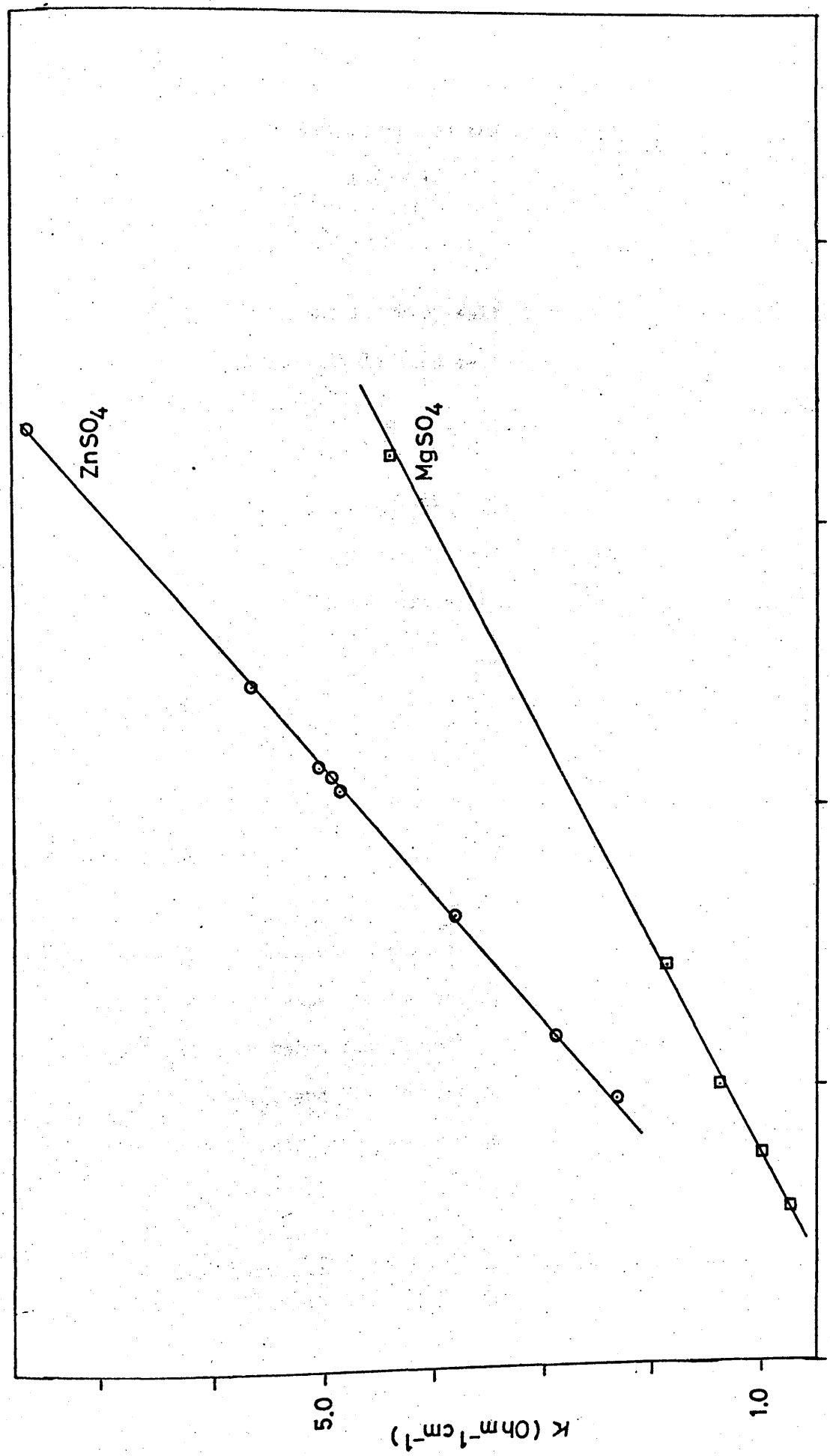

Fig. 7.1

ΔC_{12}, and hence the observed diffusion coefficient, D_{obs}, is identical with the diffusion coefficient of the free ions, D_{12}, as well as that of the bulk salt, D_s. Hence :-

$$D_{obs} = D_s = D_{12} \qquad (7.1)$$

Defining the flows of salt, free ions, and ion pairs as J_s, J_{12} and J_m respectively then :-

$$J_s = J_{12} + J_m \qquad (7.2)$$

and by Ficks 1st law :-

$$D_s\left(-\frac{\partial c_s}{\partial x}\right) = D_{12}\left(-\frac{\partial c_{12}}{\partial x}\right) + D_m\left(-\frac{\partial c_m}{\partial x}\right) \qquad (7.3)$$

where D_m is the diffusion coefficient of the ion pair with units of cm^2/sec, and concentrations are expressed in moles/cm^3. By combining equations (7.1) and (7.3) with the identity $c_s = c_{12} + c_m$ where c_m is the concentration of the ion pair we get equation (7.4)

$$D_s = D_{12} = D_m = D_{obs} \qquad (7.4)$$

Thus Harned and Hudson's results can be considered to give the Diffusion coefficient of any of the three species in solution, total salt, free ions, or ion-pairs, since all three quantities are equal. Harned & Hudson chose to consider D_{obs} as D_s, and to use Fuoss-Onsager theory along with experimental activity data to calculate this quantity. It will be shown below that a better result is obtained if D_{obs} is considered as D_{12}, and F.O. theory used, along with an activity correction calculated from an extended Debye-Huckel expression, to calculate this quantity.

7.3 Calculation of Diffusion Coefficients by F.O. theory

7.3.1 Definitions The irreversible thermodynamic definition of

the diffusion coefficients of a binary system is given by equation (2.55)

$$J_s = \frac{D_s}{1000} \left| - \frac{\partial c_s}{\partial x} \right| = \bar{M}_s \left| - \frac{\partial \mu_s}{\partial x} \right| \qquad (2.55)$$

where D_s is the S.F. diffusion coefficient in $cm^2 s^{-1}$. It was also shown in chapter 2 that the thermodynamic and experimental diffusion coefficients are related by equation (2.58)

$$D_s = 1000\ rRT \left| \frac{\bar{M}_s}{c_s} \right| \left| 1 + \frac{\partial \ln y^{\pm}}{\partial \ln c_s} \right| \qquad (2.58)$$

It is not possible to obtain explicit functions for J_{12} and J_m from the formal irreversible thermodynamic analysis, but if local equilibrium is assumed $\mu_s = \mu_{12} = \mu_m$ and hence the forces on total salt, ion pairs, and free ions are defined. In this case, by analogy with equations (2.55) and (2.58) equations (7.5) and (7.6) can be written :-

$$J_{12} = D_{12} \left| - \frac{\partial c_{12}}{\partial x} \right| = \bar{M}_{12} \left| - \frac{\partial \mu_{12}}{\partial n} \right| \qquad (7.5)$$

$$D_{12} = 1000\ rRT \left| \frac{\bar{M}_{12}}{C_{12}} \right| \left| 1 + \frac{\partial \ln y_{12}}{\partial \ln C_{12}} \right| \qquad (7.6)$$

7.3.2 Frame of Reference Effects The thermodynamic diffusion coefficient, $\bar{M}$, is frame of reference independent, but the measured diffusion coefficient is not, and is usually referred to a volume, or solvent, fixed frame of reference (D_v or D_o respectively). The relationship between the three quantites is given by equation (7.7) :

$$1000\ rRT \left| \frac{\bar{M}}{C} \right| = \frac{D_v}{fn\gamma^{\pm}} = \frac{D_o}{fny^{\pm}} \qquad (7.7)$$

where $\gamma^{\pm}$ and $y^{\pm}$ are the mean molal and molar activity coefficients respectively, and fnx denotes a function of the form $(1 + \frac{\partial \ln x}{\partial \ln c})$. The experimentally obtained quantity was D_v, and the calculated quantity will

will be D_o, but at the concentrations considered the ratios of $\gamma^{\pm}/y^{\pm}$ and c/m are respectively 1.002 and 1.003, and therefore D_v and D_o do not differ significantly.

7.3.3 Equations for $\frac{\overline{M}}{c}$ and fny_{12}

The equations used to calculate the ionic mobility term, $\frac{\overline{M}_{12}}{C_{12}}$ and activity term, fny_{12}, were taken from Harned and Owen's standard text[109], and will be quoted here without any attempt at derivation. The mobility term is given for symmetrical electrolytes by equation (7.8)

$$\frac{\overline{M}_{12}}{C_{12}} \times 10^{20} = \frac{1.0748}{Z} \cdot \frac{\lambda 1^{o} \lambda 2^{o}}{\Lambda^{o}} - \frac{.4404}{\overset{o}{a}\eta_o} \left| \frac{\lambda 1^{o} - \lambda 2^{o}}{\Lambda^{o}} \right| \frac{\kappa a}{1 + \kappa a} + \left| \frac{Z}{\overset{o}{a}} \right|^2 \cdot \frac{36790}{\eta_o \mathfrak{D} T} (\kappa a)^2 \Phi(\kappa a) \quad (7.8)$$

where $\lambda_1^{o}, \lambda_2^{o}$ are the limiting equivalent conductances of cation and anion respectively, Λ^{o} is $\lambda_1^{o} + \lambda_2^{o}$, Z is the number of equivalents per mole of solute, $\overset{o}{a}$ is the distance of closest approach of the ions in Ångstrom units, κ is the reciprocal distance of Debye-Huckel theory, η_o is the viscosity of the pure solvent in poise, $\mathfrak{D}$ is the solvent dielectric constant, and $(\kappa a)^2 \Phi(\kappa a)$ is a complex exponential function, tabulated in Harned & Owen[109]. The first term gives the limiting mobility at infinite dilution, and the next two are the first and second electrophoretic correction terms.

The activity coefficients for the salts were required for the calculation of the degree of dissociation from the association constants. The Debye-Huckel-Onsager equation was used, equation (7.9)

$$\log y_{12} = \frac{-.5091\, W\sqrt{C_{12}}}{1 + \kappa a} \qquad (7.9)$$

and $$W = (r_1 z_1^2 + r_2 z_2^2)^{3/2} / \sqrt{2} \qquad (7.10)$$

where r_1 and r_2 are the stoichiometric coefficients for ionisation. Differentiation of equation (7.9) gives an expression for the activity term, equation (7.11)

$$f_{my_{12}} = 1 - \frac{.5862\, W\sqrt{C_{12}}}{(1 + \kappa a)^2} \qquad (7.11)$$

The term κa appearing in equations (7.8), (7.9) and (7.11) is a function of the ionic concentration given by :-

$$\kappa a = .3286\, W^1 \sqrt{C_{12}} \qquad (7.12)$$

where $$W^1 = (rW\sqrt{2})^{1/3} / \sqrt{2} \qquad (7.13)$$

and $$r = r_1 + r_2$$

For aqueous solutions at 25°C equations (7.6), (7.8) and (7.11) give equation (7.14)

$$D_{12} = 24.789 \times 10^{12} r \left(\frac{\bar{M}}{C_{12}}\right) f_n y_{12} \qquad (7.14)$$

7.3.4 Method of Calculation The diffusion coefficient D_{12} was required as a function of total salt concentration C_s. Therefore values of α, the degree of dissociation, were required for each concentration in order to calculate C_{12}. These α values were calculated from the association constant K_a using the standard expression :-

$$K_a = \frac{\alpha\, C_{12}}{1 - \alpha} \cdot y_{12}^2 \qquad (7.15)$$

Table 7.1 Diffusion Coefficient for Zinc Sulphate

C mol dm^{-3}	α	$\frac{\overline{M}}{C} \times 10^9$ mol $J^{-1}cm^{-1}l^{-1}s^{-1}$	fny_{12}	$D_{12} \times 10^5$ cm^2s^{-1}
.0	1.0	1.7095	1.0	.848
.0005	.939	1.7335	.908	.780
.0010	.902	1.7470	.878	.760
.0015	.875	1.7582	.858	.746
.0020	.854	1.7682	.841	.736
.0025	.836	1.7776	.826	.728
.0030	.820	1.7859	.814	.720
.0035	.806	1.7931	.804	.714
.0040	.796	1.7995	.795	.710
.0045	.786	1.8057	.786	.703

$K_a = .0049$ $\quad \overset{\circ}{a} = 3.64\ \overset{\circ}{A}$

Table 7.2 Diffusion Coefficient of Magnesium Sulphate

C mol dm^{-3}	α	$\frac{\bar{M}}{\bar{C}} \times 10^{9}$ mol J^{-1}cm^{-1}l^{-1}g^{-1}	$f_{ry_{12}}$	$D_{12} \times 10^{5}$ cm^{2} g^{-1}
0	1.0	1.7144	1.0	.850
.0005	.931	1.7358	.909	.782
.0010	.891	1.7507	.879	.763
.0015	.860	1.7619	.858	.750
.0020	.837	1.7718	.843	.740
.0025	.818	1.7802	.829	.732
.0030	.801	1.7872	.818	.724
.0035	.787	1.7940	.808	.718
.0040	.775	1.8005	.798	.713
.0045	.763	1.8063	.789	.708
.0050	.754	1.8118	.782	.704
.0055	.745	1.8164	.776	.700
.0060	.736	1.8211	.770	.696
.0065	.729	1.8260	.764	.692

K_a = 0.0050 $\quad\quad$ $\overset{o}{a}$ = 3.87 $\overset{o}{A}$

Table 7.3 Diffusion coefficient of Cadmium Sulphate

C mol dm^{-3}	α	$\frac{\overline{M}}{\overline{C}} \times 10^{9}$ mol $J^{-1}cm^{-1}l^{-1}g^{-1}$	fny_{12}	$D_{12} \times 10^{5}$ $cm^{2}s^{-1}$
0	1.0	1.7231	1.0	.854
.01	.705	1.862	.737	.676
.02	.644	1.910	.678	.642
.03	.615	1.944	.647	.624
.04	.600	1.970	.626	.610
.05	.587	1.991	.610	.601
.06	.579	2.006	.597	.594
.07	.573	2.020	.587	.588
.08	.568	2.032	.579	.583
.09	.564	2.042	.572	.580
.10	.561	2.051	.567	.578

$K_a = 0.0049$ $\quad \overset{o}{a} = 3.87 \overset{o}{A}$

Table 7.4 Diffusion coefficient of Copper Sulphate

C mol dm^{-3}	α	$\frac{\overline{M}}{C} \times 10^9$ mol $J^{-1} cm^{-1} l^{-1} \beta^{-1}$	$f n y_{12}$	$D_{12} \times 10^5$ $cm^2 \beta^{-1}$
0	1.0	1.725	1.0	.855
.005	.760	1.827	.780	.706
.010	.700	1.871	.725	.674
.015	.667	1.904	.693	.654
.020	.646	1.929	.670	.640
.025	.633	1.950	.657	.627
.030	.622	1.969	.634	.618
.040	.607	1.997	.610	.604
.050	.596	2.019	.592	.592
.060	.590	2.038	.578	.584
.070	.585	2.056	.566	.576
.080	.581	2.071	.557	.571
.090	.577	2.082	.550	.567
.100	.575	2.094	.542	.562

$K_a = 0.0044$ $\quad \overset{o}{a} = 3.64 \overset{o}{A}$

The numerical computations were carried out by computer using the Algol programme reproduced in the Appendix. Values of the ionic concentration, c_{12}, and the distance of closest approach, $\mathring{a}$, were chosen, and the corresponding values of total salt concentration, c_s, the degree of dissociation, α, the mean molar activity coefficient of the free ions, y_{12}, the ionic activity term, fny_{12}, and the diffusion coefficient of the free ions, D_{12}, were calculated.

The calculations were performed for the four 2:2 salts for which suitable experimental data were available. These were the sulphates of zinc[57], magnesium[104], cadmium[112], and copper[110]. The values of the association constants for each of these salts were also available in the literature.[106,107,113-116]

7.4 Results and Discussion The results of the computations outlined above are given for zinc, magnesium, cadmium and copper sulphates in tables 7.1, 7.2, 7.3 and 7.4 respectively and compared with the published experimental values in Figs (7.2), (7.3), (7.4) and (7.5) respectively, where the solid lines are theoretical plots and the points are experimental data. The value of the distance of closest approach, $\mathring{a}$, was taken as an adjustable parameter, and the best agreement between theory and experiment sought. In all four cases this was obtained when $\mathring{a}$ corresponded to the sum of the crystallographic radii of the ions concerned. This finding coincides with the experience of other workers who have attempted to interpret theoretically the electrochemical properties of these solutions,[57,107] although Stokes[117] has commented that such low values of $\mathring{a}$ are physically unrealistic. As an indication of the magnitude of the effect of $\mathring{a}$ on the calculated diffusion

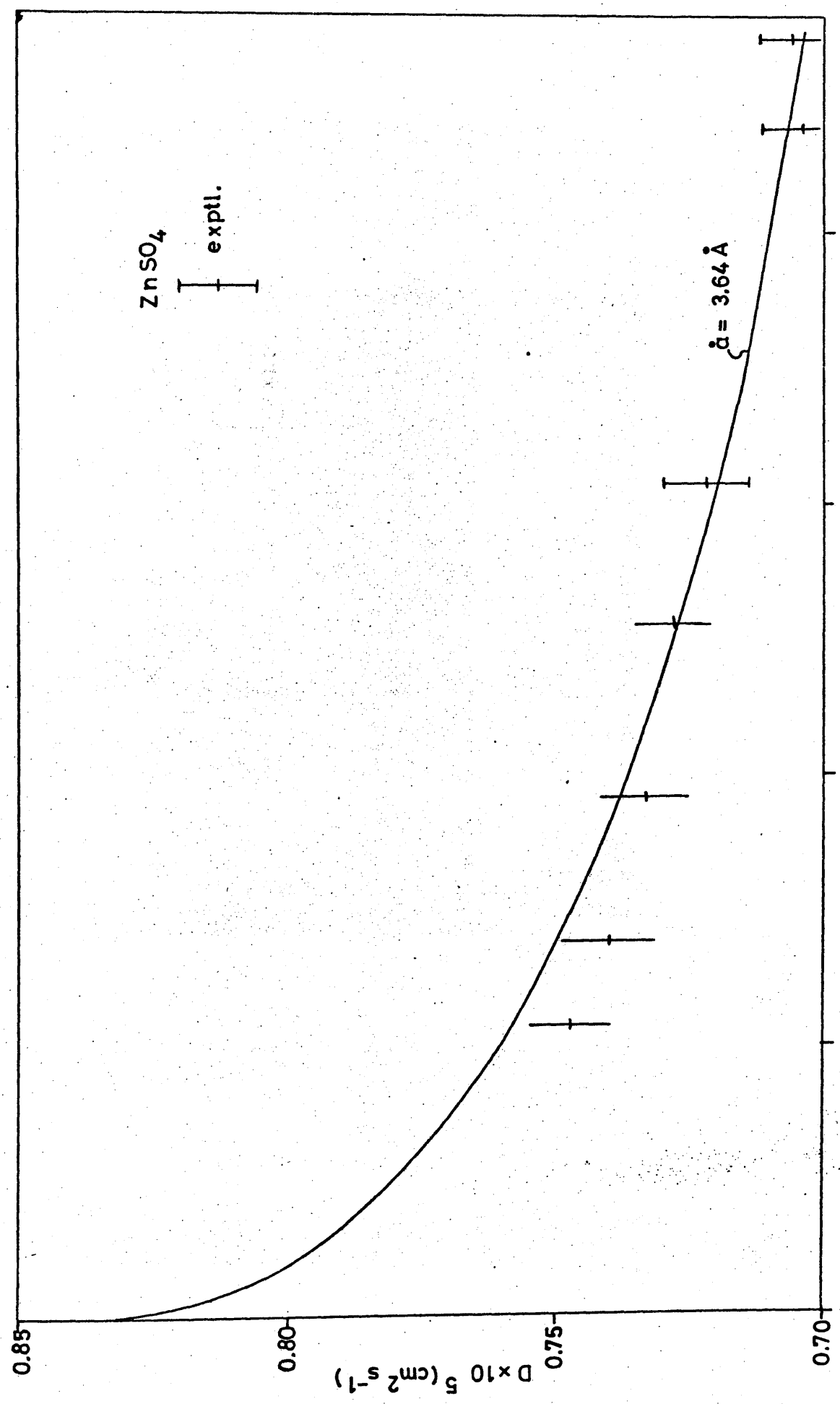
ZnSO4
expt.
å = 3.64 Å
0.85
0.80
0.75
0.70
D × 10 5 (cm2 s-1)
0
0.001
0.002
0.003
0.004
Molarity

Fig. 7.2

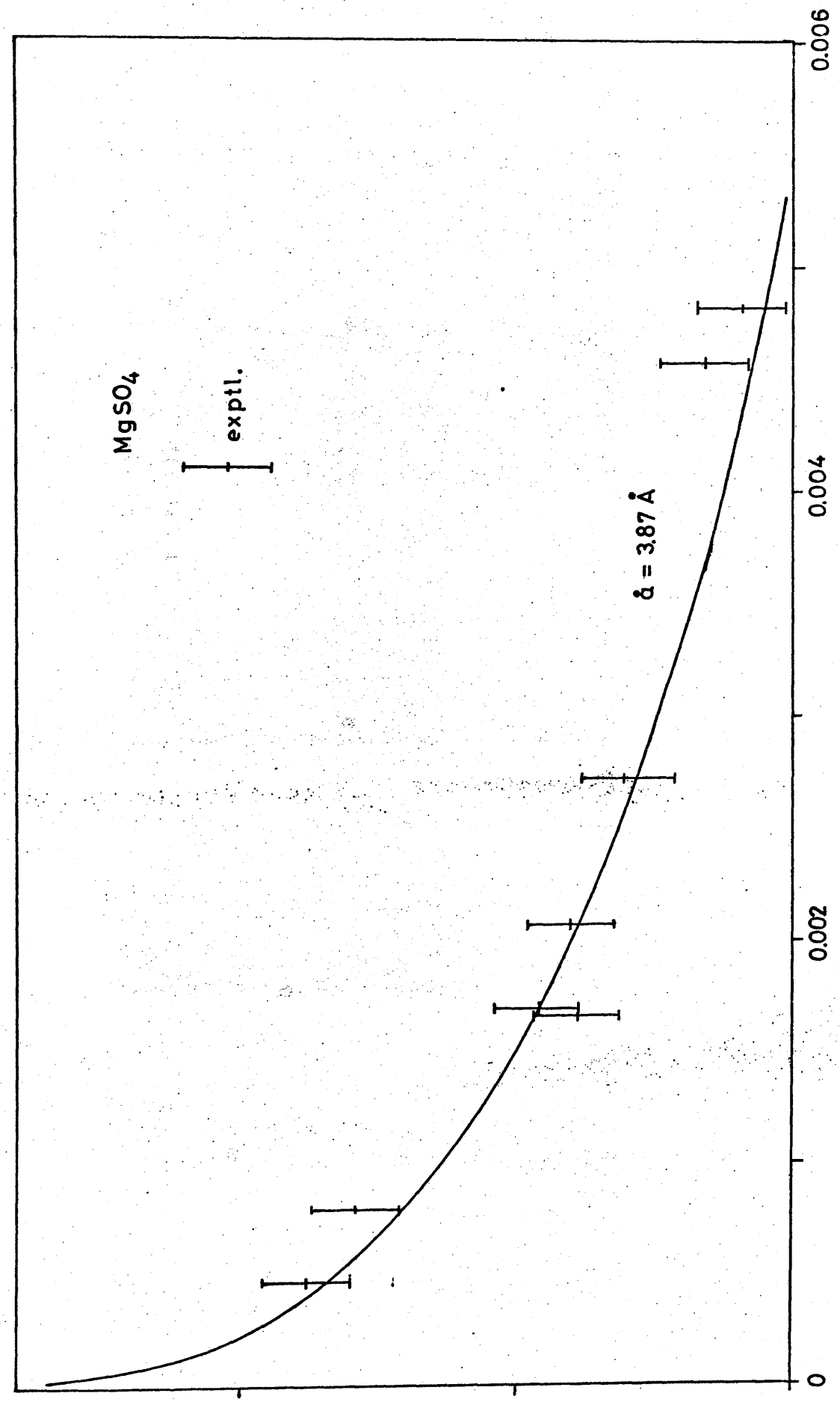
MgSO4
exptl.
å = 3.87 Å
D×10^5(cm^2s^-1)
0.80
0.75
0.70
0
0.002
0.004
0.006
Molarity

Fig. 7.3

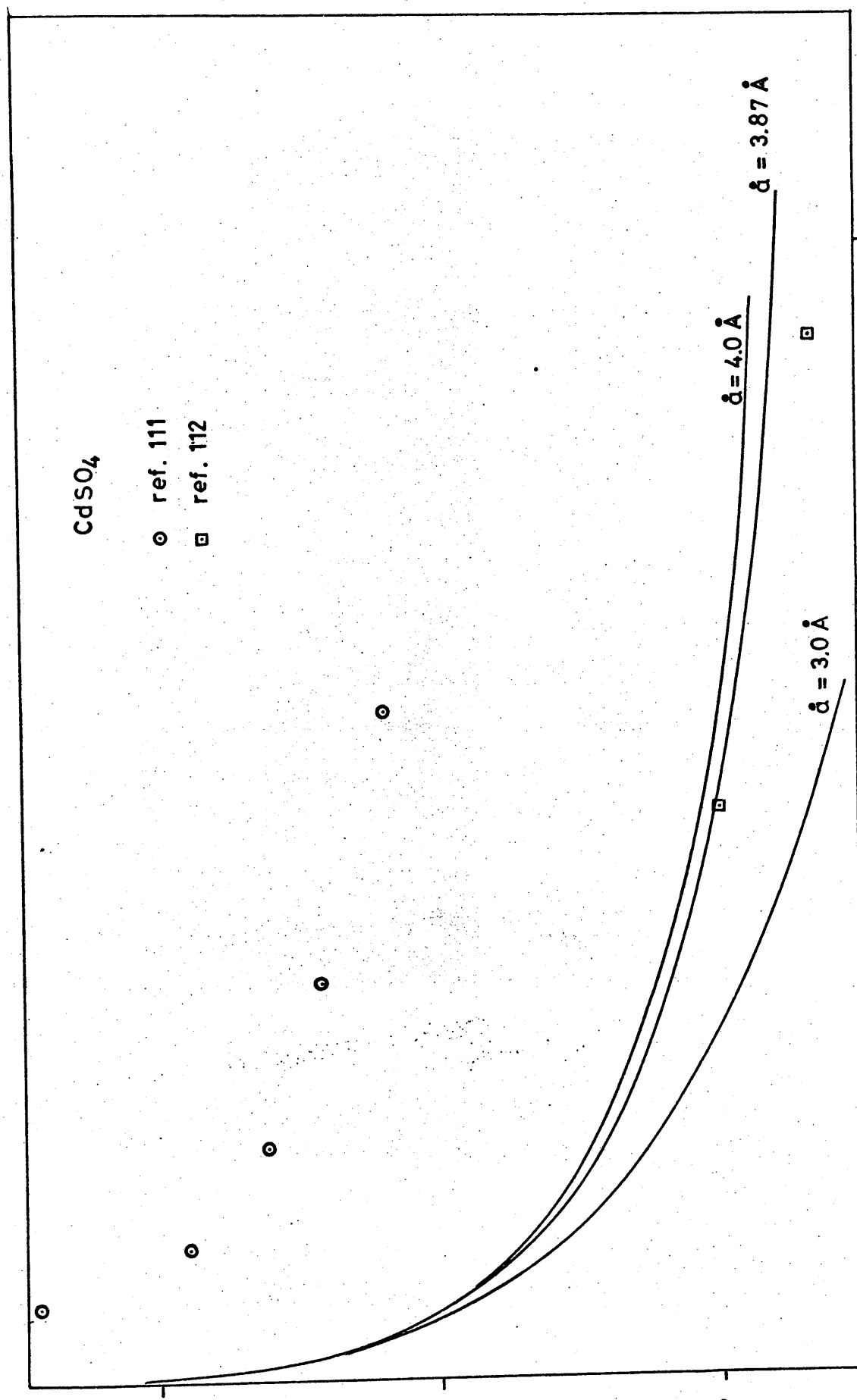
CdSO4
ref. 111
ref. 112
å = 4.0 Å
å = 3.87 Å
å = 3.0 Å
D x10^5 (cm^2 s^-1)
0.8
0.7
0.6
0
0.05
0.10
Molarity

Fig. 7.4

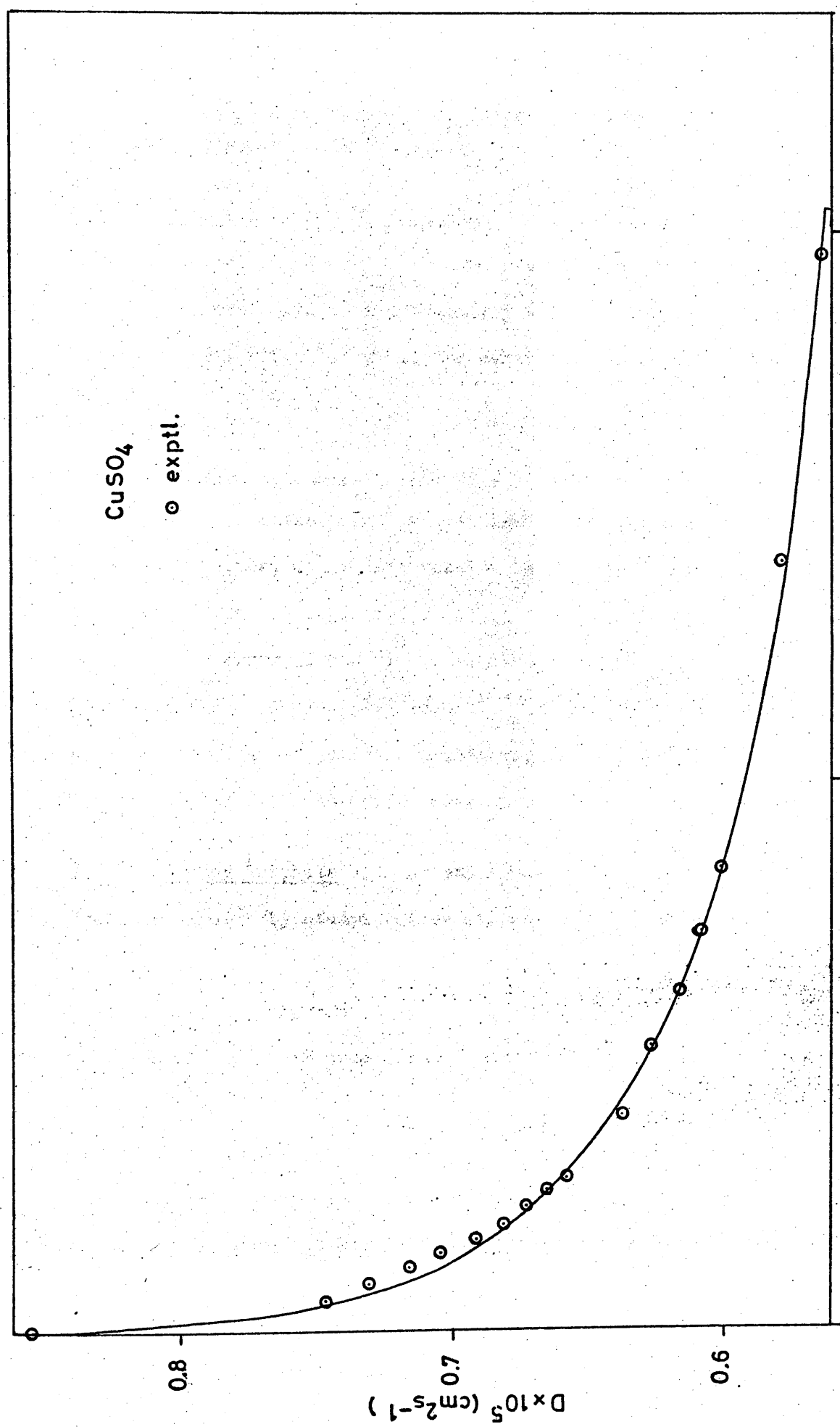

Fig. 7.5

coefficient Fig (7.4), showing the results for cadmium sulphate, includes the results obtained using $\mathring{a} = 3\mathring{A}$ and $\mathring{a} = 4\mathring{A}$ as well as the best fit, obtained using $\mathring{a} = 3.87\mathring{A}$.

7.4.1 Zinc and Magnesium Sulphates The experimental data are those of Harned and Hudson[57,104] and were obtained by the conductimetric method to a precision of approximately $\pm$ .5%. The agreement between theory and experiment is good, the maximum deviation being approximately 1%.

7.4.2 Cadmium Sulphate Two sets of experimental results are reported in the literature, by Gokstien[111] and by Longsworth[112]. The two sets do not agree, Gokstien's results being some 10% higher than Longsworth's in the region of overlap. Gokstien's results are almost certainly in error as his first two results are higher than the Nernst limit for the diffusion coefficient. Longsworth's results are all, unfortunately, at higher concentrations, but his first two points, at 0.05 molar and 0.1 molar, lie close to the theoretical line.

7.4.3 Copper Sulphate The experimental results were obtained by Eversole et al[110] by studying free diffusion of salt into a tall column of distilled water, using the optical density of the solution as a measure of concentration. Values of the diffusion coefficient are reported from 0.003 M upwards. No estimation of experimental error is given, but as the temperature control during the experiment was poor the results are unlikely to have an accuracy much better than $\pm$ 1%. The agreement between theory and experiment is excellent up to a concentration of 0.1 molar, with the exception of the first five experimental points in the most dilute region which lie about 2% above the theoretical line.

This can probably be ascribed to experimental error, since poor temperature control tends to increase the apparent value of the diffusion coefficient by encouraging the onset of convection currents.

7.5 Diffusion in Aqueous Solutions of Weak Acids

The aqueous 2:2 salt solutions considered above are examples of systems which are only slightly associated. The maximum degree of association encountered was approximately 40%. In the weak acids, however, the degree of association is much higher, being typically in the region of 90% - 100% in the concentration ranges which can conveniently be studied. The character of the associated species is also different. It is a covalently bonded neutral molecule rather than a loose electrostatic ion pair, as is the case for the 2:2 salts. For these reasons it is hardly surprising that the relation, $D_s = D_{12} = D_m$ does not hold.

The diffusion coefficients of three aqueous weak acid systems, acetic,[91,118] chloroacetic,[119] and citric[120] acids, have been measured. In each case the workers concerned have measured the bulk diffusion coefficient of the acid, D_s, calculated D_{12}, and used equation (7.3) to estimate D_m. The values of D_m obtained in this way were then plotted against the total acid concentration, C_s, and found to give, as expected, a straight line plot. This was extrapolated to zero concentration to give a value for the diffusion coefficient of the undissociated acid molecule at infinite dilution, D_m^o.

Some doubts as to the validity of this extrapolation were raised by the work of Holt and Lyons on dilute aqueous solutions of

acetic acid.[118] These authors measured the diffusion coefficients of extremely dilute solutions of acetic acid and attempted to predict their results using values of D_m obtained from the work of Vitagliano and Lyons on more concentrated acetic acid solutions.[91] Their predicted values were low, a result which they were unable to explain, but which could be accounted for by the values of D_m obtained from the extrapolation being low.

It was considered that this might be an indication of a general trend, and that the identity $D_s = D_{12} = D_m$ was approached for aqueous weak acid systems as the degree of dissociation.increased. Unfortunately no data exist to test this hypothesis. The data required would be experimental values of the bulk diffusion coefficient of a weak acid in the concentration range where the degree of dissociation is appreciable. One system which could be used to provide such data is aqueous chloroacetic acid, where the degree of dissociation is approximately 40% at a concentration of 0.002 molar. Such data could only be obtained by the conductimetric method. However the only data available for chloroacetic acid are the measurements of Garland, Tong, and Stockmayer,[119] obtained at concentrations of 0.2 molar and above by the porous frit technique.

In order to provide more data on the diffusion of chloroacetic acid a few measurements were made in dilute solutions using the optical method described in chapter 4. The results are given in table (7.5). The lowest concentration reported, 0.05 molar, represents the lower limit for which accurate measurements can be made by this method.

Table 7.5

Concentration (mol l^{-1})	$D_s \times 10^5$ (cm^2 sec^{-1})
.09957	1.1045
.08289	1.1091
.07592	1.1042
.05097	1.1290

In the following sections rigorous relationships between D_s, D_{12} and D_m, are derived and used to process the available experimental data for weak acid systems.

7.6.1 Relationship Between D_s, D_{12} and D_m This can be derived from equation (7.3) using the relations between C_3, C_{12} and C_m derived from the law of mass action.

$$C_{12} = \alpha C_s$$
$$C_m = (1 - \alpha)C_s \qquad (7.16)$$

Differentiating equations (7.16) with respect to the distance parameter, x, gives the following relations :-

$$\frac{\partial C_{12}}{\partial x} = \left(\alpha + C_s \frac{\partial \alpha}{\partial C_s}\right)\left(\frac{\partial C_s}{\partial x}\right) \qquad (7.17)$$

$$\frac{\partial C_m}{\partial x} = \left[(1-\alpha) - C_s \frac{\partial \alpha}{\partial C_s}\right]\frac{\partial C_s}{\partial x} \qquad (7.18)$$

$$\frac{\partial C_s}{\partial x} = \frac{1}{\alpha^2}\frac{\partial C_{12}}{\partial x}\left(\alpha - C_{12}\frac{\partial \alpha}{\partial C_{12}}\right) \qquad (7.19)$$

$$\frac{\partial C_m}{\partial x} = \frac{1}{\alpha^{22}}\frac{\partial C_{12}}{\partial x}\left[\alpha(1-\alpha) - C_{12}\frac{\partial \alpha}{\partial C_{12}}\right] \qquad (7.20)$$

The factors $C_s \frac{\partial \alpha}{\partial C_s}$ and $C_{12} \frac{\partial \alpha}{\partial C_{12}}$ can be calculated by differentiating the expression for the dissociation constant of the acid K_D with respect to either C_s or C_{12} respectively. The dissociation constant can be written

$$K_D = \frac{\alpha C_{12} y_{12}^2}{1-\alpha} = \frac{C_s y_{\pm}^2}{1-\alpha} \qquad (7.21)$$

using the relation $y_{\pm} = \alpha y_{12}$ given by Davies [121] Differentiating gives :-

$$-C_s \frac{\partial \alpha}{\partial C_s} = (1-\alpha)(2fn y_{\pm} - 1) \qquad (7.22)$$

and

$$-C_{12} \frac{\partial \alpha}{\partial C_{12}} = \alpha(1-\alpha)(2fn y_{12} - 1) \qquad (7.23)$$

Substituting equations (7.17), (7.18), and (7.22) in (7.3) gives

$$D_s = (\alpha-1).2fn y_{\pm} + 1 \; D_{12} + (1-\alpha)2fn y_{\pm} . D_m \qquad (7.24)$$

and substituting equations (7.19), (7.20) and (7.23) in (7.3) gives

$$\alpha + (1-\alpha)2fn y_{12} \; D_s = \alpha D_{12} + (1-\alpha) 2fn y_{12} \cdot D_m \qquad (7.25)$$

Equations (7.24) and (7.25) are the required relations between D_s, D_{12} and D_m. Equation (7.24) can only be used when experimentally determined activity or osmotic coefficients are available to permit the calculation of $fn\, y_{\pm}$. Equation (7.25) is used when the activity term, $fn\, y_{12}$, must be calculated using electrolyte theory. As no experimental activity data is available for the weak acids studied equation (7.25) was used. If activity corrections are neglected $fn\, y_{12}$ becomes unity and equation (7.25) reduces to the approximate expression derived by Müller and Stokes [120] :-

$$D_s = \frac{\alpha}{2-\alpha} D_{12} + \frac{2(1-\alpha)}{2-\alpha} D_m \qquad (7.26)$$

Table 7.6 Diffusion Coefficient of Acetic Acid

C_s mol dm^{-3}	α	$f n_{y_{12}}$	$D_{12} \times 10^5$ $cm^2\ s^{-1}$	$D_s \times 10^5$ $cm^2\ s^{-1}$	$D_m \times 10^5$ $cm^2\ s^{-1}$	$D_m \times 10^5$ $cm^2\ s^{-1}$
0	1.0	1.0	1.951	1.951		
.00241	.083	.992	1.929	1.278	1.249	1.248
.00524	.057	.990	1.924	1.259	1.239	1.239
.00913	.044	.989	1.921	1.246	1.230	1.230
.01407	.036	.987	1.917	1.253	1.222	-
.02004	.030	.986	1.914	1.227	1.216	1.216
.02705	.026	.985	1.911	1.220	1.211	-
.03078	.023	.984	1.908	1.214	1.206	1.206
.04119	.020	.983	1.906	1.210	1.203	-
.05417	.018	.983	1.904	1.207	1.201	1.201
.07725	.016	.981	1.900	1.203	1.197	-
.10429	.013	.980	1.896	1.199	1.194	1.194
.13523	.012	.978	1.893	1.194	1.190	-
.17004	.011	.977	1.890	1.188	1.184	1.184
.20868	.0096	.976	1.887	1.181	1.179	1.179
.25112	.0088	.975	1.884	1.175	1.172	-

Values of D_m in the penultimate column are calculated using equation (7.2.6) and those in the last column from equation (7.25)

Table 7.7 Diffusion Coefficient of Chloroacetic Acid

C_s mol dm^{-3}	α	fny_{12}	$D_{12} \times 10^5$ $cm^2\ s^{-1}$	$D_s \times 10^5$ $cm^2\ s^{-1}$	$D_m \times 10^5$ $cm^2\ s^{-1}$	$D_m \times 10^5$ $cm^2\ s^{-1}$
0	1.0	1.0	2.007	2.007	1.075	1.072
.04677	.171	.955	1.888	1.134	1.056	1.053
.1262	.111	.944	1.858	1.098	1.051	1.048
.1981	.091	.938	1.843	1.079	1.041	1.038
.2841	.077	.933	1.831	1.057	1.025	1.022
.3836	.068	.928	1.820	1.034	1.005	1.003
.4962	.060	.924	1.810	1.010	.984	.982
.6214	.055	.921	1.801	.984	.960	.958
.7586	.050	.918	1.793	.958	.936	.934
.8318	.048	.916	1.789	.944	.923	.921

Values of D_m in the penultimate column are calculated using equation (7.26) and those in the last column from equation (7.25)

Table 7.8 Diffusion Coefficient of Citric Acid

C_s mol dm^{-3}	α	$f_{\gamma_{12}}$	$D_{12} \times 10^5$ $cm^2\ s^{-1}$	$D_s \times 10^5$ $cm^2\ s^{-1}$	$D_m \times 10^5$ $cm^2\ s^{-1}$	$D_m \times 10^5$ $cm^2\ s^{-1}$
0	1.0	1.0	1.474	1.474	.660	.659
.0792	.101	.956	1.374	.688	.649	.648
.1190	.084	.951	1.365	.676	.644	.643
.1661	.072	.948	1.356	.664	.637	.636
.2203	.064	.944	1.349	.653	.629	.628

Values of D_m in the penultimate column are calculated using equation (7.26) and those in the last column from equation (7.25)

The above relations are completely general for symmetrical electrolytes, and would apply also to the diffusion coefficients of 2:2 salts if not rendered trivial by the equality of these coefficients.

7.6.2 Calculation of the Diffusion Coefficients of Undissociated Weak Acid Molecules These calculations were carried out for the three weak organic acids for which experimental diffusion data were available, i.e. acetic,[91,118] chloroacetic [119] and citric [120] acids. Values of D_{12}, fny_{12}, C_s and α, were obtained using the computer programme described above in section (7.3.4). These values were combined with the experimental diffusion coefficients using equation (7.26) to give approximate values for D_m and equation (7.25) to give exact values for D_m. The results are shown in tables 7.6, 7.7 and 7.8 and in Figs (7.6), (7.7) and (7.8) for acetic, chloroacetic and citric acids respectively. In each case the results given by equations (7.26) and (7.25) are equal within experimental error.

7.6.3 Discussion of Results The diffusion coefficients of undissociated citric acid and chloroacetic acid exhibit the behaviour expected of a typical non-electrolyte by showing a linear variation with concentration. As expected from the results of Holt and Lyons [118] the coefficient for acetic acid varies linearly with concentration from 0.04 molar upwards, but deviates positively from the extrapolated line at lower concentrations. For all three acids an extrapolation from the linear region to zero concentration gives values of the limiting diffusion coefficient of the undissociated acid which are in good agreement with those obtained by the original workers. These values are given in table (7.9).

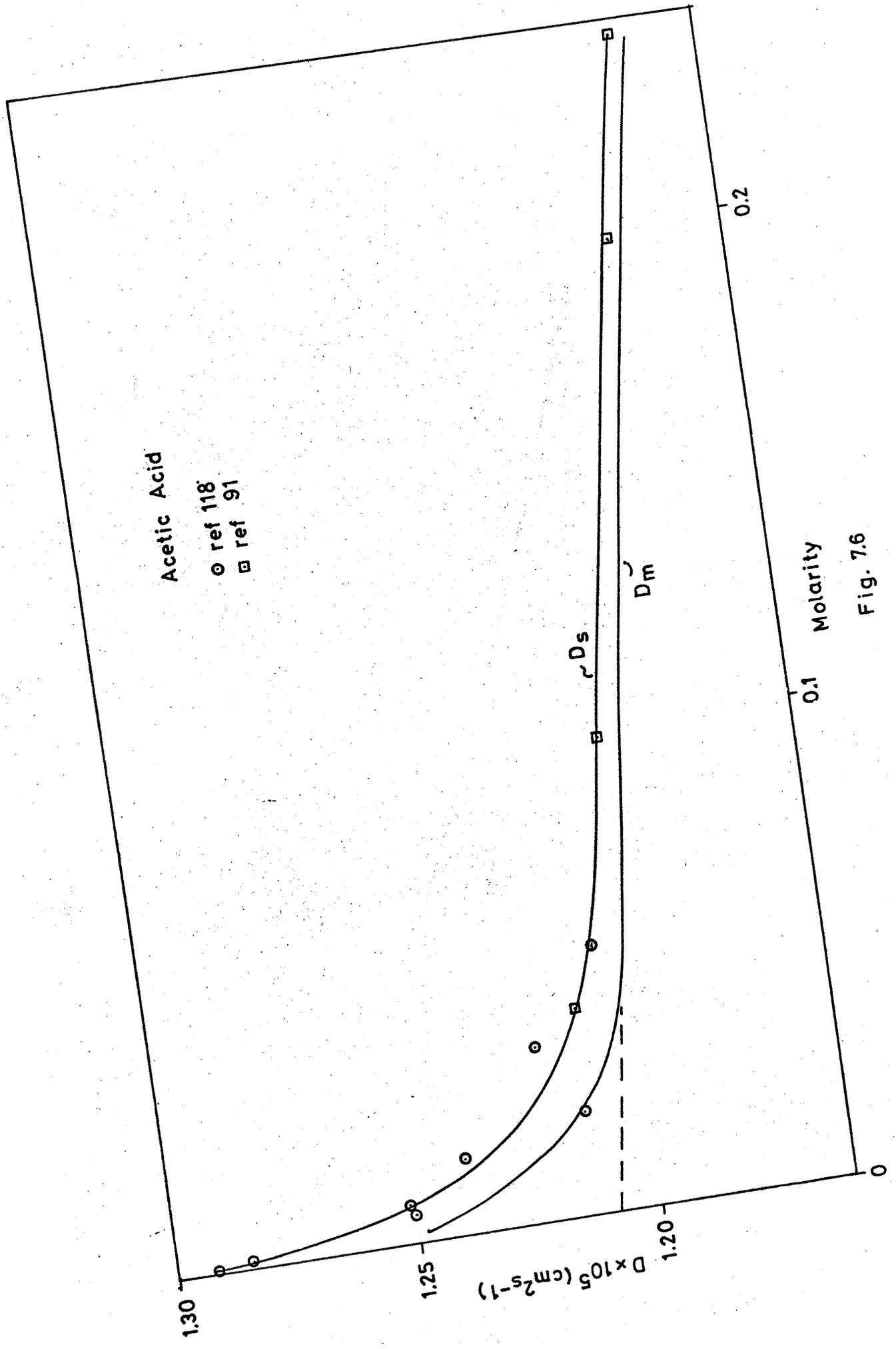
Acetic Acid
⊙ ref 118
⊡ ref 91
D_s
D_m
$D \times 10^5$ ($cm^2 s^{-1}$)
1.30
1.25
1.20
0
0.1
0.2
Molarity

Fig. 7.6

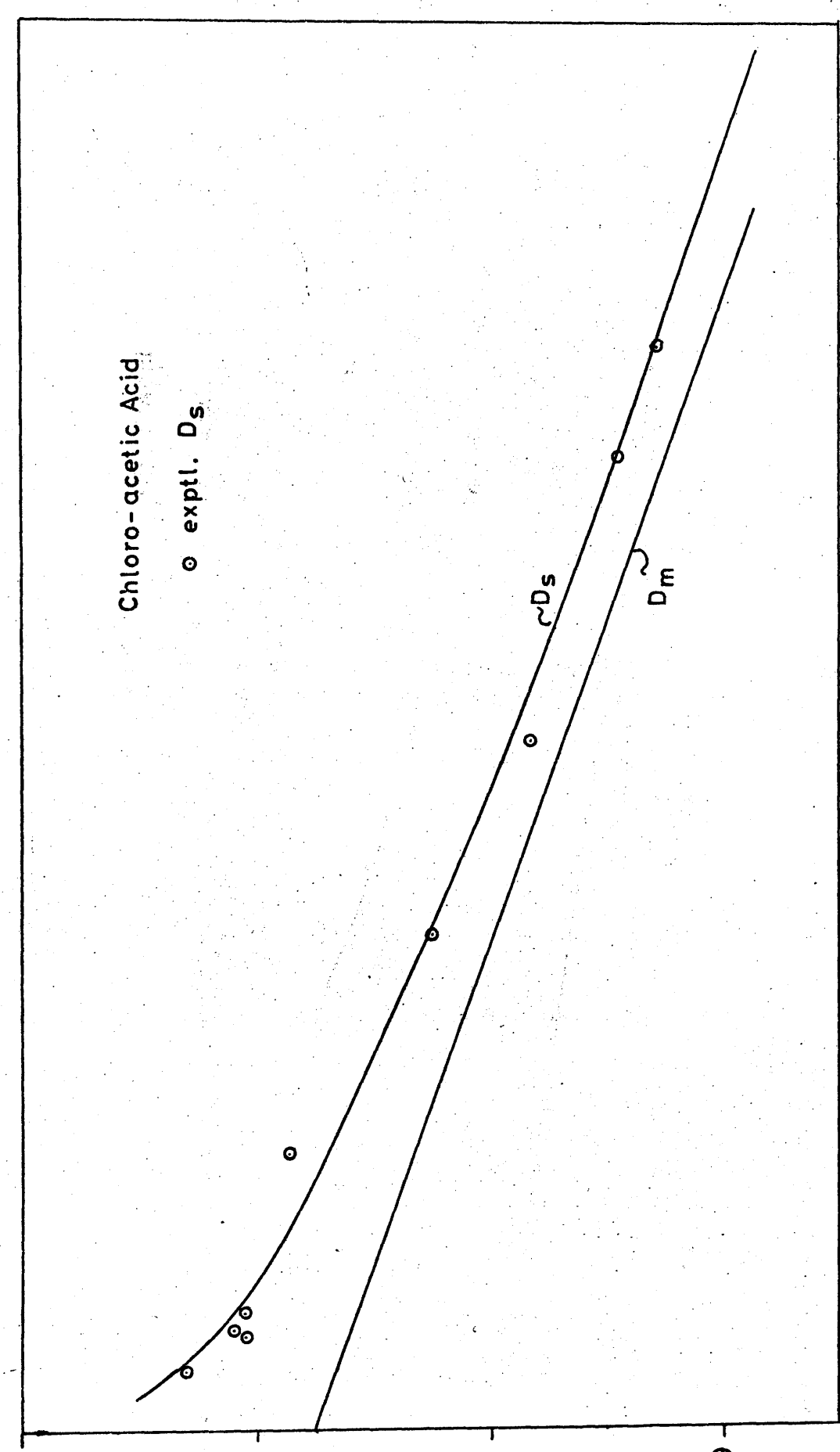
Chloro-acetic Acid
⊙ exptl. D_s
D_s
D_m
$D \times 10^5$ ($cm^2 s^{-1}$)
1.2
1.1
1.0
0.9
0
0.5
1.0
Molarity

Fig. 7.7

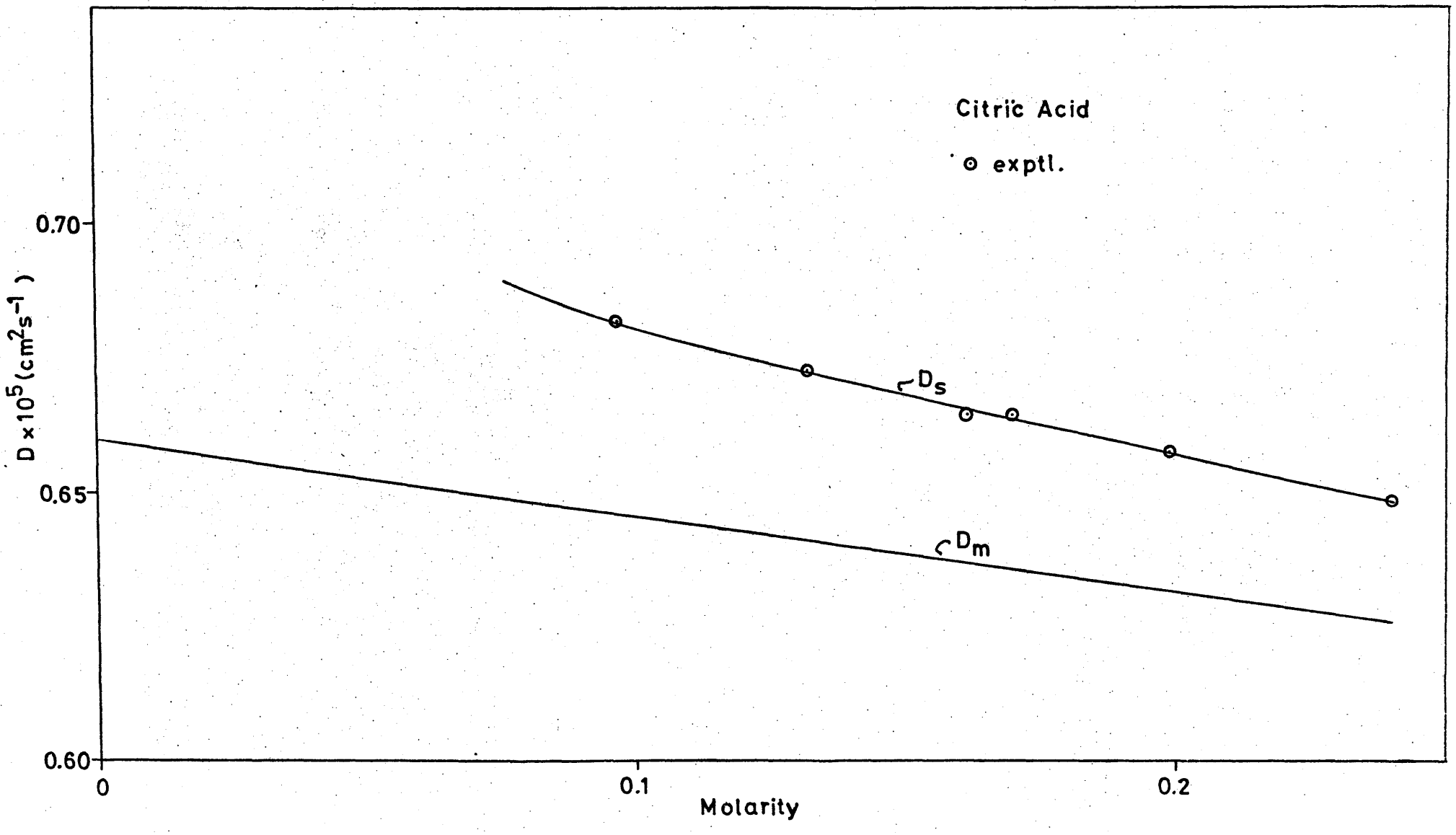
Citric Acid
⊙ exptl.
0.70
0.65
0.60
D x 10^5 (cm^2 s^-1)
Ds
Dm
0
0.1
0.2
Molarity

Fig. 7.8

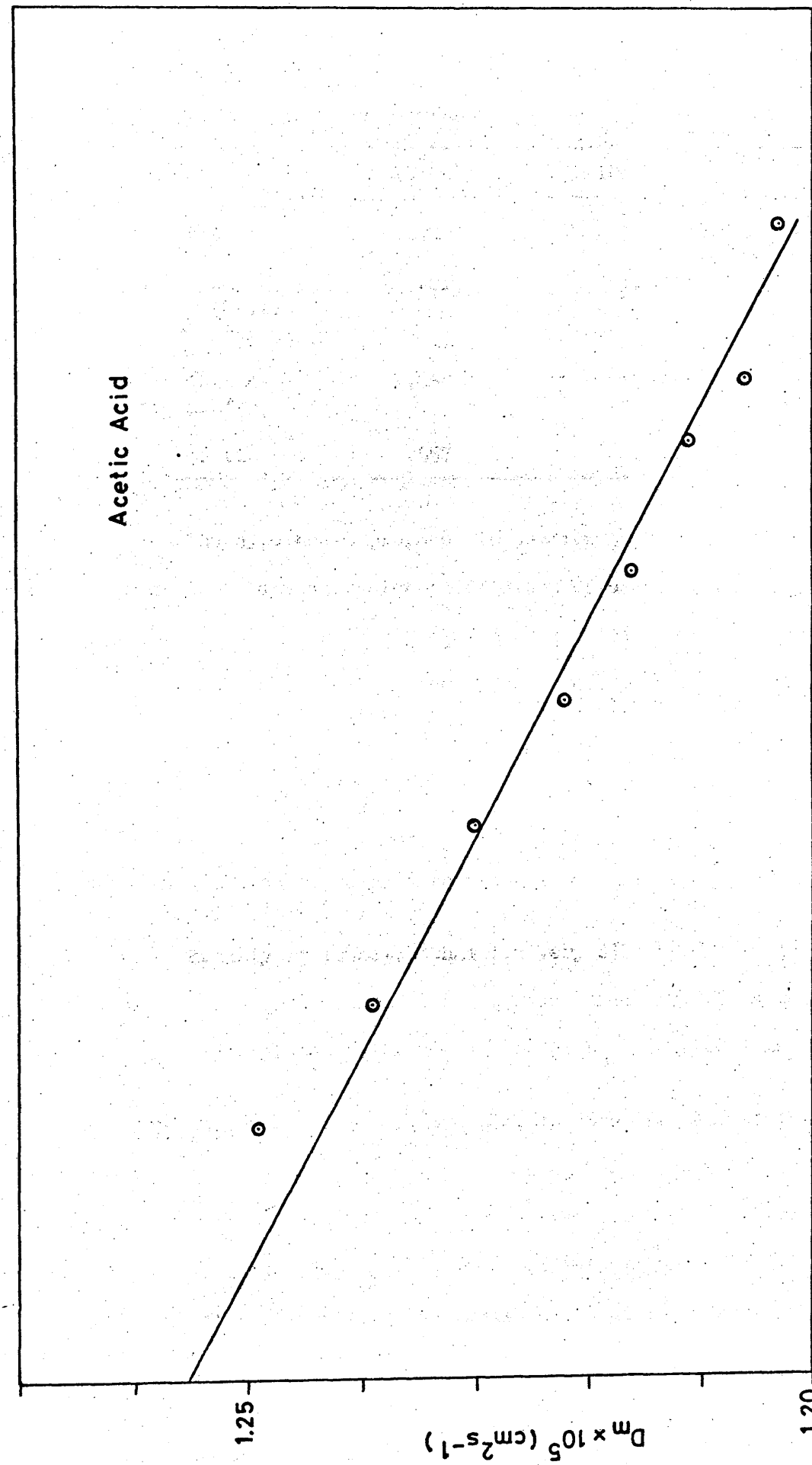

Fig. 7.9

Table 7.9

Acid	D_m^o (original)	D_m^o (present work)
	x $10^5 cm^2 s^{-1}$	x $10^5 cm^2 s^{-1}$
Acetic	1.201	1.209
Acetic (lower conc)	(1.201)	1.260
Chloro-acetic	1.08	1.075
Citric	.657	.660

The hypothesis proposed in section 5 is not supported by these results. The diffusion coefficient of undissociated chloro-acetic acid is a linear function of concentration until 0.05 molar, in which solution the degree of dissociation is 17%, whereas that of acetic acid deviates substantially from linearity at a concentration of 0.02 molar, where the degree of dissociation is only 3%. More experimental work on very dilute weak acid solutions will be required before any decision on which type of behaviour is typical can be made.

Finally it is noted that for very dilute acetic acid solutions a plot of D_m against $\sqrt{C}$, (shown in Fig (7.9)) is essentially linear and extrapolates to give a value for D_m^o of 1.260 x $10^{-5} cm^2 sec^{-1}$.

7.7 Conclusions The original aim, to show that Harned & Hudson's results could be interpreted as free ion diffusion coefficients, has been accomplished. In addition it has been shown that the calculations outlined in section (7.3) give a good estimate of the salt diffusion coefficient of a 2:2 salt in aqueous solution up to concentrations of

0.1 M; well beyond the range of concentration where Fuoss-Onsager theory is expected to be valid. It seems likely that such a calculation will be applicable to any aqueous 2:2 salt solution, and may well prove useful where an estimate of the diffusion coefficient is required.

For the weak acids, however, no such convenient relation exists. In these systems the major contribution to the bulk diffusion coefficient is given by the undissociated acid molecule, which behaves as a typical non-electrolyte. The contribution of the free ions appears only as a relatively minor correction term in the bulk diffusion coefficient.

Appendix.

The programs reproduced here are written in the version of the Algol language suitable for use with the Edinburgh Regional Computer Centre's I.B.M. 370/158 computer. They may need some slight modification before being used with other computing systems.

Program 1

This program reads in sets of data, (x,y), and then calculates the straight line fit between ln(y) and x.

```
'begin''real' sx, sy, sx2, sxy, m, c, sy2, m1, r, ses, sigx;
'integer' n, k, i, j, f;
repeat: n:=read; 'begin''array' x, y, y1, dy, a, b(/1:n/);
'for'i:=1'step'1'until'n'do' a(/i/):=read;
'for'i:=1'step'1'until'n'do'b(/i/):=read; f:=n;
more: k:=read; 'if'k=1'then'r:=read; n:=f;
'for'i:=1'step'1'until'n'do''begin'x(/i/):=a(/i/); y(/i/):=b(/i/);
'if'k=1'then'y(/i/):=y(/i/) + r; y(/i/):= ln(y(/i/)); 'end';
paperthrow; copytext('('*')');
redo: sx:=sy:=sx2:=sy2:=sxy:=0; newlin(2);
'for'i:=1'step'1'until'n'do''begin' sx:=sx + x(/i/);
sy:=sy + sy(/i/); sx2:=sx2 + x(/i/)**2; sxy:=sxy + x(/i/)*y(/i/);
sy2:=sy2 + y(/i/)*2; 'end'; m:= (n*sxy-sx*sy)/(n*sx2-sx**2);
c:=(sx"*sy-sx*sxy)/(n*sx2-sx**2); m1:=(sxy*n-sx*sy)/(n*sy2-sy**2);
r:=sqrt(m*m1); 'if'r**2>1'then''begin'writet('('R TEST FAILS')');
'goto'miss; 'end'; sigx:=(n*sx2-sx**2)/n**2; ses:=sigx*sqrt(1-r**2);
j:=0; writet('('  X  Y OBS  ')');
writet('(' Y CAL  DIFF')');
'for'i:=1'step'1'until'n'do''begin'y(/i/):=m*x(/i/) + c;
dy(/i/):=y(/i/)-y1(/i/); newlin(1); print(x(/i/),0,6);
print(y(/i/),0,6); print(y1(/i/),0,6); print(dy(/i/),0,6);
'if'abs(dy(/i/))≤2*ses'then''begin'j:=j+1; x(/j/):=x(/i/);
y(/j/):=y(/i/); 'end';'end';
miss: newlin(2); writet('('M =  ')'); print(m,0,6); newlin(2);
writet('('C =  ')'); print(c,0,6); newlin(2);
writet('('REGRESSION COEFFICIENT = ')'); print(r,0,6); newlin(2);
writet('('STANDARD ERROR OF ESTIMATE = ')'); print(ses,0,6);
```

```
'if'j<n'then''begin' n:=j; 'if'n  3'then''goto'zed; 'goto'redo; 'end';
zed:   k:=read;  'if'k=2'then''goto'more; 'end';
       'if'k=1'then''goto'repeat;  'end'
```

Data input for Program 1.

Number of sets of data points, (x,y);

All values of x, x_1 .... x_n;

All values of y, y_1 .... y_n;

Control digit, always equal to 1;

Correction factor, r, to be added to each value of y;

Title*

Second control digit; 0 if no more data follows;

1 if fresh data follows;

2 if a second correction factor is to replace the current value. The control digit, 1, and the fresh value of r should follow.

Program 2.

This program reads in the coefficients, a_i, of the curve fit expression of y against x and then uses the method of Rutledge to calculate $\frac{dy}{dx}$ at various values of x. If required it will also read in coefficients of the curve fit expression of x against z and output values of $\frac{dy}{dx}$ and corresponding values of z.

```
'begin''real' xstart, xfin, h, no, conc;
'integer'i, j, k, n, m, l, p;
'real''array' b(/0:5/);
p:=read;  'if' p=0 'then''goto' redo; l:=read;
'for' i:=0 'step'1'until' l 'do' b(/i/):=read;
'for' i:=l+1 'step'1'until' 5 'do' b(/i/):=0;
redo:  'begin''array' a(/0:5/), x(/-3:2/), y(/-2:2/); paperthrow;
copytext('('*')'); k:=read;  newlin(2);
'for' i:=0 'step'1'until' k 'do' a(/i/):=read;
'for' i:=k+1 'step'1'until' 5 'do' a(/i/):=0;
moredo:  xstart:=read; xfin:=read; h:=read; no:=abs((xstart-xfin)/h);
n:=entier(no);
'begin''array' r,s,t,e(/1:n/); x(/-3/):=xstart - h;
'for' j:=2 'step'1'until' n-2'do''begin''for'i:=-2'step'1'until'2'do'
'begin' x(/i/):=x(/i-1/)+h;  y(/i/):=a(/0/)+x(/i/)*(a(/1/)+x(/i/)*
(a(/2/)+x(/i/)*(a(/3/)+x(/i/)*(a(/4/)+x(/i/)*a(/5/))))); 'end';
x(/-3/):=x(/-2/);
t(/j+1/):=(-3*y(/-2/)-10*y(/-1/)+18*y(/0/)-6*y(/*/)+y(/2/))/(12*h);
r(/j/):=(y(/-2/)-8*y(/-1/)+8*y(/1/)-y(/2/))/(12*h);
s(/j+1/):=(-y(/-2/)+6*y(/-1/)-18*y(/0/)+10*y(/1/)+3*y(/2/))/(12*h);
e(/j-1/):=x(/-1/); e(/j/):=x(/0/); e(/j+1/):=x(/1/);  'end';
r(/1/):=s(/1/):=s(/2/):=1.0;  j:=n-2;
t(/j+1/):=r(/j+1/):=s(/j+1/);  t(/j/):=(s(/j/)+r(/j/))/2;
'if'p=1'then''goto' altern;
writet('('        DERIV 1        DERIV 2        DERIV 3        AVERAGE')');
```

```
writet('('          X VALUE')'); newlin(2);
'for'i:=1'step'1'until'j+1'do''begin' space(4); print(t(/i/),3,4);
space(3); print(r(/i/),3,4); space(3); print(s(/i/),3,4);
space(3); h:=(t(/i/)+r(/i/)+s(/i/))/3; print(h,3,4); space(3);
print(e(/i/),3,6); newlin(1); 'end'; 'goto' next;
altern: writet('('          DERIV 1       DERIV 2       DERIV 3')');
writet('('      AVERAGE        DELTA E        MOLARITY')');
newlin(2); 'for'i:=1'step'1'until'j+1'do' 'begin'
conc:=a(/0/)+e(/i/)*(a(/1/)+e(/i/)*(a(/2/)+e(/i/)*(a(/3/)+e(/i/)*
      (a(/4/)+e(/i/)*a(/5/))))); space(4); print(t(/i/),3,4);
space(3); print(r(/i/),3,4); space(3); print(s(/i/),3,4);
space(3); h:=(t(/i/)+r(/i/)+s(/i/))/3; print(h,3,4);
space(3); print(e(/i/),3,6); space(3); print(conc,3,5);
newlin(1); 'end';
next: 'end'; m:=read; 'if'm=1'then''goto'redo;
'if'm=2'then''goto'moredo; 'end'; 'end'
```

Data input for program 2

Control digit:- 1 if conversion between x and z is required, otherwise 0; If the control digit is 1 then:-

Degree of the curve fit expression between x and z;

Coefficients of the curve fit expression between x and z;

Title*

Degree of the curve fit expression between x and y;

Coefficients of the curve fit expression between x and y;

Starting value of x; Final value of x; Step in x;

Control digit:- 1 if a fresh expression between x and y is to follow;

2 if a fresh starting value of x is to follow for the original x/y curve fit;

0 if no more data follows;

Program 3.

This program reads in sets of molarity, density or molality, equivalent conductance, cation transference number, diffusion coefficient, and thermodynamic activity term, and then calculates corresponding sets of the mobility and frictional coefficients defined in chapter 2.

```
'begin''real' r, f, t, m, q;
      'integer' rs, r1, r2, n, z, z1, z2, fs, md, i;
copytext('('*')');
repeat:   r:=read; f:=read; t:=read;
again:    newlin(2);  copytext('('*')');  m:=read; r1:=read;  r2:=read;
z1:=read;  z2:=read;  rs:=r1 + r2;  newlin(2); z:=read; n:=read;
md:=read;
'begin''array' c, d, ms, t1, lda, ds, l11; l12; l22; r11; r22; r12;
                r10, r20, r00, f12, x, y, act(/1:n/);
'for'i:=1'step'1'until'n'do''begin'  c(/i/):=read;  ds(/i/):=read;
lda(/i/):=read;  t1(/i/):=read;  d(/i/):=read;  act(/i/):=read; 'end';
q:=10**(-4)*r*t*rs*r1*z1;   'for'i:=1'step'1'until'n'do''begin'
x(/i/):=d(/i/)/(q*act(/i/));  y(/i/):=lda(/i/)/(10**(-9)*f**2);
'if'md=3'then'ms(/i/):=ds(/i/)'else'ms(/i/):=c(/i/)/(ds(/i/)-.001*
c(/i/)*m);
l11(/i/):=y(/i/)*t1(/i/)**2/z1**2 + r1**2*x(/i/);
'if'c(/i/)=0.0'then'l12(/i/):=0.0'else'
    l12(/i/):= y(/i/)*t1(/i/)*(1-t1(/i/))/z1*z2 + r1*r2*x(/i/);
l22(/i/):= y(/i/)*(1-t1(/i/))**2/z2**2 + r2**2*x(/i/);
x(/i/):= l11(/i/)*l22(/i/) - l12(/i/)**2;  x(/i/):=0.1*x(/i/);
r11(/i/):= l22(/i/)/x(/i/);     r12(/i/):= -l12(/i/)/x(/i/);
r22(/i/):=  -r12(/i/)*y(/i/);  r22(/i/):= l11(/i/)/x(/i/);
'if'md=3'then''begin''if'c(/i/)=0.0'then'x(/i/):=0.01807/z'else'
x(/i/):=18.015*ms(/i/)/(1000*z*c(/i/));'end''else'
x(/i/):=18.015/(z*(1000*ds(/i/) - m*c(/i/)));
```

```
r10(/i/):= -(r1*r11(/i/) + r2*r12(/i/))*x(/i/)*100;
r20(/i/):= -(r1*r12(/i/) + r2*r22(/i/))*x(/i/)*100;
r00(/i/);= -(r1*r10(/i/) + r2*r20(/i/))*x(/i/)*100;  'end';
writet('('          C        M       EQV COND      T+     D(V)*5')');
writet('('     ACTERM ')');  newlin(2);
'for'i:=1'step'1'until'n'do''begin' space(5);  print(c(/i/),2,4);
print(ms(/i/),2,6); print(lda(/i/),4,3); print(t1(/i/),2,4);
print(d(/i/),2,4);  print(act(/i/),2,4); newlin(1); 'end'; newlin(3);
writet('('         SQRT S    L11/N     L12/N     L22/N      ')');
writet('('F12       Q12')');  newlin(1);
writet('('          *10       **12      **12      **12')');newlin(2);
'for'i:=1'step'1'until'n'do''begin' space(5); f:=10*sqrt(z*c(/i/)*
(z1 - z2)/2); print(f,2,4); print(l11(/i/),2,4); print(l12(/i/),2,4);
print(l22(/i/),2,4); print(f12(/i/),2,4);
f:=l12(/i/)/sqrt(l11(/i/)*l22(/i/)); print(f,2,4); newlin(1); 'end';
newlin(3);
writet('('         SQRT S    NR11      -NR12     NR22       Q10')');
writet('('       Q20')');  newlin(1);
writet('('          *10       **-11       **-11     **-11')'); newlin(3);
'for'i:=1'step'1'until'n'do''begin'  space(5);
f:=10*sqrt(z*c(/i/)*(z1 - z2)/2); print(f,2,4); r12(/i/):=r12(/i/);
print(r11(/i/),2,4); print(r12(/i/),2,4); print(r22(/i/),2,4);
r12(/i/):=-r12(/i/);  f:= -r10(/i/)/sqrt(r11(/i/)*r00(/i/));
print(f,2,4); f:= -r20(/i/)/sqrt(r22(/i/)*r00(/i/));
print(f,2,4); newlin(1); 'end'; newlin(3);
writet('('         SQRT S    -R10      -R20      -COR10    -COR20')');
writet('('     R00/N')');  newlin(2);
writet('('          *10       **9       **-9      **-11      **-11')');
writet('('       **-7')'); newlin(3);
'for'i:=1'step'1'until'n'do''begin' space(5);
```

```
f:=10*sqrt(z*c(/i/)*(z1 - z2)/2);  print(f,2,4);
r10(/i/):=-r10(/i/); r20(/i/):=-r20(/i/); print(r10(/i/),2,4);
print(r20(/i/),2,4); r10(/i/):=0.01*r10(/i/)/(z*x(/i/));
r20(/i/):=0.01*r20(/i/)/(z*x(/i/)); print(r10(/i/),2,4);
print(r20(/i/),2,4); print(r00(/i/),2,4); newlin(1); 'end'; 'end';
n:=read;  f:=96493;
'if'n=1'then''goto'again'else''if'n=2'then''goto'repeat; 'end'
```

Data input for program 3.

Title; Gas constant; Faraday's constant; Absolute temperature;

Title;

Molecular weight of the solute; r_1; r_2; z_1; z_2; Number of equivalents per mole of solute; Number of data points to be entered, n;

Control digit; 1 if density is entered in data.

3 if molality is entered in data.

n sets of data, consisting of:-

molal concentration; density or molal concentration; equivalent conductance; cation transference number; diffusion coefficient; activity term;

Control digit; 1 if fresh data at the same temperature follows.

2 if fresh data at a new temperature follows.

0 if no more data follows.

Program 4

This program calculates values of the diffusion coefficient of aqueous solutions of salts or acids in which ion assocciation is present using the theories of Debeye-Hückel and Fuoss-Onsager.

```
'begin''real' lamda, lamda1, lamda2, z1, z2, z, r1, r2, r, m, m1, a,
        alstart, alfin, alstep, pk, b, t1, t2, t3, t4, t5, t6,
        t7, t8, t9, w, w2, ka, dterm, logy, anot, astart, afin,
        astep;   'integer' p, i, n1, n2;
again:  copytext('('*')'); lamda1:=read; lamda2:=read;
lamda:=lamda1 + lamda2; z1:=read; z2:=read; z:=read; r1:=read;
r2:=read; r:=r1 + r2; m:=read; m1:=read; astart:=read; afin:=read;
astep:=read;  alstart:=read; alfin:=read; alstep:=read;  pk:=read;
p:=read; 'if'p=0'then'pk:=exp(2.302585*(-pk));
copytext('('*')');  t1:= 1.0748*lamda1*lamda2/(lamda*z);
t2:= 49.2122*(lamda1-lamda2)**2/lamda**2;   t3:= 175.5616*z**2;
t5:= 0.001*(18.015*r - m);
w:=(sqrt(r1*z1**2 + r2*z2**2))**3/(r*sqrt(2));
w2:=(w*r*sqrt(2))**(1/3)/sqrt(2);  n2:=entier((alfin-alstart)/alstep);
'begin''array' alphac(/-1:n2/), mbarc, acterm, d, y, alpha, c(/0:n2/);
anot:=astart-astep;
newa:  anot:=anot+astep;  a:=0.3286*w2*anot;
alphac(/-1/):=alstart-alstep; 'for'i:=0'step'1'until'n2'do''begin'
alphac(/i/):=alphac(/i-1/)+alstep;  ka:=a*sqrt(alphac(/i/));
'if'ka=0'then''begin' t4:=0.0; 'goto'skip; 'end';
'if'ka<0.9'then''begin' ka:=ln(ka);
t4:=-2.4047+ka*(0.21848+ka*(-0.35319+ka*(-0.03803-0.000857*ka)));
t4:=exp(t4); ka:=exp(ka); 'end';
'if'ka≥0.9'then't4:=0.04201+ka*(0.081968+ka*(-0.03974+ka*0.00562));
skip:   t6:=t2*ka/(anot*(1+ka));  t7:=t3*t4/anot**2;
mbarc(/i/):=t1-t6+t7;  mbarc(/i/):=mbarc(/i/)*1'-20;
```

```
dterm:=(m1+t5)/((m1*alphac(/i/)+0.99707)+alphac(/i/)*t5);
dterm:=dterm*alphac(/i/);  t8:=(1+ka)**2;
t9:=0.586178*w*sqrt(alphac(/i/));  acterm(/i/)1-(t9/t8);
d(/i/):=r*24.7894'12*mbarc(/i/)*acterm(/i/);  t8:=sqrt(t8);
t9:=t9*0.868508; logy:=t9/t8;  y(/i/):=exp(-2.3026*logy);
alpha(/i/):=pk/(alphac(/i/)*y(/i/)**2+pk);
c(/i/):=alphac(/i/); 'end';  newlin(1);  writet('(' A = ')');
print(anot,2,5);  newlin(2);
writet('('  MOLARITY       ALPHA       ALPHA*C       Y12')');
writet('('      ACTIVITY TERM      M/C          D12')');
newlin(");  'for'i:=0'step'1'until'n2'do''begin' print(c(/i/),0,5);
print(alpha(/i/),0,5); print(alphac(/i/),0,5); print(y(/i/),0,5);
print(acterm(/i/),0,5); print(mbarc(/i/),0,5); print(d(/i/),0,5);
newlin(1); 'end';  paperthrow; 'if'anot<afin'then''goto'newa; 'end';
n1:=read;  'if'n1=2'then''goto'again; 'end'
```

Data input for program 4.

Title; Limiting equivalent conductances of the cation and anion resp.;

z_1; z_2; Number of equivalents of salt per mole;

r_1; r_2; Gradient of density with concentration(mol.dm^{-3});

Initial value

Final value distance of closest approach, Å;

step in value of

Initial value

Final value molar concentration of free ions;

Step in value of

Assocciation constant of salt, K_a; Control digit = 1; or

pK_a; Control digit = 0;

Title*

Control digit - 2 if fresh data follows otherwise 0.

References for the Introduction.

1. Onsager, L. Phys. Rev., 1931 37 405;
   1931 38 2265.
2. Meixner, J. Ann. Physik. 1941 39 333; 1942 41 409; 1943 43 244.
3. Casimir, H.B.G. Rev. Mod. Phys. 1945 17 343.
4. Prigogine, I. 'Etude Thermodynamique des Phenomenes Irreversibles', Dunod, Paris, Desoer, Liege, 1947.
5. Guggenheim, E.A. J. Phys. Chem. 1923 33 842; 1924 34 1540.
6. Miller, D.G. J. Phys. Chem. 1966 70 2639; 1967 71 616; 1967 71 3588.
7. Dunsmore, H.S., Jalota, S.K. and Paterson, R. J. Chem. Soc. A., 1969, 1061.
8. Paterson, R., Jalota, S.K. and Dunsmore, H.S. J. Chem. Soc. A., 1971, 2116.
9. Jalota, S.K. and Paterson, R., J. Chem. Soc. Faraday Trans. 1, 1973 69 1510.
10. Jalota, S.K. Ph.D. Thesis, Glasgow, 1971.
11. Harris, A.C. and Parton, H.N., Trans. Farad. Soc. 1940 36 1139.
12. Irish, D.R., McCarrol, B. and Young, T.F. J. Chem. Phys. 1963 39 3436.
13. Stokes, R.H. and Levien, B.J. J. Amer. Chem. Soc. 1946 68 333.

References for Chapters 2 - 7.

1. Onsager, L. Phys. Rev, 1931 37 405; 1931 38 2265.

2. Meixner, J. Ann. Physik, 1941 39 333; 1942 41 409; 1943 43 244.

3. Casimir, H.B.G. Rev. Mod. Phys. 1945 17 343.

4. Prigogine, I. Etude Thermodynamique des Phenomenes Irreversibles, Dunod, Paris and Desorr, Liege, 1947.

5. Katchalsky, A. and Curran, P. 'Non-equilibrium Thermodynamics in Biophysics', Harvard Univ. Press, Cambridge, 1965.

6. Prigogine, I. 'Introduction to Irreversible Thermodynamics', 3rd Ed. Interscience New York 1967.

7. De-Groot S.R. and Mazur, P., 'Non-equilibrium Thermodynamics', North Holland, Amsterdam, 1962.

8. Fitts, D.D., 'Non-equilibrium Thermodynamics', McGraw Hill, New York, 1962.

9. Miller, D.G. (a) J. Phys. Chem. 1966 70 2639;
(b) J. Phys. Chem. 1967 71 616;
(c) J. Phys. Chem. 1967 71 3588.

10. Ref. 6 pp 34-36.

11. Ref. 5 pp 74-80.

12. Ref. 7 pp 43-45.

13. Miller, D.G. Chem. Rev. 1960 60 15.

14. Miller, D.G. and Pikal, M.J. J. Solution Chem. 1972 1 111.

15. McQuillan, A.J. J. Chem. Soc. Faraday Trans. 1 1974 70 1558.

16. Onsager, L. Ann. N.Y. Acad. Sci. 1945 46 241.

17. Laity, R.W. J. Phys. Chem. 1959 63 80.

18. Ref. 9(a) Appendix 1.

19. Ref. 9(a) Appendix 2.

20. Hamilton, R.T. and Butler, J.A.V. Proc. Roy. Soc. (Lon.) A 1932 138 450.

21. Lunden, A. J. Electrochem. Soc. 1962 109 260.

22. Scatchard, G. and Tefft, R.F., J. Amer. Chem. Soc. 1930 52 2272.

23. Robinson, R.A. and Stokes, R.H. Trans. Farad. Soc. 1940 36 740.

24. Harris, A.C. and Parton, H.N., Trans. Farad. Soc. 1940 36 1139.

25. Stokes, R.H. J. Phys. Chem. 1961 65 1242.

26. Hasse, R., Saurrmann, P.F. and Duecker, K.H. Z. Physik. Chem. NF. 1965 47 224.

27. Vogel, A.I. Quantitative Inorganic Analysis 3rd Ed. Longmans, London, 1961.

(a) pp 192 (b) pp 433

(c) pp 401 (d) pp 950

(e) pp 154

28. Gran, G. Acta. Chem. Scand. 1950 4 559.

29. Gran, G. Analyst 1952 77 661.

30. Shedlovsky, T. and Shedlovsky 'Physical Methods of Chemistry' Vol. I Part IIA, Weissberger, A. and Rossiter, B.W. (Eds.), Chap. 3, Wiley-Interscience 1970.

31. Robinson, R.A. and Stokes, R.H. 'Electrolyte Solutions', 2nd Ed., Butterworths, London, 1959.

32. Evans, D.F. and Matesich, M.A. Techniques of Electrochemistry, Vol. 2, Chapter 1, Yeager, E. and Salkind, A.J. (Eds.) Wiley-Interscience 1973.

33. Jalota, S.K. Ph.D. Thesis, Glasgow 1971 Chapter 5.

34. Dunsmore, H.S., Jalota, S.K. and Paterson, R. J. Chem. Soc. A. (1969) 1061.

35. Jones, G. and Bollinger, G.M. J. Amer. Chem. Soc. 1931 53 411.

36. Stokes, R.H. J. Phys. Chem. 1961 65 1277.

37. Jones, G. and Bollinger, G.M. J. Amer. Chem. Soc. 1935 57 280.

38. Jones, G. and Bradshaw, B.C. J. Amer. Chem. Soc. 1933 55 1780.

39. Rabinowitsch, W. Z. Physik. Chim. 1921 99 338.

40. Jones, H.C. Carnagie Inst. Pub. 1912 170 12.

41. Ref. 31 Chapter 10.

42. Geddes, A.L. and Pontius, R.B., Ref. 30 Vol. I, Part 2, Chapt. 16.

43. Bierlein, J.A. and Becsey, J.G. Ref. 32 Chapter 4.

44. Longsworth, L.G. Ann. N.Y. Acad. Sci. 1945 61.

45. Ref. 33 Chapter 4.

46. Wall, F.T., Grieger, P.F. and Childers, C.W. J. Amer. Chem. Soc. 1952 74 3562.

47. Harned, H.S. and French, D.M., Ann. N.Y. Acad. Sci. 1945 61

48. Coulson, C.A., Cox, J.T., Ogston, A.G. and Philpot, J. St. L., Proc. Roy. Soc. (Lon.) A 1948 192 382.

49. Gosting, L.J. and Onsager, L. J. Amer. Chem. Soc. 1952 74 6066.

50. Hall, J.R., Wishaw, B.F. and Stokes, R.H. J. Amer. Chem. Soc. 1953 75 1556

51. Philpot, J. St. L. and Cook, G.H., Research 1948 1 234.

52. Longsworth, L.G., Rev. Sci. Inst. 1950 21 524.

53. Longsworth, L.G., J. Amer. Chem. Soc. 1952 74 4155.

54. Chapman, T.W. Ph.D. Thesis, University of California, UCRL-17768, 1967.

55. Svenson, H., Acta. Chem. Scand. 1951 5 72.

56. Zernicke, F., Physik. Z. 1937 38 994.

57. Harned, H.S. and Hudson, R.M. J. Amer. Chem. Soc. 1951, 73, 3781.

58. Spiro, M. Chapter 4 of Ref. 30.

59. Ref. 31 Chapter 5.

60. Kay, R.L. Chapter 2 of Ref. 32.

61. Kaimakov, E.A. and Varshavskaya, N.L. Russ. Chem. Rev. 1966 35 89.

62. Irish, D.R., Davies, A.R., Plane, R.A. J. Chem. Phys. 1969 50 2262-3.

63. Harris, A.C. and Parton, H.N. Trans. Farad. Soc. 1940 36 1139.

64. Stokes, R.H. and Levien, B.J. J. Amer. Chem. Soc., 1946 68 333.

65. McBain, J.W. Proc. Wash. Acad. Sci. 1907 9 1.

66. Hittorf, W. Z. Physic. Chim. 1903 43 249.

67. MacInnes, D. and Dole, M. J. Amer. Chem. Soc.

68. Pikal, M.J. and Miller, D.G. J. Phys. Chem. 1970 74 1337.

69. Pikal, M.J. and Miller, D.G. J. Chem. Eng. Data. 1971 16 226.

70. Ives, D.J.G. and Janz, G.J. 'Reference Electrodes' Academic Press (Lon.) 1961.

71. Hamer, W.J. J. Amer. Chem. Soc. 1935 57 662.

72. Rutledge, G. Phys. Rev. 1932 40 262.

73. Lutfullah, Dunsmore, H.S. and Paterson, R. Private communication.

74. Parton, H.N. and Mitchell, J.W. Trans. Farad. Soc. 1939 35 758.

75. Stokes, R.H. and Levien, B.J. J. Amer. Chem. Soc. 1946 68 1852.

76. Egan, D.M. and Partington, J.R. J. Chem. Soc. 1943 157.

77. Stokes, R.M. Trans. Farad. Soc. 1948 44 296.

78. Gilbert, B. Bull. Soc. Chim. Belges 1967 76 493.

79. Kechi, Z. Spectrochim. Acta. 1962 18 1165.

80. Delwaulle, M.L. Bull. Soc. Chim. France (1955) 1294.

81. Delwaulle, M.L. Compt. Rend. 1955 240 2132.

82. Quicksall, C.O. and Spiro, T.G. Inorg. Chem. 1966 5 2232.

83. Irish, D.E., McCarrol, B. and Young, T.F. J. Chem. Phys. 1963 39 3436.

84. Beer, J., Crow, D.R., Grzeskew, R. and Turner, I.D.M. Inor. Nuc. Chem. Lett. 1973 9 35.

85. Morris, D.F.C., Short, E.L. and Waters, D.N. J. Inorg. Nuc. Chem. 1963 25 975.

86. Jones, M.M., Jones, E.A., Harmon, D.F. and Semmes, R.T. J. Amer. Chem. Soc. 1961 83 2038.

87. Davies, C.W. and Thomas, G.O., J. Chem. Soc. (1958) 3660.

88. Dye, J.L., Faber, M.P. and Karl, D.J. J. Amer. Chem. Soc. 1960 82 314.

89. Frei, V. and Podlahova, J. Chemiker. Z. 1963 67 47.

90. Lyons, P.A. and Riley, J.F. J. Amer. Chem. Soc. 1954 76 5216.

91. Vitagliano, V. and Lyons, P.A. J. Amer. Chem. Soc. 1956 78 1594.

92. Pikal, M.J. J. Phys. Chem. 1971 75 3124.

93. Gurney, R.W. 'Ionic Processes in Solution', McGraw-Hill, N. York, 1953.

94. Spiegler, K.S. Trans. Farad. Soc. 1958 54 1409.

95. Jalota, S.K. and Paterson, R. J. Chem. Soc., Farad. Trans. I 1973 69 1510.

96. Reilly, P.J. and Stokes, R.H. Aust. J. Chem. 1970 23 1397.

97. Bates, R. J. Amer. Chem. Soc. 1941 63 399.

98. Short, E.L. and Morris, D.F.C. J. Inorg. Nuc. Chem. 1961 18 192.

99. Shchukarev, S.A., Lilich, L.S. and Latysheva, Z.A. Neorg. Khim. 1956 1 225.

100. Marcus, Y. and Maydan, D. J. Phys. Chem. 1963 67 979.

101. Scibona, G., Orlandini, F. and Danesi, P.R. J. Inor. Nuc. Chem. 1966 28 1313.

102. Onsager, L. and Fuoss, R.M. J. Phys. Chem. 1932 36 2689.

103. a. Harned, H.S. and Hildreth, C.L. J. Amer. Chem. Soc. 1951 73 650.

b. Harned, H.S. and Nuttal, R.L., IBID. 1947 69 737.

c. Harned, H.S. and Blake, C.A. IBID. 1950 72 2265.

d. Harned, H.S. and Hudson, R.M. IBID. 1951 73 652.

104. Harned, H.S. and Hudson, R.M. J. Amer. Chem. Soc. 1951 73 5880.

105. Pikal, M.J. J. Phys. Chem. 1971 75 663.

106. Davies, C.W. 'Ion Association', Butterworths, London, 1962.

107. Owen, B.B. and Gurrey, R.W. J. Amer. Chem. Soc. 1938 60 3074.

108. Dunsmore, H.S. and James, J.C. J. Chem. Soc. 1951, 2925.

109. Harned, H.S. and Owen, B.B., 'The Physical Chemistry of Electrolyte Solutions', 3rd Ed., Reinhold Publishing Corp., N.Y. 1958.

110. Eversole, W.G., Kindsvater, H.M. and Petersen, J.D. J. Phys. Chem. 1942 46 370.

111. Gokstien, Y.R., Zhur. Fiz. Khim. 1952 26 224.

112. Longsworth, L.G.

113. Davies, W.G., Otter, R.J. and Prue, J.R. Disc. Farad. Soc. 1957 24 103.

114. Bale, W.D., Davies, E.W. and Monk, C.B. Trans. Farad. Soc. 1956 52 816.

115. Brown, P.G.M. and Prue, J.R. Proc. Roy. Soc. London, A. 1955 232 320.

116. Davies, C.W. J. Chem. Soc. 1938, 2093.

117. Ref. 31 pp

118. Holt, R.L. and Lyons, P.A. J. Phys. Chem. 1965 69 2341.